KARST GEOMORPHOLOGY OF UPPER SINKING COVE, FRANKLIN COUNTY, TENNESSEE

by

JERRY DOUGLAS DAVIS

A.B., Georgia State University, 1976

A Thesis Submitted to the Graduate Faculty

of the University of Georgia in Partial Fulfillment

of the

Requirements for the Degree

MASTER OF ARTS

ATHENS, GEORGIA

1982

KARST GEOMORPHOLOGY OF UPPER SINKING COVE,

FRANKLIN COUNTY, TENNESSEE

by

JERRY DOUGLAS DAVIS

Approved:

George A. Brook Date July 30, 1982
Major Professor

Vernon Mecutchen Date 30 July 1982
Chairman, Reading Committee

Approved:

John Dowling
Graduate Dean

August 10, 1982
Date

TABLE OF CONTENTS

ILLUSTRATIONS

LIST OF TABLES

ACKNOWLEDGMENTS

The writer would like to thank Dr. George A. Brook for his assistance in this research. Field assistance (especially in cave survey and exploration) was given by members of the Athens Speleological Society: Ann Davis, Ken Davis, George Holland, Sally Holland, and Mike Weems; graduate students in the Department of Geography: Neil Carrier, Mark Hanson, and Andy McFadden; and others: Becky Baker, Lawrence Camp, John Catmur, Glenn Davis, Lewis Davis, Bill Holland, Mary Holland, Helen Johnston, Danny Marshall, and John Rice. Rick Buice (Rome, Ga.) provided unpublished maps of Sinking Cove Cave, and he and Will Chamberlin (Athens) provided information on the 17 caves known prior to this study in Upper Sinking Cove. Ken Davis (Dept. of Geology, UGA) analyzed rock samples in thin-section. Chin-Hong Sun (Dept. of Geography) provided a FORTRAN program for analysis of joint and cave passage orientations. Climatic datawere provided by the Data Management Section (Robert Beebe, supervisor), Tennessee Valley Authority. J. F. Quinlan (Uplands Research Laboratory) provided technical advice on dye-tracing techniques. Photographic assistance was provided by Roy Doyon (Dept. of Geography) and Don Hunter (Athens, Ga.).

Field equipment for hydrologic and solution chemistry studies was provided by the Department of Geography. Fluorometry laboratory facilities and equipment was provided by James Porter, Department of Zoology, University of Georgia.

CHAPTER I

INTRODUCTION

The unique drainage and morphogenetic characteristics of karst landscapes (a predominance of underground drainage, rapid underground flow rates, cavern development, and ground-surface subsidence and collapse) have produced special problems of water supply, water quality, and general land use in these areas. An illustration of this was the extensive sinkhole collapse in Florida during 1981, which resulted from man's removal of groundwater from a karst aquifer and extreme drought conditions. The need to resolve specific management and engineering problems in karst areas has led to research into the nature of karst processes.

Karst research has worldwide scope: more than 11% of the earth's land surface is underlain by soluble rocks (Sweeting, 1973). The manner in which these terranes become karstified (i.e., develop underground drainage and characteristic landforms) is dependent upon factors of the local geology and climate. Global models of karst morphogenesis have been developed (e.g., Lehmann, 1936; Corbel, 1959), but are generally hampered by a lack of information on regional differences in karst processes. Further study of karst landforms and processes in a wide variety of environments is needed to provide information for the refinement of the present models.

The purpose of this study is to examine the landforms and processes of Upper Sinking Cove, a karst area situated along the southeastern flank of the Cumberland Plateau in south-central Tennessee. The study has four basic objectives:

1. To examine the landforms and the geologic and climatic setting of the study area through fieldwork and a literature review (Chapter II).

2. To analyze the present hydrologic system in the study area, and to interpret paleohydrologic conditions from cave evidence. In Chapter III, past and present characteristics of surface and groundwater flow are examined, and the effect of possible geologic controls assessed.

3. To analyze solutional denudation in the study area. In Chapter IV, spatial and seasonal variations in stream chemistry and soil air CO_2 conditions are interpreted. A denudation rate derived from these findings, together with that determined from direct erosion measurements, is used to relate denudational conditions in Upper Sinking Cove to those in other areas of the world.

4. To model karst landform development in Upper Sinking Cove, using the results of process studies (Chapter V).

Karst Hydrology, Solution Chemistry, and Landforms: A Literature Review

Theories of Karst Hydrology

The nature of water circulation through karst rocks is not well understood. Since carbonates generally have low porosity but high secondary permeability along solutionally widened fractures, karst

groundwater flow is highly localized. In the literature, there has been considerable debate as to whether karst drainage patterns are similar to those in other rocks, and whether Darcy's Law of groundwater flow through porous media can be applied.

Single-Aquifer Theories

In these theories, karst groundwater is considered to be similar to that in other rocks, and a watertable is considered to exist. Groundwater flow below the soil-moisture zone is classified into three hydrologic zones: vadose (above the watertable), intermediate (zone through which the watertable fluctuates), and phreatic (below the watertable).

In an interpretation of the Dinaric Karst early this century, Grund developed a karst hydrologic model in which groundwater moved downward through the vadose zone, laterally toward the sea at a seasonally-fluctuating watertable, and was stagnant in the phreatic zone (Sweeting, 1973).

Davis (1930) also presented a single-aquifer theory, but differed in his emphasis on flow through the phreatic zone, which he believed to follow paths defined by Darcy's Law (Fig. 1.1).

Multiple-Aquifer Theories

As karst groundwater does not generally move through intergranular pores but through fractures and cave passages, speleologists such as Martel (1921) have refuted the application of Darcy's Law to karst hydrologic systems. In some areas, the close proximity of dry and water-filled wells drilled in limestone has been used as evidence that there is no continuous (single-aquifer) watertable in karst.

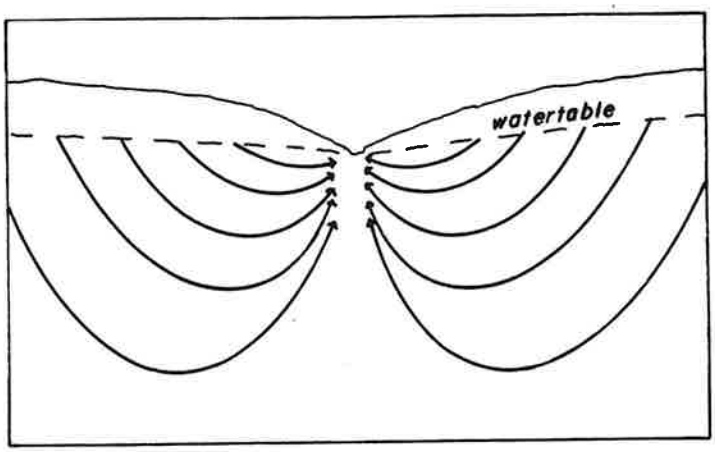

Fig. 1.1. Generalized model of phreatic karst groundwater flow, following Darcy's Law of flow through a porous medium. After Davis (1930).

Instead, a multiple-aquifer system of independent underground channels is considered to exist (Thrailkill, 1968). Stream tracing experiments, such as those of Drew (1966) in the Mendip Hills (U.K.) have shown that drainage channels can cross one another underground.

Compromise Views

Lehmann (1932) presented a compromise to these viewpoints, combining single- and multiple-aquifer theories into an evolutionary model. From an initial surface drainage system, zones of weakness underground are opened up, developing into a mature complex system of independent conduits. An approximation of a watertable is developed at a later stage, as passages are increasingly interconnected.

In the Austrian Calcareous Alps, Zötl (1965) used spore stream tracing experiments to show that underground conduit systems evolve interconnections much earlier in their history than envisaged by Lehmann (1932). Spores were recovered from multiple outlets surrounding plateau-top inputs. Trunk channels are developed, however, since spores injected near these arteries often had single outlets.

Jennings (1971) has argued that differences in local conditions have led to the development of the various bodies of theory surrounding groundwater flow through karst rocks. Considerable differences in local relief, geology, climate, and past conditions have produced a multitude of karst hydrologic types. Since data are lacking from a great many locations with unique conditions, Jennings concludes, "It is clear that a complete body of theory in this subject cannot be expected yet" (p. 97).

Theories of Cavern Development

Theories of cavern development are closely interrelated with those of karst groundwater flow. If a watertable concept is rejected, or if development is said to occur in the vadose zone, excavation occurs not only through corrosion (chemical erosion), but also through corrasion (mechanical erosion) under gravity flow (Fig. 1.2a). Other theories relate cavern development to the two other groundwater zones of single-aquifer theories: deep phreatic (Fig. 1.2b) and intermediate (water-table caves) (Fig. 1.2c). Each of the three groundwater zones has been emphasized over the others by certain authors in the past, but it is generally agreed that caves exhibit features developed in more than one regime (Jennings, 1971).

Passages initiated under deep phreatic conditions (following flow lines defined by Darcy's Law) were noted by Davis (1930). Bretz (1942) expanded upon this work and described cave features indicative of phreatic solution: spongework passages, bedding plane and joint anastomoses, wall and ceiling pockets, joint wall and ceiling cavities, ceiling half tubes, continuous rock spans across cave chambers, and two- or three-dimensional networks or mazes of passages.

Bretz identified entrenched meandering passages as later vadose modifications of caves initially developed in the phreatic zone (Fig. 1.3). Other vadose modifications have been identified, including vertical shafts (Pohl, 1955) and wall scallops (Coleman, 1945).

The input of fresh chemically aggressive water into a karst aquifer is intensified at the watertable. Swinnerton (1932) argued

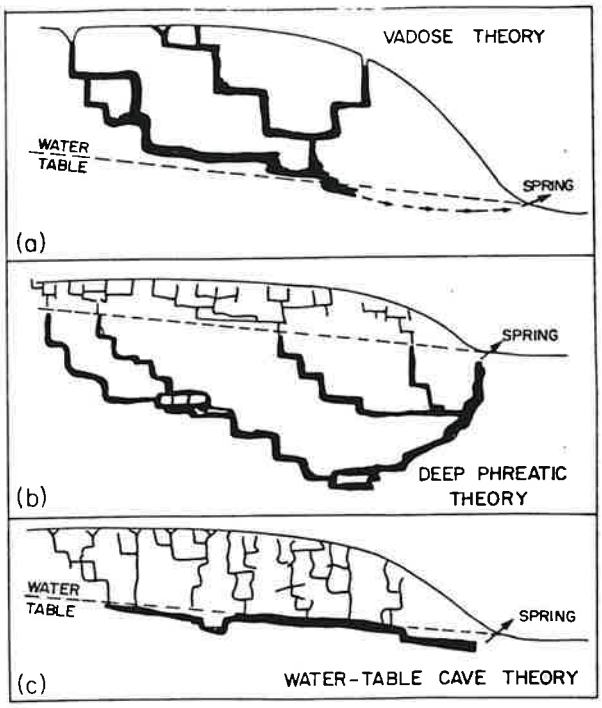

Fig. 1.2. Three general models of cavern development, applying vadose theory, deep phreatic theory, and watertable cave theory. After Ford and Ewers (1978).

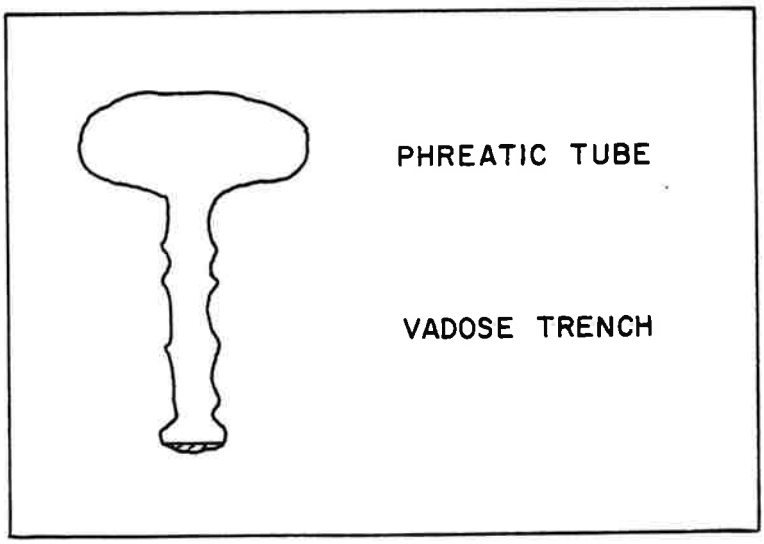

Fig. 1.3. Cave passage cross-section, showing the effect of vadose entrenchment of an original phreatic tube.

from this that most solution occurs at or near the top of the phreatic zone (see Fig. 1.2c). A similar model was presented by Rhoades and Sinacori (1941), though Darcy's Law of deep phreatic flow was applied in initial cavern formation (Fig. 1.4).

Where horizontal passage development predominates in steeply dipping or vertical beds, as in Punchbowl-Signature Caves, N.S.W., Australia (Jennings, 1971), watertable control is clearly indicated.

Ford and Ewers (1978) proposed a model relating cavern genesis to local conditions. Phreatic and watertable caves are end members of a spectrum differentiated by fissure frequency. Where fractures and bedding planes are infrequent, water takes lengthy phreatic loops approximating Darcy flow lines, resulting in deep phreatic ("bathyphreatic") caves. In cases of increasing fissure frequency, the watertable end member is approached (Fig. 1.5).

In Ford and Ewers' model, vadose caves may be developed in, or be independent from, a previously formed phreatic skeleton. Two types of vadose caves are proposed. A drawdown vadose cave is formed in phreatic tubes following lowering of the piezometric surface as lower networks are enlarged. An invasion vadose cave (from Malott, 1937) results from the presence of impervious materials located adjacent to, or overlapping, the limestone, to which aggressive water is directed (Fig. 1.6).

To summarize, features of cave passages have been used to interpret past groundwater flow conditions. Cave passages have been shown to indicate paleoflow above a watertable (essentially the same as predicted by multiple-aquifer theories), at a watertable, or deep in the phreatic

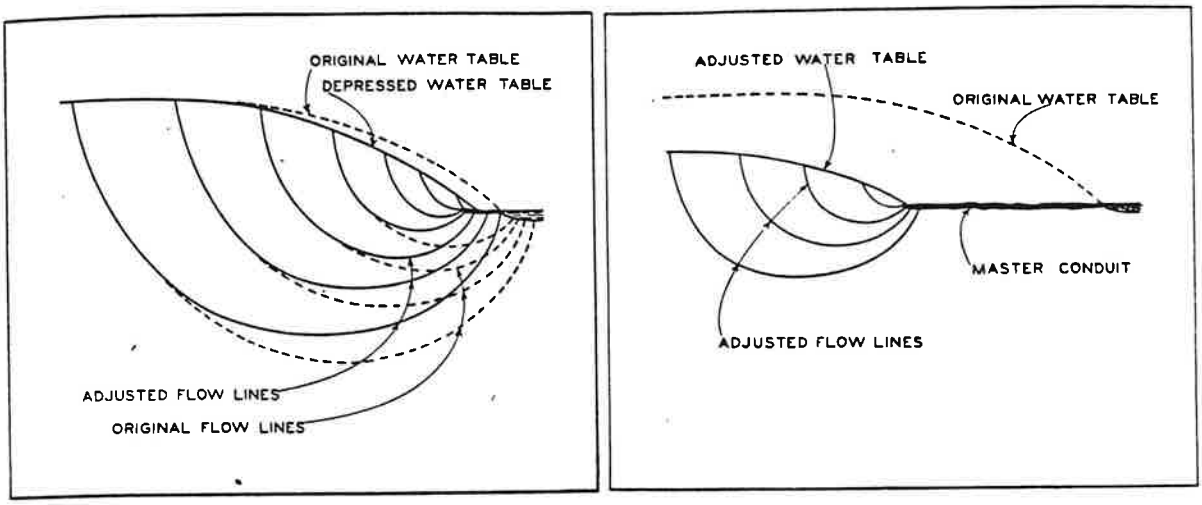

Fig. 1.4. The Rhoades and Sinacori model of cavern development, in which flow lines and the watertable are adjusted as a master conduit cave is enlarged. After Rhoades and Sinacori (1941).

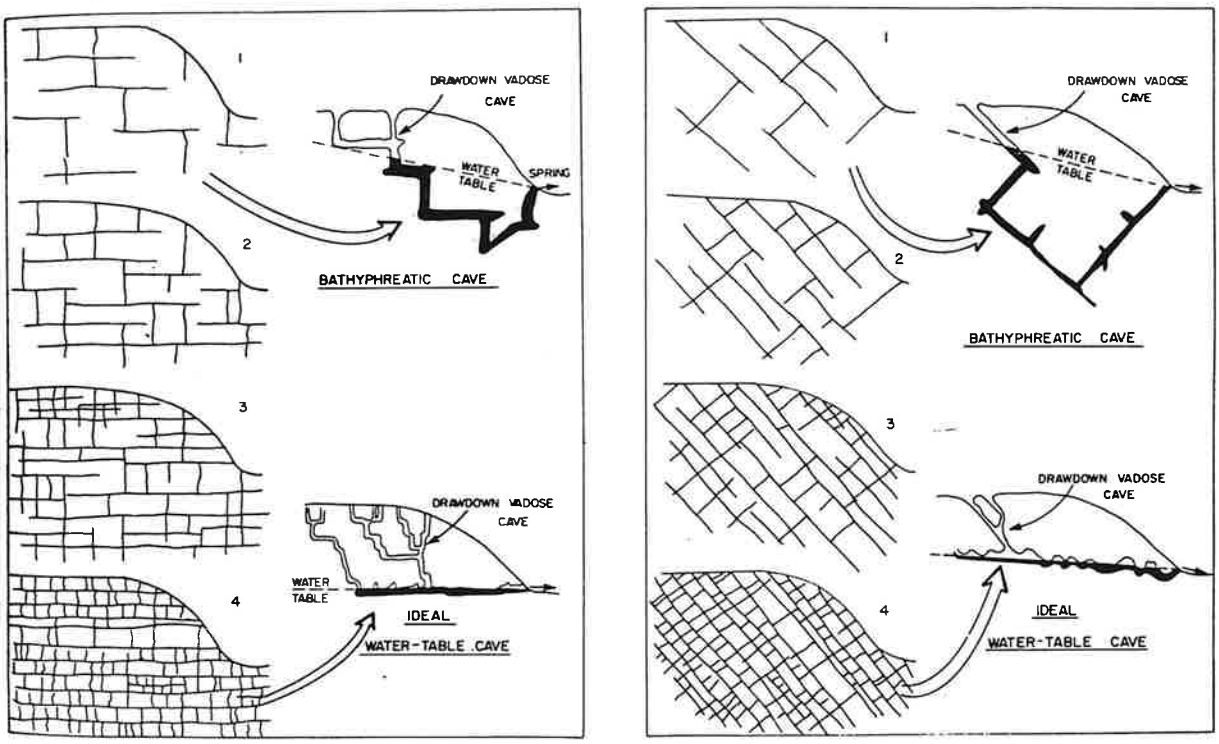

Fig. 1.5. Deep phreatic and watertable caves as endmembers of the Ford and Ewers model, in which geologic structure (fissure frequency and local dip) controls the development of specific cavern morphologies. After Ford and Ewers (1978).

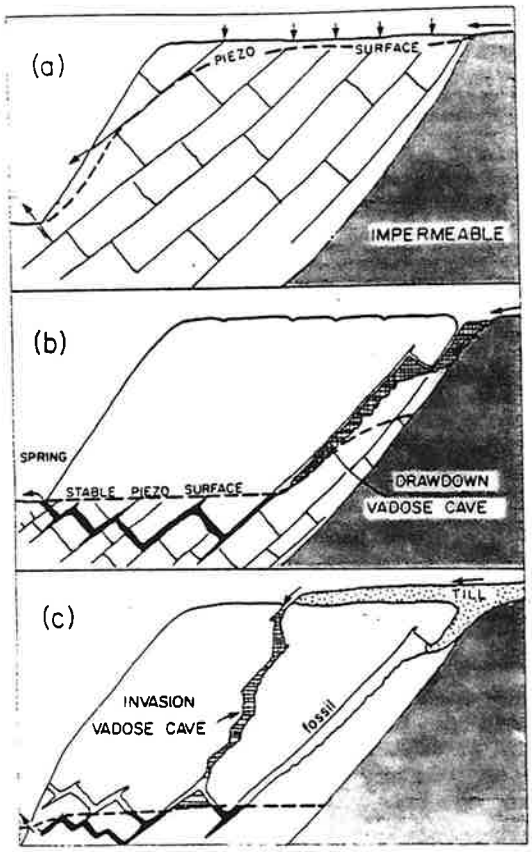

Fig. 1.6. The development of two distinct types of vadose caves from an initial exposed limestone surface (a). A drawdown vadose cave (b) results from the presence of low-level phreatic passages which lower the piezometric surface. Introduction of a surface cover (e.g., glacial till) results in the development of an invasion vadose cave (c), as aggressive water is directed into previously-excavated phreatic passages. After Ford and Ewers (1978).

zone. One objective of this research is to use cave evidence to interpret the paleohydrologic conditions of the study area.

The Solution Process in Karst Environments

The dissolution of limestone takes place in a system of chemical compounds of the type CO_2-H_2O-$(Ca,Mg)CO_3$. Chemical and physical processes occur at the interfaces of solid, liquid, and gaseous components of the system (Bogli, 1980):

1. CO_2 present in overlying air is physically diffused in water bodies.

2. Subsequent hydration of the CO_2 results in the production of carbonic acid, dependent upon the temperature of the water:

$$CO_2 + H_2O = H_2CO_3$$

3. The carbonic acid is dissociated into bicarbonate and hydrogen ions (first oxidation level):

$$H_2CO_3 = HCO^-_3 + H^+$$

4. Water in contact with carbonate rock allows ionization of carbonate minerals, in a physical process involving destruction of the crystal lattice:

$$CaCO_3 = Ca^{2+} + CO^{2-}_3$$

5. The carbonate ions produced may then combine with hydrogen ions from the dissociation of carbonic acid, forming bicarbonate ions:

$$CO^{2-}_3 + H^+ = HCO^-_3$$

6. Chemical equilibria are disturbed:

a. between the activities of Ca^{2+} and CO^{2-}_3 (equation 4), resulting in renewed dissolution of $CaCO_3$

b. between carbonic acid and its first oxidation product (equation 3), resulting in renewed hydration of CO_2 and thus increased diffusion from the air.

An equation combining these reactions may be written:

$$CaCO_3 + CO_2 + H_2O = Ca^{2+} + 2HCO_3^-$$

The total amount of limestone which can be dissolved is thus highly dependent upon the availability of CO_2. According to Henry's Law, the solubility of CO_2 is in direct proportion to CO_2 partial pressure. Atmospheric carbon dioxide partial pressures, typically on the order of 0.03%, are insufficient for the production of significant amounts of carbonic acid. Soil air, however, may have a higher percentage of CO_2 and is therefore an important factor in the solution of limestone in water (Adams and Swinnerton, 1932). Carbon dioxide is produced in soils by a combination of decay of organic matter and root respiration (Douglas, 1968), producing CO_2 partial pressures (PCO_2) of 1-2%, or greater.

Diffusion of CO_2 is only possible in an open system where the water is continually exposed to air. If water becomes isolated from air (closed system), only the previously diffused CO_2 will be available for carbonic acid production, thus allowing an attainment of equilibrium with limestone dissolution. A theoretical PCO_2 is maintained in equilibrium with the dissolved CO_2.

Assuming equilibrium is reached, renewed exposure to air with a different PCO_2 produces a condition of disequilibrium which must be balanced by CO_2 diffusion in the direction of lower PCO_2. If CO_2 is diffused out of the water in sufficient amounts, precipitation of calcite will result. This is often the case in caves, where saturated

percolation waters release CO_2 upon exposure to low-PCO_2 cave air, and calcite is precipitated in the form of stalactites, stalagmites, and flowstone.

If waters are undersaturated with calcite, continued limestone dissolution is possible, and the water is referred to as 'aggressive.'

Hydrologic conditions may be important in controlling the solution process. The rate of aggressive water supply will govern the solution of exposed limestone. Water of a given chemistry will dissolve more limestone, in a given time, if supplied at a faster rate, since solution rates are most rapid during the first second of limestone-water contact (Douglas, 1968). On the other hand, a given volume of water might dissolve less total limestone if the amount of rock-contact time (residence time) is insufficient for saturation to be reached.

Seasonality is an important factor governing the CO_2 component of the chemical system. Carbon dioxide solubilities, for instance, are inversely related to water temperature (Corbel, 1959). This tendency, however, is overshadowed by seasonal cycles of biogenic soil CO_2 production, considered to be at a peak during the summer months (Smith, 1965).

A given sample of water may be characterized by its chemistry. Field measurements of water temperature, pH, and alkalinity may be combined with titrated total and calcium hardness values to describe a sample. From these measured quantities other variables may be derived (Chapter IV), including theoretical values of equilibrium PCO_2, and saturation indices with respect to calcite (SI_C), dolomite (SI_D), and gypsum (SI_G).

Seasonal variations in temperature, pH, hardness, HCO_3^- concentration (assumed identical to alkalinity), and saturation indices were used by Shuster and White (1971) to differentiate groundwater flow systems above sampled springs. Two endmember types of flow systems were proposed: (1) diffuse flow along small (less than one centimeter) interconnected openings in bedrock, and (2) conduit flow of often turbulent water through larger solution passages. Diffuse flow springs were found to exhibit constant hardness values year-round and were near saturation. Conduit flow springs were more variable in hardness, this reaching a minimum during high-flow periods, and were generally undersaturated. PCO_2 was considered to be representative of the source area of recharge.

Global Models of Karst Landform Systems and Karst Denudation

Interpretations of karst landform assemblages in various areas of the world have led to the development of explanatory models for karst systems. The earliest attempts at modelling karst landform development were in the early 1900's. They were proposed by researchers studying the Classical Karst of Yugoslavia, and were evolutionary models in which one form of karst developed from an earlier one. An unkarstified surface might thus evolve into a mature karst via a series of stages from the initial surface through (i) a doline karst, with partially-developed underground drainage, (ii) a uvala and polje karst, with laterally extended depressions, to, (iii) a cone karst, in which essentially all drainage was underground (Lehmann, 1960).

Apparent differences between assemblages observed in humid tropical areas (e.g., cockpit and tower karsts) and temperate and arid

areas (e.g., mid-latitude doline karsts) led, in the 1930's and 1940's, to models emphasizing climate as the controlling factor in karst landform development.

Hydrochemical evidence has often been applied in support of morphoclimatic models. Corbel (1959) used the inverse relationship between solubility of CO_2 in water and temperature of the water to predict that chemical erosion rates of limestone would be greater in colder climates. He made broad use of denudation rates derived from spot water chemical samples and runoff estimates to support his model. Denudation was calculated using the formula:

$$X = \frac{4ETn}{100}$$

where

X = erosion rate ($m^3/km^3/yr$, or mm/1000 yr)

E = runoff (dm)

T = concentration of dissolved $CaCO_3$ (mg/L)

1/n = proportion of basin underlain by limestone.

This was later modified by Douglas (1964), to:

$$X = \frac{TQ}{AD}$$

where T and X are the same as above, and

Q = discharge (m^3/yr)

A = drainage area (km^2)

D = density of rocks in drainage area (g/cm^3)

Later workers felt that Corbel's work was based on insufficient sampling, and that denudation rates derived from this type of analysis were not representative of true erosional environments. Positive

relationships between water temperature and (i) total hardness, (ii) saturation with respect to calcite, (iii) bicarbonate ion concentration, and (iv) PCO_2 for sites in North America (Harmon et al., 1975; Drake and Wigley, 1975; Drake, 1980) suggested that temperature was the major factor controlling erosion rates (per unit volume of runoff) in karst areas. By avoiding the impact of runoff, their results differed greatly from those of Corbel; specific erosion rates were shown to be greater in warmer areas. This they attributed to the impact of greater biogenic CO_2 production in warm humid areas.

A limitation to the use of temperature as a predictor of PCO_2 in soils and groundwater is the lack of consideration of precipitation. Biogenic CO_2 production is dependent upon total biologic activity, and thus must be less in drier climates. A more meaningful predictor of PCO_2 appears to be actual evapotranspiration (AET), which responds to the availability of both energy and moisture (Brook et al., in press).

Criticism of the use of simple climatic models was presented during the 1960's by workers who felt that the impact of geologic structure had been largely overlooked. Douglas (1968) and others, noting the great diversity among forms in similar climatic situations, argued that geologic factors such as the relative solubility, porosity, and fracture characteristics of the bedrock in karst areas must be considered.

The use of multiple factors in the interpretation of a given area's karst assemblage was presented as a whole systems approach by Marker (1980). She listed five overall factors leading to the production of a karst system: geology (including cover, lithology,

structure, and thickness), tectonics (including local relief, planation levels, and fractures), hydrology (including location of a saturated zone, and flow rates), climate (precipitation and temperature), and biotic CO_2 environment (vegetation cover and growth period). These relate to two features of a karst system: a suitable parent rock and an active solution process. The production of any given karst landform assemblage would be influenced by two additional factors: time (incorporating the age of the rock, the amount of time it was exposed, and the impact of past events) and the ratio of non-karstic surface processes. This approach, while avoiding specific explanations for individual karst assemblages, provides a means of systematically describing the factors involved in their production, thus enabling comparisons to be made among karst areas of the world.

Rethinking of previous concepts of karst landform evolution has resulted largely from the discovery and exploration of unique karst areas throughout the world. Anomalies exist which do not conform to classifical climatic classification schemes. The Nahanni Karst, N.W. Territories, Canada (61°-62°N latitude), for example, contains features previously considered tropical in nature, including karst towers (Brook and Ford, 1978).

The need for continued exploration and study of karst areas throughout the world is clearly necessary before any reliable explanatory model of karst morphogenesis can be expected. Regional studies of individual karst areas, with analysis of the interactions among the various processes active in producing a given karst system, are needed to complete the picture.

This study will provide data from a karst area of the Cumberland Plateau in Tennessee.

CHAPTER II

THE STUDY AREA: UPPER SINKING COVE, FRANKLIN COUNTY, TENNESSEE

The Cumberland Plateau is a broad (up to 40 km wide) upland surface extending northeast to southwest through east-central Tennessee (Fig. 2.1). In the southern half of the state, the plateau rises to elevations of 500-700 m. To the north the plateau grades into the Cumberland Mountains which extend into Kentucky.

The general stratigraphy of the plateau consists of a caprock of predominantly flat-lying Pennsylvanian conglomerates, sandstones, and shales, underlain by 200-400 m of Mississippian carbonates, with interbedded sandstones and shales. Resistant beds of cherty and sandy limestones occur below this sequence, and produce a lower plateau surface, the Highland Rim, which borders the Cumberland Plateau on its northwestern escarpment.

Along the margins of the plateau, valley incision has produced steep-walled, flat-floored valleys called "coves," which extend headward into the plateau as narrow canyons. Dry and blind valleys are common because surface streams typically sink soon after leaving the plateau surface. Large springs occur on resistant beds at the base of the escarpment. Stream caves, which connect sinks and springs, are also common.

This study deals with an area at the head of one of the blind valleys, Sinking Cove, which indents the southeastern escarpment of the

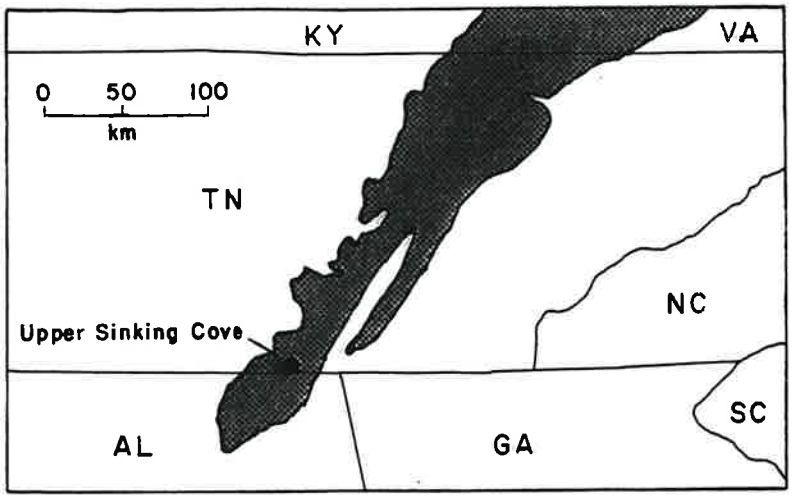

Fig. 2.1. Extent of the Cumberland Plateau in Tennessee and northern Alabama and the location of Upper Sinking Cove.

plateau in south-central Tennessee (Fig. 2.2). Upper Sinking Cove (35°03'N, 86°01'W) is typical of the headward canyon segments of these valleys, in that it contains large depressions and associated cave systems.

Previous Research on the Cumberland Plateau

In 1894, Hayes and Campbell suggested that the upper surface of the Cumberland Plateau had developed by erosion during the Cretaceous period. They argued that, following a period of uplift, renewed planation during the Tertiary resulted in the development of the lower Highland Rim surface. Hack (1966) disputed this interpretation suggesting that the horizontal surfaces were not the result of peneplanation processes, but instead reflected structural controls, particularly the presence of relatively resistant, flat-lying beds of rock. Hack argued that parallel slope retreat occurred because of sapping in soluble beds and collapse of overlying sandstone and conglomerate beds which form the resistant caprock for the plateau.

Crawford (1978) has outlined a model for the Cumberland Plateau escarpment which relates caprock removal by slope retreat to conduit cavern development. In this model, canyon advancement into the plateau is preceded by subterranean stream invasion of surface drainage originating on the caprock. This normally occurs near the contact between caprock and limestone where streams flow down the escarpment. If a structural high exists behind the escarpment, limestone is exposed and invasion occurs at this point. Crawford refers to the resulting depressions as solution valleys.

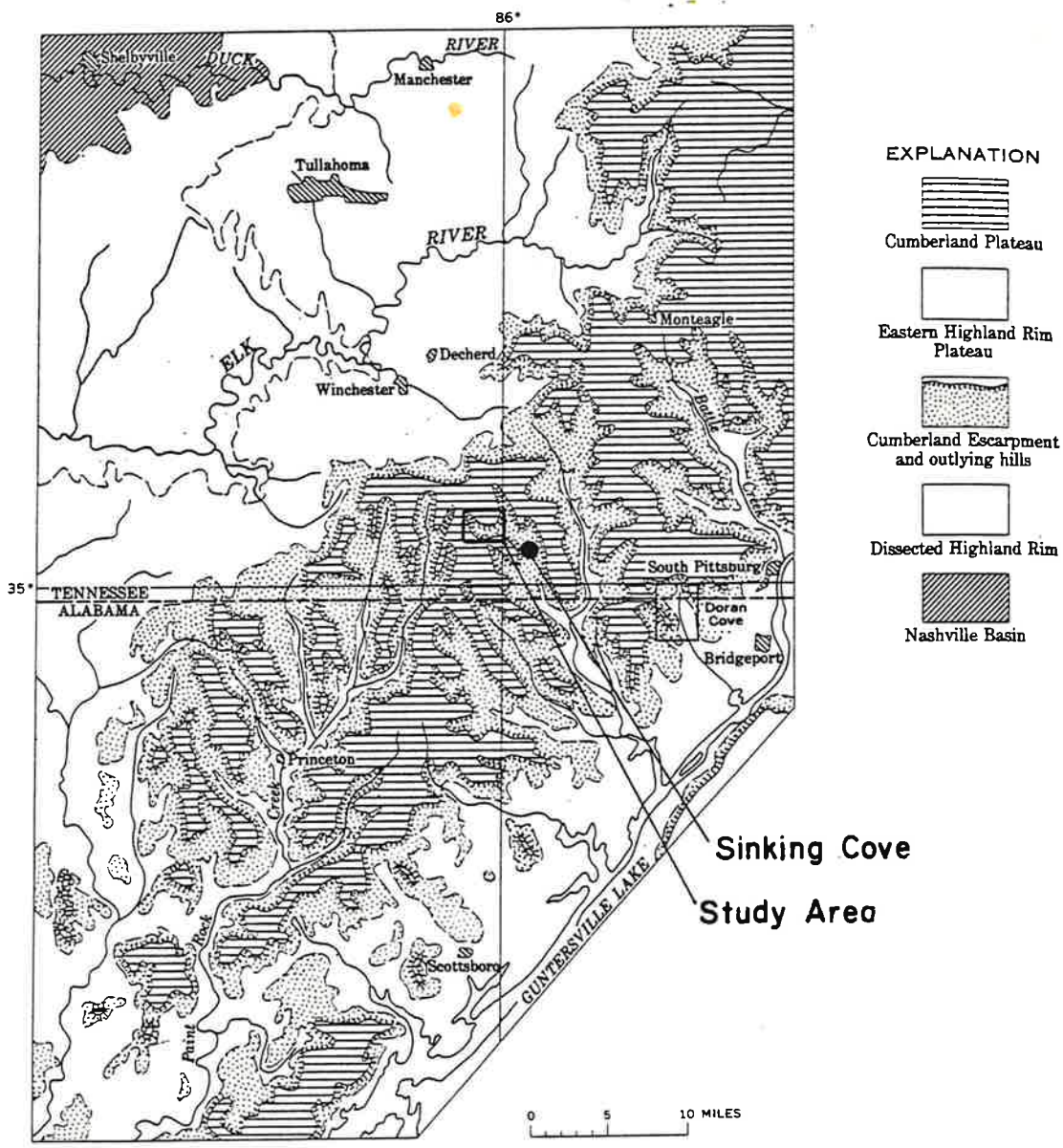

Fig. 2.2 Location of the study area, with respect to the southern Cumberland Plateau in Tennessee and northern Alabama. Modified after Hack (1966).

The process of invasion in Crawford's model is initiated when aggressive stream water from the caprock flows through joints and bedding planes to a spring at the base of the escarpment. Conduit caverns continue to enlarge, primarily as a result of input of aggressive water from the caprock, entering the caves at swallets. This enlargement is considered to be greatest during floods, when both corrosion and corrasion are intensified.

According to Crawford, diffuse percolation input does not play a major role in cavern enlargement since it supersaturates with respect to calcium carbonate upon loss of CO_2 to cave air, but is important in dissolving limestone at the regolith/bedrock interface.

Crawford contends that cavern development is influenced most by geologic factors including dip, lithology, and joint orientation. Although dip of strata controls the general direction of groundwater flow, cave passages generally develop along joints. Crawford has determined that resistant beds produce local base levels for cavern development but do not produce perched watertables. Solution at or below a watertable is not, therefore, considered an important factor in cave development. Crawford suggests that most caves are of the vadose conduit variety.

In his 1978 dissertation, Crawford introduces Upper Sinking Cove as an example of caprock retreat and conduit cavern development in the southern portion of the Cumberland Plateau escarpment. He states that the presence of a thinner Pennsylvanian caprock in this area resulted in a process of stream invasion somewhat different to that proposed for areas to the north. Instead of developing by headward advance into the plateau, the drainage system in Upper Sinking Cove is

considered to have evolved as a result of downward erosion of a stream on the caprock. Subterranean stream invasion is thought to have occurred behind the escarpment due to local thickening of the uppermost major limestone unit, the Bangor Limestone. As surface stream valleys were deepened, these relatively nonresistant limestones were exposed upvalley from the escarpment. Subterranean stream invasion then led to the development of depressions, or solution valleys in the plateau.

Apart from the work of Crawford (1978) most published accounts of Upper Sinking Cove relate to the discovery and exploration of caves (Bloxsom, 1955; Johnson, 1978; Smith, 1978). T. C. Barr visited the area, while compiling data for Caves of Tennessee (1961) and referred to the system of depressions as "illustrative of the manner in which coves may extend headward into the Plateau by underground solution and karst development."

The Climate and Geology of Upper Sinking Cove

Climate

The study area has a humid subtropical climate, with an average annual temperature of 13.8°C. The coldest and warmest months are January and July, with mean monthly temperatures of 3.1°C and 23.7°C, respectively.

Precipitation is primarily in the form of rainfall, though snowfall may be significant in winter. Because of orographic effects, the mean annual total, 1550 mm, is 11% higher than that of nearby lowlands. Though fairly well distributed throughout the year, a maximum occurs in winter. During the peak month, March, 167 mm of precipitation is received, and annual floods often occur. Heavy convectional

thunderstorms are common in summer. October is the driest month with 80 mm rainfall.

Geology

Ferguson and Stearns (1968) describe the stratigraphy of the Pitcher Ridge 7 1/2' Quadrangle, which includes most of the study area, to consist of sedimentary sequences of Mississippian to Pennsylvanian age. The nine stratigraphic units identified in the area are summarized in Table 2.1.

According to the geologic map of this quadrangle, the canyon and depressions, which comprise the study area, are surrounded by a plateau rim underlain by Pennsylvanian beds: the Warren Point Sandstone and Raccoon Mountain Formation. The canyon slopes and the depressions are developed in Mississippian beds: the Pennington Formation, Bangor Limestone, Hartselle Formation, and Monteagle Limestone. Underlying the alluvial floor of Sinking Cove, which begins at the lower eastern end of the study area, is the St. Louis Limestone.

Because of the possibility that geologic factors were important in controlling the morphologies and locations of caves and coves in the study area, additional structural and stratigraphic data were obtained by undertaking field investigations. Rock samples were collected at suitable surface and underground (cave) sites. Particular attention was given to geologic members which might act as aquitards, or be relatively resistant to solution. Samples were analyzed in hand specimen, and selected samples in thin section (by Ken Davis, Department of Geology, University of Georgia).

Table 2.1 Stratigraphy of Pitcher Ridge Quadrangle, Tennessee, after Ferguson and Stearns (1968)

Pennsylvanian Sequences (youngest at top):

Sewanee Conglomerate (Ps): conglomerate and sandstone
maximum thickness on quadrangle: 20 feet (6.1 m)

Warren Point Sandstone (Pwp): sandstone
thickness: 70-160 feet (21.3-48.8 m)

Raccoon Mountain Formation (Pra): siltstone and shale (upper); sandstone (lower)
thickness: 10-80 feet (3.0-24.4 m)

Mississippian Sequences (youngest at top):

Pennington Formation (Mp): shale, interbedded with limestone (upper two-thirds); silty dolomite or dolomitic limestone (lower one-third). Dolomitic limestone and dolomitic siltstone interbedded throughout formation.
thickness: 260-380 feet (79.2-115.8 m)

Bangor Limestone (Mb): limestone and dolomitic limestone, partings and thin zones of shale
thickness: 120-260 feet (36.6-79.2 m)

Hartselle Formation (Mh): shale (locally at top); limestone; sandstone (locally at base)
thickness: 0-40 feet (0-12.2 m)

Monteagle Limestone (Mm): limestone, many beds oolitic, thin chert beds; near base is Lost River Chert, grading into limestone. Partings and thin zones of shale.
thickness: 160-280 feet (48.8-85.3 m)

St. Louis Limestone (Msl): dolomitic limestone with chert, interbedded with limestone and dolomite
thickness: 100 feet (30.5 m)

Warsaw Limestone (Mw): limestone, interbedded with dolomitic limestone
maximum thickness on quadrangle: 50 feet (15 m)

Three important shale aquitards were identified in the area (Fig. 2.3). Two of these aquitards are approximately two metres thick, one at 382 m a.s.l. in the upper Bangor Limestone, and the other at 320 m a.s.l. in the Monteagle Limestone. The third aquitard was located in the Hartselle Formation. This was found to contain 14 metres of silty shales, at 344-358 m a.s.l.

Selected joints were examined in an attempt to determine if they had exerted any influence on the character of surface landforms and caves. Orientations were measured where joints were observed in caves or in surface stream beds. Orientation peaks suggest the presence of two joint sets (Fig. 2.4). Twelve joints had a mean orientation of 295.4°, closely clustered (standard deviation = 5.6°). Fifteen joints had greater dispersion (standard deviation = 12.3°), and a mean of 36.2°.

Landforms of Upper Sinking Cove

Upper Sinking Cove consists of a 2.5 km long, 1.0-1.5 km wide canyon in the floor of which are three large depressions, called coves (Fig. 2.5 and 2.6). Cave Cove, at the head of the canyon, and Farmer Cove, approximately one kilometre downvalley, lie at 390 m and 360 m a.s.l., respectively, and are developed in the Bangor Limestone. Downvalley from these and immediately upvalley from Sinking Cove is a third depression, Wolf Cove, at 295 m a.s.l. in the Monteagle Limestone. The canyon walls above these depressions are in the Bangor Limestone and the Pennington Formation.

Within these depressions, and on canyon slopes, are dry, blind, and pocket valleys, dolines, and numerous caves. Some of these caves

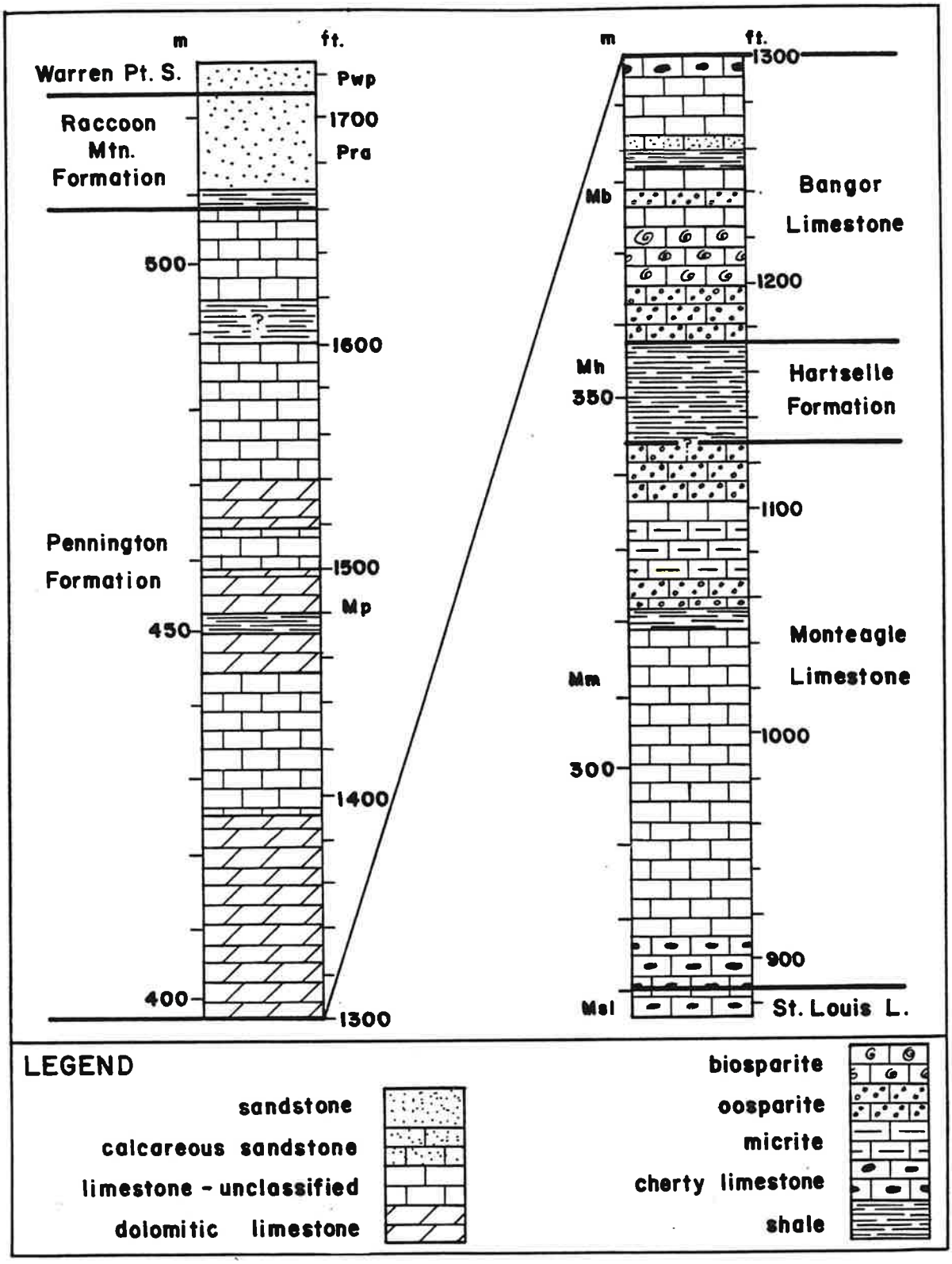

Fig. 2.3. Stratigraphy of Upper Sinking Cove.

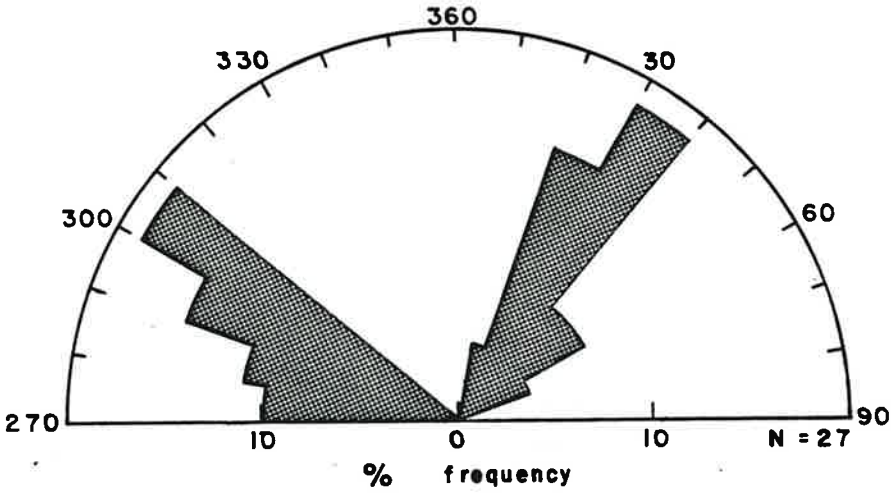

Fig. 2.4. Distribution of field-measured joint orientations, grouped in 10° classes.

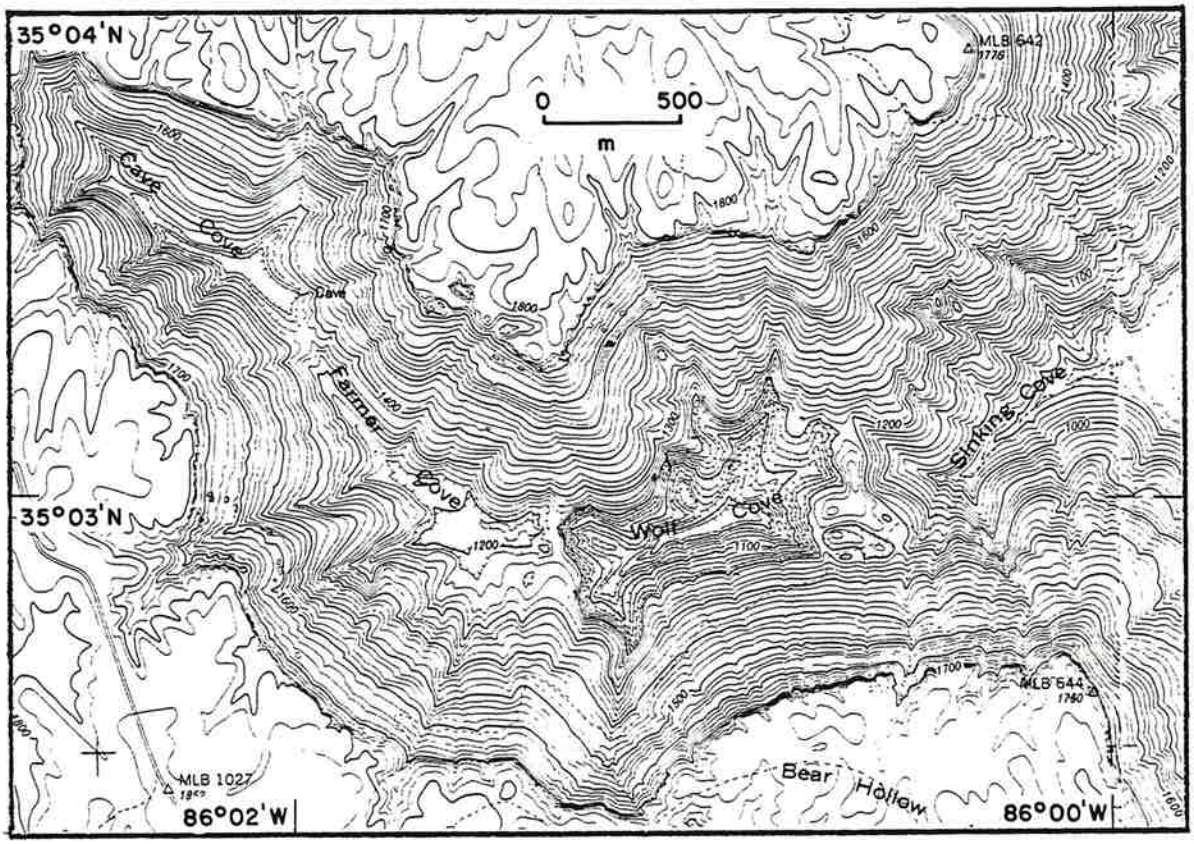

Fig. 2.5. The study area: Upper Sinking Cove, Franklin County, Tennessee.

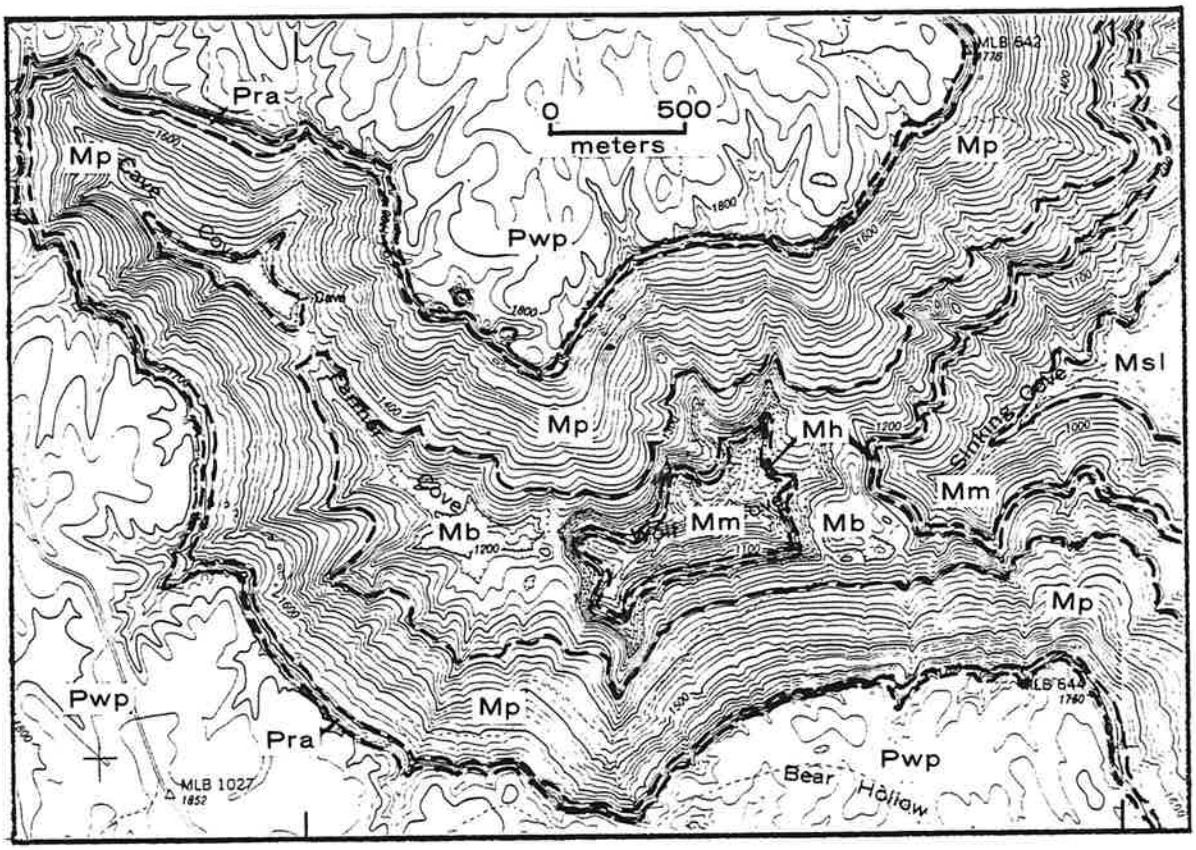

Fig. 2.6. Geology and topography of the study area. See Fig. 2.3 for stratigraphy.

function as drainage conduits for dry valleys; some connect blind and pocket valleys.

Before undertaking hydrologic and solution process research in the study area, detailed field study of the surface and underground landforms was made. Seventeen caves were already known in the area (Tennessee Cave Survey, 1980). A further seventeen caves were discovered during the course of the research. All caves now known in the area are listed in Table 2.2; locations are shown in Fig. 2.7.

The landforms are described in the following sections. Distinction is made between features in the coves themselves and features in the canyon walls above the coves. This separation is necessary for two reasons: (1) similarities in form and function exist among canyon wall features at given elevations, and among depression features in analogous locations; (2) canyon wall features may not be hydrologically related to the depressions immediately downslope.

The Coves

Cave Cove

Cave Cove is the uppermost of the three depressions; it lies at an elevation of 390 m (1280') a.s.l. (Fig. 2.8). On the basis of the highest contour that encloses it, Cave Cove is 792 m in length and 66-250 m in width. It extends, northwest to southeast, from its head to a 20 m-high saddle separating it from Farmer Cove.

The cove is composed of two blind valleys, the lowermost of which is normally dry. Surface flow is perennial from the northwest to a major streamsink in a collapse doline at the Pennington/Bangor contact (Figs. 2.9, 2.10, 2.11). The entrance to Exercise Cave (Fig. 2.12) was

Table 2.2. Caves in Upper Sinking Cove, Franklin Co., Tenn.

No.	Name	TCS[1]#	elev (m)	length[2] (m)	depth (m)	Formation
1	Racoon Bluff Cove	*	518	15	6	Mp
2	Still Cave	*	518	40	5	Mp
3	Sandstone Jumble	*	494	36	10	Mp
4	Little Dome	*	482	8	9	Mp
5	Lower Pennington Cave	*	433	60+	3+	Mp
6	Forgotten Cave	*	420	90+	3+	Mp
7	Cold Day in Well	FR181	405	**	15	Mb
8	Green Barrel Pit	FR182	393	15	15	Mb
9	Cold as a Witch's Pit	FR183	390	**	10	Mb
10	Jet Pit	FR189	393	**	12	Mb
11	Spray Well	*	415	40	17	Mb
12	Shower Cave	*	415	263+	30+	Mb
13	Blowhole Pit	*	427	15	13	Mp-Mb
14	Exercise Cave	*	415	60+	9+	Mb
C1	Cave Cove Cave	FR 33	400	2010+		Mb
C2	McFadden Entrance #1		415			Mb
C3	McFadden Entrance #2		415			Mb
15	Suicide Cellar Cave	FR173	384	107	12	Mb
16	Farmer Cove Cave	FR 10	360	(150)	6	Mb
17	Wolf Cove Cave	FR 58	400	672+	37+	Mb
18	Waterfall Cave	FR 29	360	580	24	Mb
19	C Cave	FR 54	365	25	3	Mb
20	D Cave	FR 55	347	30	**	Mm
21	(unnamed cave)	*	390	(30)	**	Mb
22	Helen Highwater Cave	*	320	(30)	3	Mm
23	Spider Tunnels Cave	*	315	(50)	3	Mm
24	Bill's Cave	*	315	(30)	3	Mm
25	Mary's Cave	*	310	(30)	3	Mm
26	Upper Sinking Cove Cave	FR 57	310	198	6	Mm
27	Marshall Cave	*	305	(20)	2	Mm
28	Raccoon Raceway Cave	FR208	310	(100)	(5)	Mm
29	Xylophone Cave	FR 56	341	73	3	Mm
30	Thorn Cave	*	300	60	12	Mm
S1	Sinking Cove Cave	FR 25	265	6435	137	Mb-Mm
S2	relict entrance		260			Mm
S3	pit entrance		266			Mm
S4	Wolf Cove entrance		320			Mm
S5	Boulder entrance		402			Mb
31	Ashlee Cave	FR174	293	152	**	Mm
32	Big Entrance Small Cave	FR180	335	15	9	Mm

[1]Tennessee Cave Survey, 1980.

[2]Figures in parentheses are approximate.

*Designates caves not registered with the TCS.

**Designates insignificant horizontal or vertical extent.

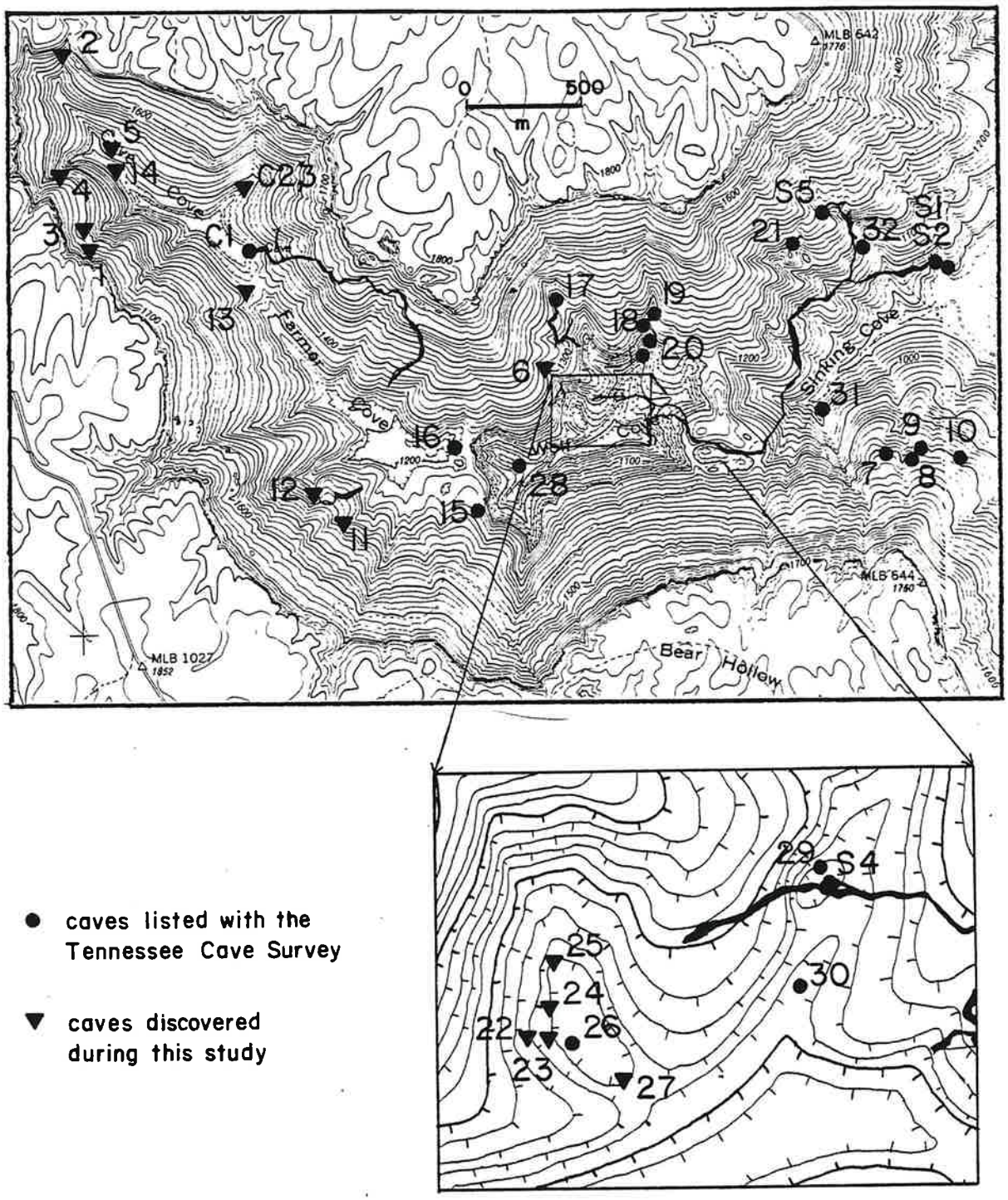

● caves listed with the Tennessee Cave Survey

▼ caves discovered during this study

Fig. 2.7. Caves of Upper Sinking Cove. See Table 2.2 for names and data.

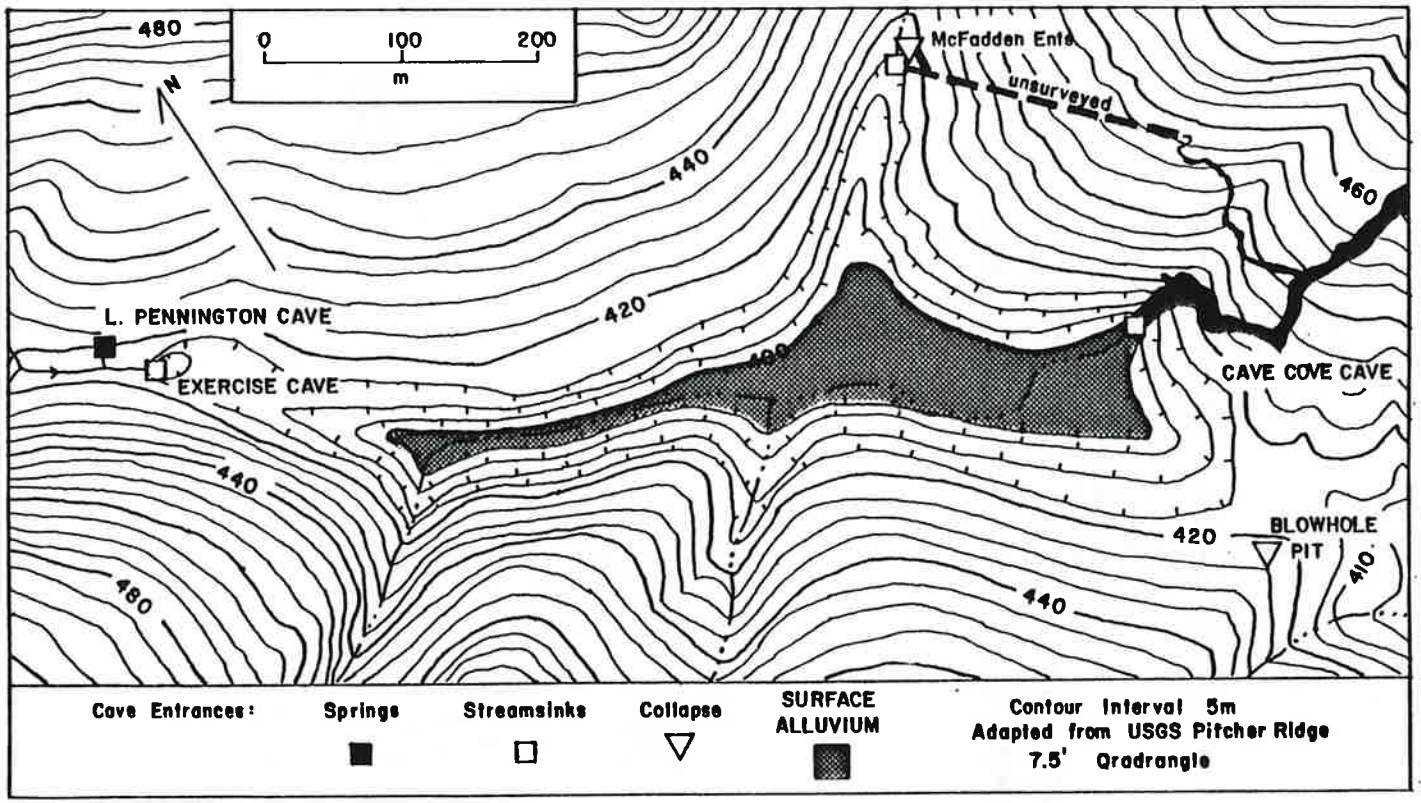

Fig. 2.8. Topography and hydrological characteristics of Cave Cove.

Fig. 2.9. Cave Cove Creek, just above Cave Cove Sink.

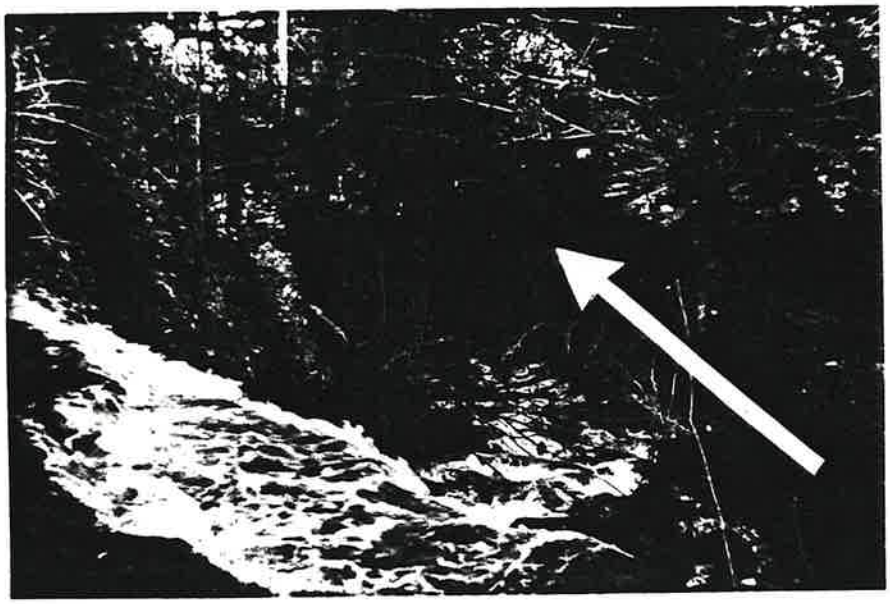

Fig. 2.10. Cave Cove Creek plunging into Cave Cove Sink, a collapse doline. Final sink during high flow conditions (arrow) is at the base of the northern wall of the depression.

Fig. 2.11. The doline at Cave Cove Sink. Cave Cove Creek plunges into the doline at the upper left. The entrance to Exercise Cave (#15) is in an overflow swallet in the foreground.

Fig. 2.12. The entrance to Exercise Cave, Cave Cove.

discovered in the walls of this doline; part of the cave extends to a point directly beneath the stream input into the depression at its northwestern edge (Fig. 2.13). Large volumes of breakdown make up the inner wall of the cave, adjacent to the doline. Exploration through the breakdown to 20 metres below the surface has shown that vertical cavern development has been an important factor at this streamsink.

For a distance of 180 m downvalley from this doline, there is no surface stream channel in the floor of Cave Cove. A channel, which is normally dry, enters the depression from the southwest after this distance, then meanders through 0.8 m of alluvium across the floor of the cove for 550 m to the entrance of Cave Cove Cave, just beneath the terminal saddle of the cove. Bed materials in the stream channel are composed primarily of sandstone, with cobbles up to 30 cm in diameter (Fig. 2.14).

More than two kilometres of passages have been mapped in Cave Cove Cave (see Map 1). Developed in the Bangor Limestone, cave passages extend from Cave Cove and pass beneath the north wall of Farmer Cove (see Fig. 2.18). Three entrances are known to the cave, all in Cave Cove. One of these, at the downvalley end of the cove, (Fig. 2.15) leads into a 5-7 m high by 10-20 m wide passage, which carries intermittent streamflow. The other entrances (McFadden Entrances: #C2 & C3) are 10 m vertical shafts, at the Pennington/Bangor contact, located at a streamsink in a northern tributary valley of Cave Cove. A small, active stream passage, Hanson's Lost Creek, leads from the base of these shafts for 500 m to an intersection with the much larger passage, described above.

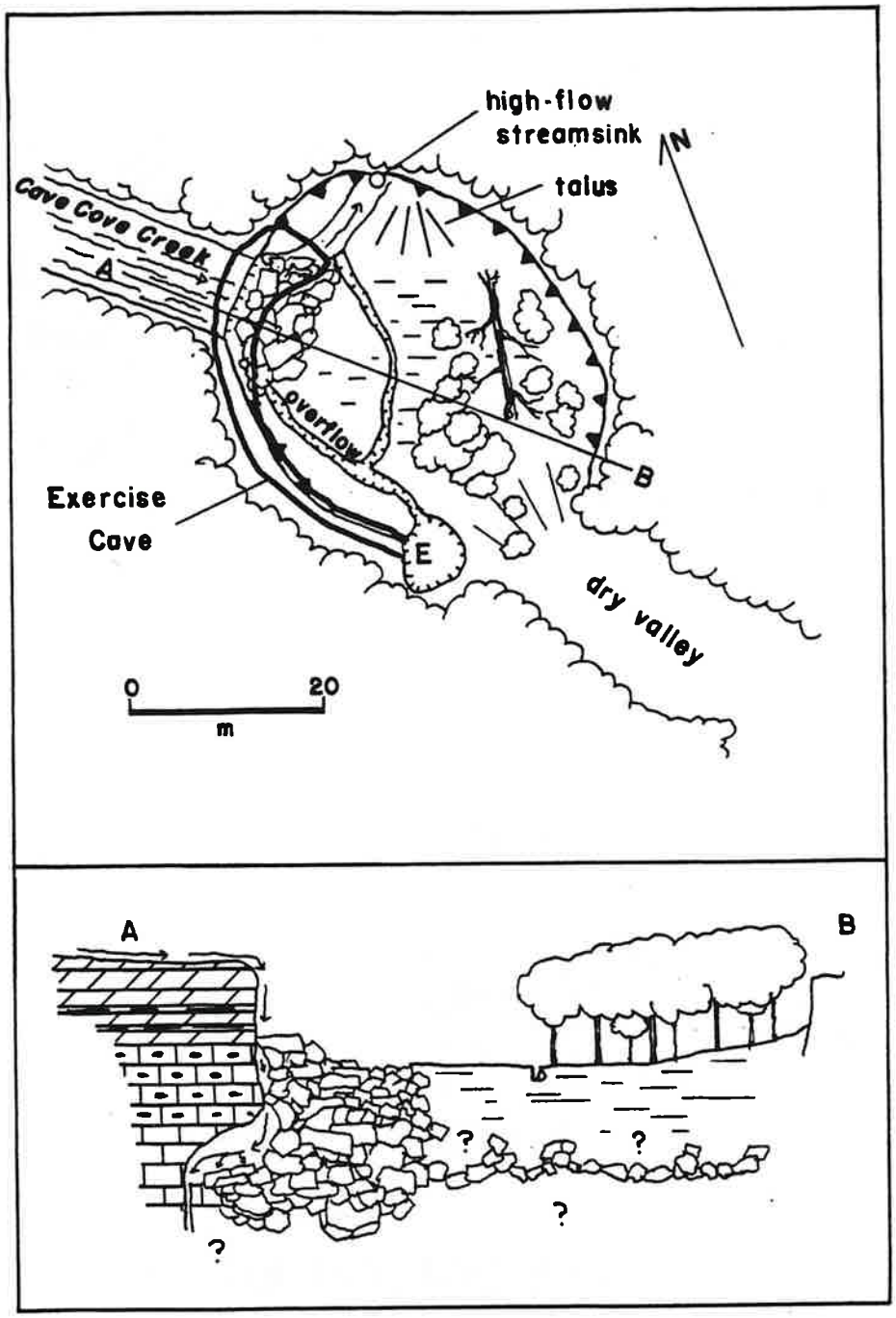

Fig. 2.13. Plan and profile of the doline at Cave Cove Sink and Exercise Cave.

Fig. 2.14. A dry streambed cut in alluvium, in the floor of Cave Cove.

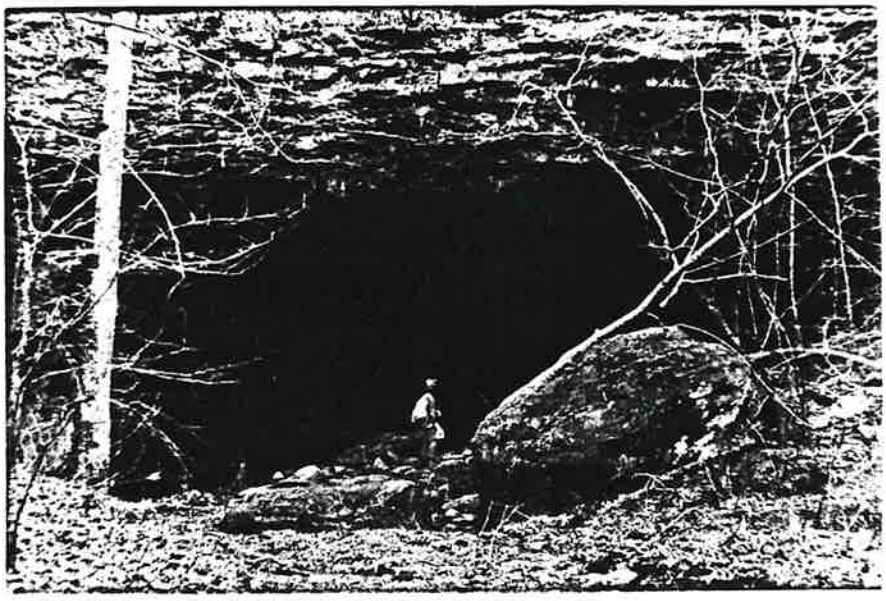

Fig. 2.15. The principal entrance to Cave Cove Cave. This entrance is located at a normally dry streamsink at the southeastern end of Cave Cove.

The main passage of the cave (Fig. 2.16) extends from this intersection for over one kilometre. Passage dimensions are typically 5 m high by 12 m wide. Extensive areas of breakdown occur in the cave, especially in the proximity of the valley wall of Farmer Cove. The stream in the cave flows on a bed of clastic gravels; relict deposits of sand and gravel, well above the present stream, are common along many passages.

At a distance of 1170 m from the Cave Cove entrance, a lower level passage is developed which absorbs all present streamflow. In contrast to the upper level, this passage is a narrow canyon with apparently constricted drainage: water remained ponded in this passage throughout the period of the present study. A recent history of higher flooding is suggested by the presence of leaf and twig fragments on the walls up to 14 m above the cave floor. Unlike upper level stream segments, the lower passage has no detectable gradient (Fig. 2.17).

Farmer Cove

The central depression in Upper Sinking Cove, Farmer Cove, lies at an elevation of 360 m (1181') a.s.l. (Fig. 2.18). A 20 m high saddle separates this 600 m long, 130-240 m wide depression from Wolf Cove which lies to the east.

Farmer Cove is composed of two blind valleys. A stream channel, which is normally dry, enters from the direction of Cave Cove, to the northeast, and meanders across the 5 m of alluvium covering the floor of the cove (Fig. 2.19) to a streamsink at the north wall. A second stream channel, fed by Farmer Cove Spring, enters from the southwest to meander across the alluvium to the cove's lowest point in the east

Fig. 2.16. The main upper-level passage of Cave Cove Cave. Streamflow through the passage is on sand and gravel beds.

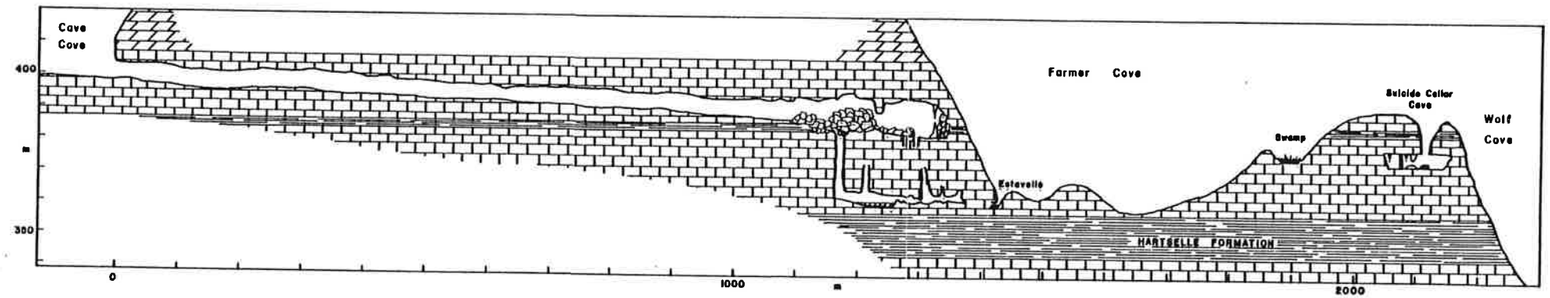

Fig. 2.17. Longitudinal section of Cave Cove Cave and Suicide Cellar Cave. Note ponded water level in Cave Cove Cave and Farmer Cove Estavelle. Vertical exaggeration 5x.

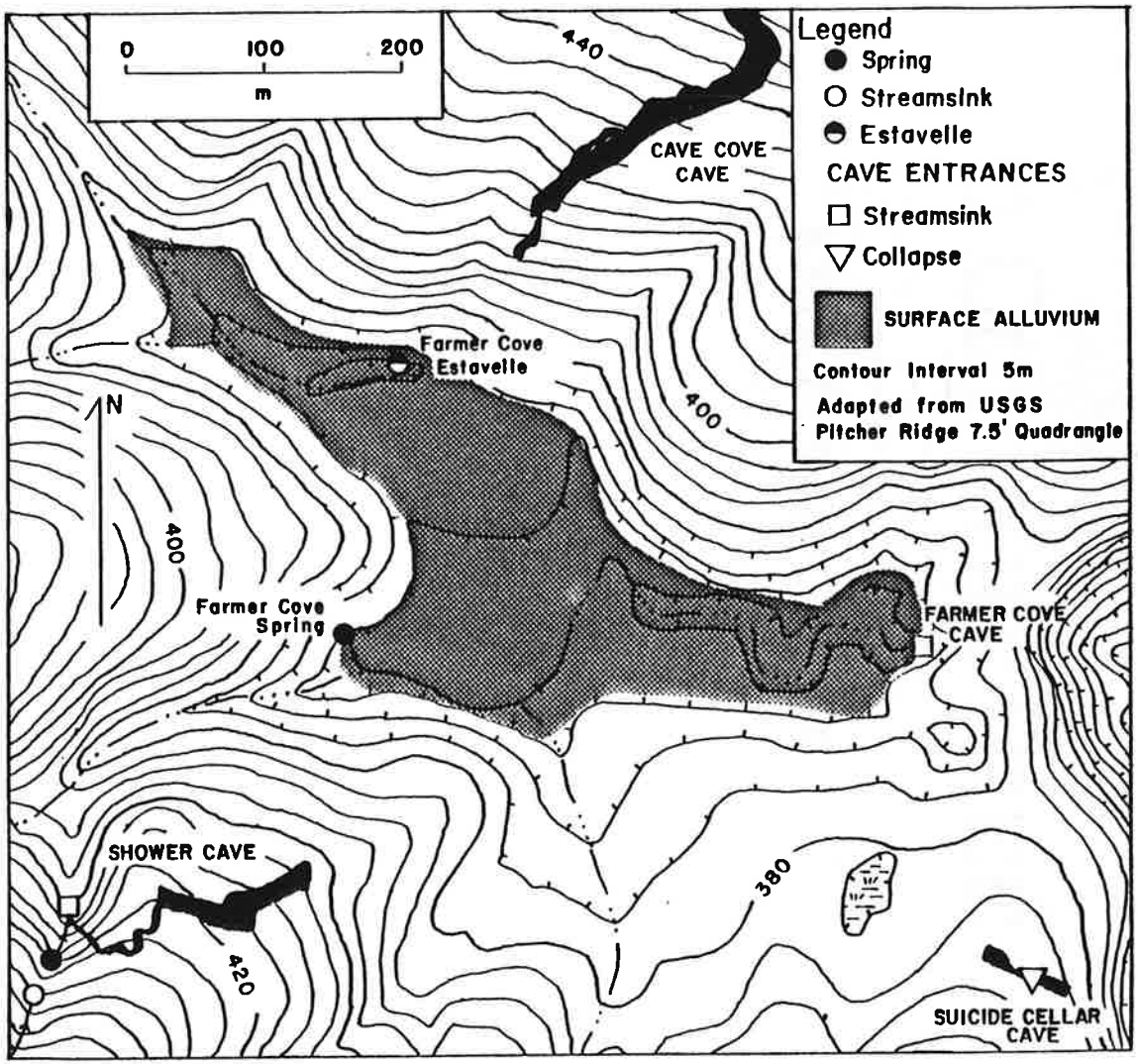

Fig. 2.18. Topography and hydrological characteristics of Farmer Cove.

Fig. 2.19. Alluvium in the floor of Farmer Cove. The sediments exposed in this bank are 4.5 m thick.

(Fig. 2.20). Under all but high flow conditions the stream never reaches this low point, water being lost underground all along the channel.

Passages of Cave Cove Cave approach the surface near the upper streamsink of the cove. A flooded cave entrance was found at this point, at the same level and only 100 m from the farthest point of exploration in the lower levels of Cave Cove Cave (Fig. 2.21).

A cave entrance was discovered at the lower streamsink of Farmer Cove. This cave, Farmer Cove Cave, appears incidental to the streamsink, with major passage development perpendicular to the direction of surface streamflow. A small stream passage is encountered at the bottom of the cave, but ends after 10 m in a sump (ponded water reaches the ceiling).

A short distance above and to the south of the saddle separating Farmer Cove and Wolf Cove is a cave of probable significance in the geomorphic history of the area. The entrance to Suicide Cellar Cave (#15) was formed by collapse (Fig. 2.22). The cave is a straight 107 m passage developed along a prominent joint oriented at 295°. Both ends of this passage are truncated by breakdown and calcite deposition. The elevation, location, and passage characteristics of Suicide Cellar Cave suggest the possibility that it may be a relict segment of a trunk passage which once extended from Cave Cove Cave across what is now Farmer Cove (see Fig. 2.17 and 2.18). Since enlargement ended at the time of separation from Cave Cove Cave, passage dimensions in Suicide Cellar (4 m high by 8 m wide) are less than in Cave Cove Cave.

Fig. 2.20. Final stream sink at the eastern end of Farmer Cove.

Fig. 2.21. Farmer Cove Estavelle. This is located at the end of the upper of two blind valleys in the cove. Water is ponded inside the estavelle, which probably connects with ponded passages in Cave Cove Cave.

Fig. 2.22. Suicide Cellar Cave entrance, a collapse feature between Farmer Cove and Wolf Cove.

A surface depression (containing a swamp), located over what was possibly the former route of the Cave Cove Cave/Suicide Cellar Cave system, may be a collapse doline. Free drainage was not established since no perennial surface streams flow into this depression, and so a swamp developed here (Fig. 2.23).

Wolf Cove

Wolf Cove, 1080 m in length and 325-650 m in width, is a 70 m deep depression composed of four minor depressions (Fig. 2.24). Three of these are blind valleys entering the cove from the north, west, and southwest; another is a collapse doline. All but one of the depressions have lower elevations of 310-315 m (1017-1033'), in the Monteagle Limestone.

Wolf Cove's principal blind valley, into which the other valleys appear to feed, extends from southwest to east across the cove, descending to near 295 m (968') a.s.l. Upstream segments of this blind valley are narrow; bed materials include slope-derived sandstone and limestone cobbles up to 40 cm in diameter (Fig. 2.25). Near its lower end, where the valley broadens, the floor is covered by 1.5 m of alluvium, which is dotted with small collapse dolines. The channel which meanders through this lower stretch only rarely carries stream-flow, and bed materials decrease in size to small gravels and sands at the terminal sinkpoint (Fig. 2.26).

The blind valley entering Wolf Cove from the west (i.e., from the direction of Farmer Cove) has at its head a group of springs emerging at the Hartselle Formation. During wet weather, these combine to flow downvalley to a ponor, Raccoon Raceway Cove (#28), at the valley's eastern end.

Fig. 2.23. Swamp in a depression near Suicide Cellar Cave. The depression may have resulted from collapse of cave passages formerly connecting Cave Cove Cave and Suicide Cellar Cave.

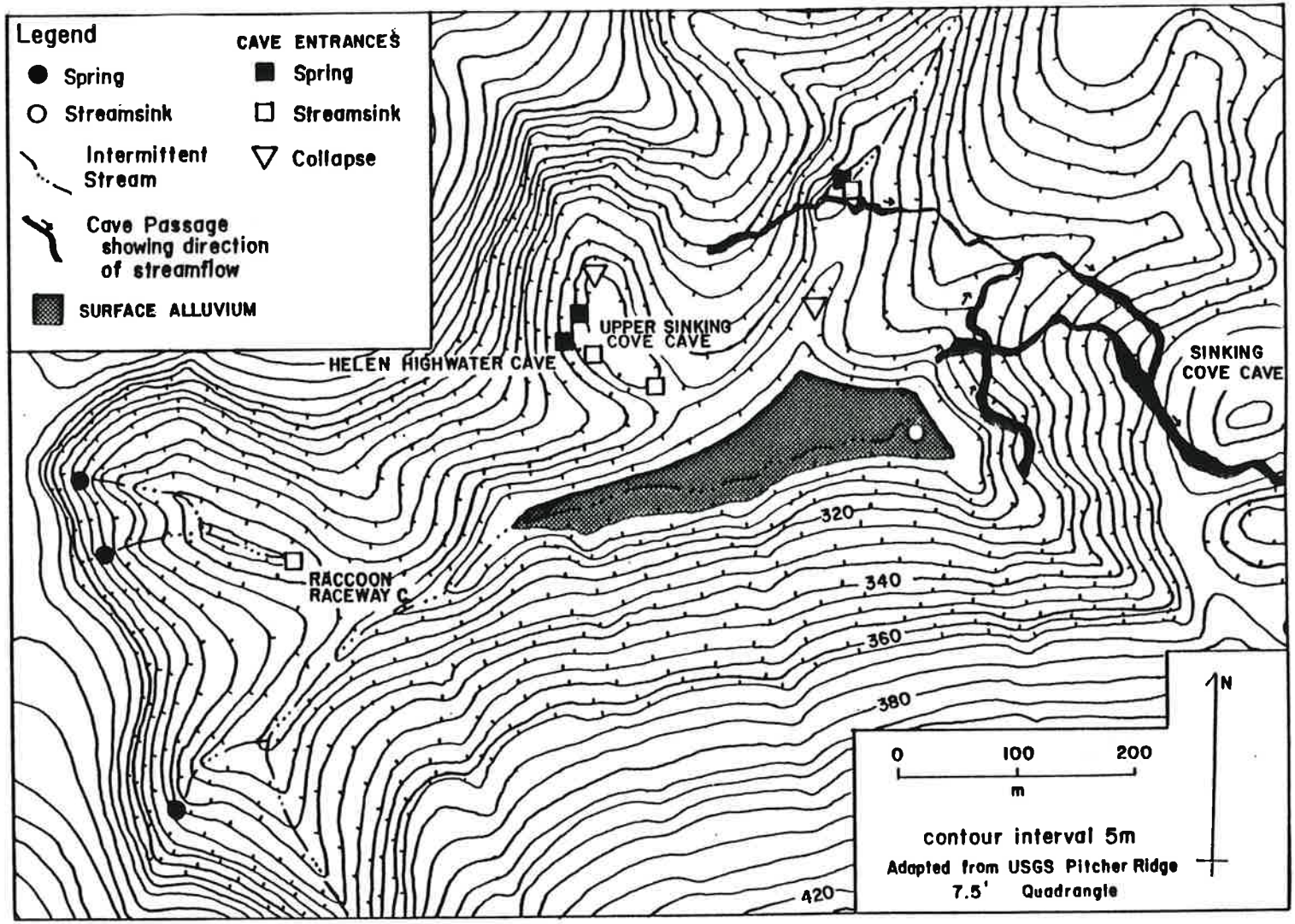

Fig. 2.24. Topography and hydrological characteristics of Wolf Cove.

Fig. 2.25. Streambed in the main blind valley of Wolf Cove. The channel contains slope-derived limestone cobbles.

Fig. 2.26. Streambed cut in alluvium near the final streamsink of the main blind valley of Wolf Cove. Note the lack of larger sediments.

Two depressions adjoin the main valley to the north. One of these is a collapse doline, separated from the lower valley by a 15 m high saddle. Major springs occur along the western side of this doline at 320 m (1050') a.s.l., on a 2 m shale bed in the Monteagle Limestone.

Caves are associated with these springs. Helen Highwater Cave (#22; Fig. 2.27) is the largest of these and contributes most of the flow. A stream passage of walking to stooping dimensions can be followed for 15 m upstream to a 4 m dome. A waterfall emerges from a small impenetrable passage at the ceiling, and is the source of most of the water flowing through the cave. Upon exiting the cave, the water from this and other springs (Bill's Cave, #24) flows over a series of waterfalls and into a ponor, Upper Sinking Cove Cave (frontispiece).

Two relict caves were also found in this doline. Mary's Cave (#25), at the northern end, has no present streamflow and is partially filled with calcite deposits. Marshall Cave (at the southern end of the doline) (#27) may once have functioned as a ponor; it is now dry, and partially filled with sediment.

The other depression to the north is a prominent blind valley which terminates in a 12 m deep doline (Fig. 2.28). There are entrances to three caves in this doline. A stream emerges from one of these, Xylophone Cave (#29), and flows over a shelf into another, Sinking Cove Cave (entrance S4).

Between this doline and the principal blind valley of the cove is a smaller collapse depression. A 12 m high relict cave passage,

Fig. 2.27. The spring at Helen Highwater Cave, in Wolf Cove.

Fig. 2.28. A 12 m deep doline at the end of a blind valley entering Wolf Cove from the north. The stream cascading at center exits Xylophone Cave (upper left) and enters Sinking Cove Cave (lower right).

Thorn Cave (#30; Fig. 2.29), extends from this depression for 60 m to a terminal collapse of surface debris.

Sinking Cove and Sinking Cove Cave

Beyond the Wolf Cove saddle, a dry valley descends 104 m to the alluvial floor of Sinking Cove. Located in a branch of this valley, and apparently serving as that branch's drainage route, is Ashlee Cave. A 1-2 m high stream passage oriented roughly parallel to the valley branch can be followed for 140 m upstream.

Connecting Wolf Cove and Sinking Cove is the most extensive cave discovered to date in the study area, Sinking Cove Cave (Fig. 2.30). More than six kilometres of passage have been mapped (R. Buice, personal communication). Discovery in 1978 of the Boulder Entrance at the Pennington/Bangor contact has given the cave a total depth of more than 135 m (Smith, 1978).

The Wolf Cove entrance to Sinking Cove Cave is in a depression; water from Xylophone Cave enters at this point. A 150 m stream passage (Fig. 2.31) leads to a junction with a larger passage which contributes the major amount of streamflow in the cave. This trunk passage may be followed upstream for 250 m south from this junction to a breakdown choke, where the valley wall of Wolf Cove is approached (see Fig. 2.30).

Downstream, this trunk passage continues for 2.2 km to a spring entrance at the head of Sinking Cove. This passage passes under depressions developed in the saddle separating Wolf Cove and Sinking Cove, and then parallels the dry valley descending into the lower cove.

The cave is developed on several levels. The uppermost level is in the Bangor Limestone and consists of a tributary passage leading

Fig. 2.29. Thorn Cave, in Wolf Cove. A 4 m high, dry passage extends for 60 m to a terminal fill of surface debris.

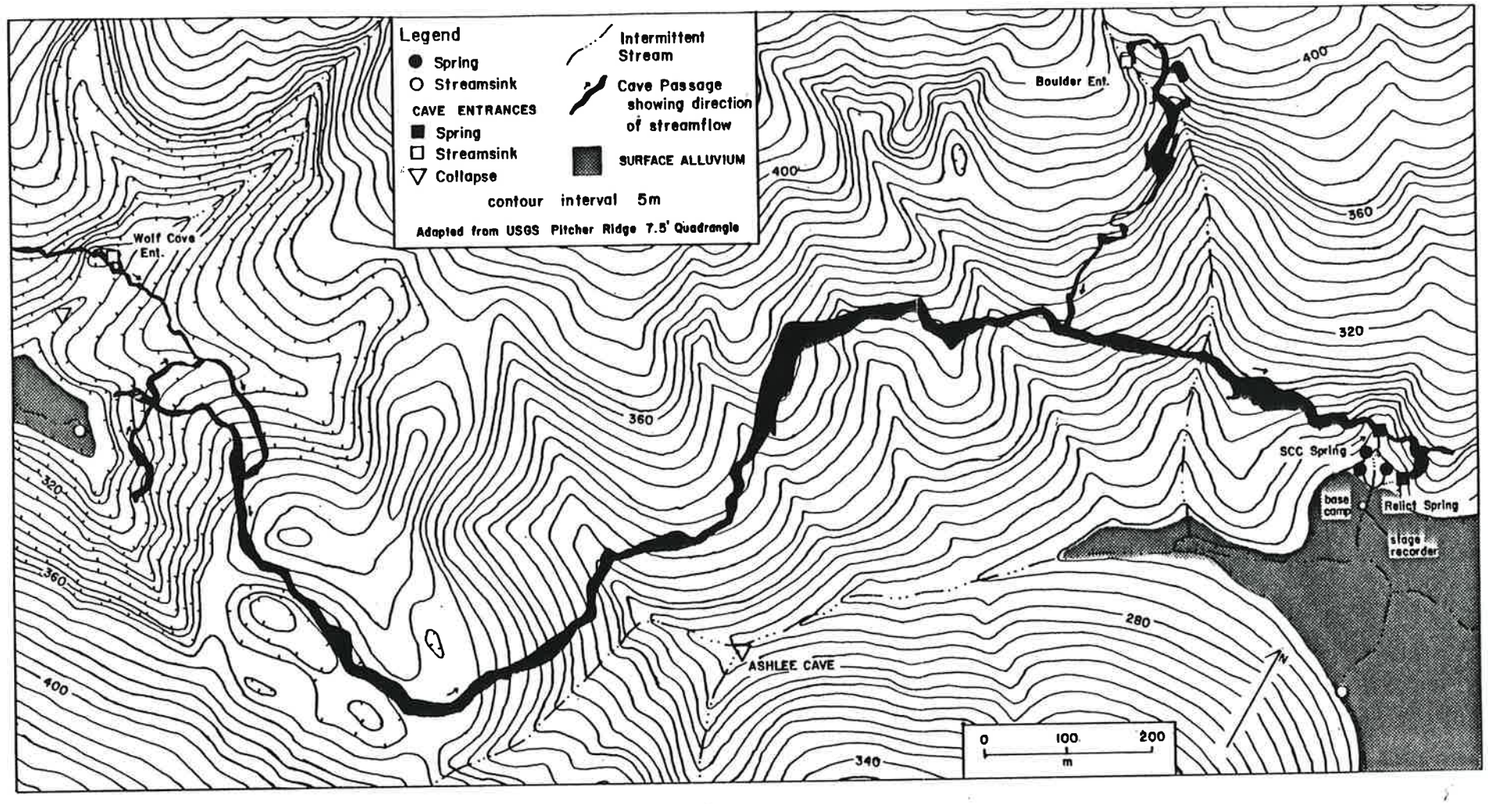

Fig. 2.30. Map of Sinking Cove Cave showing the entrances in Wolf Cove (left), Sinking Cove (right), and at the Pennington/Bangor contact (top). Cave plan supplied by R. Buice.

Fig. 2.31. Tributary passage in Sinking Cove Cave connecting with the Wolf Cove entrance. Passage height is 4 m.

from the Boulder Entrance at the Pennington/Bangor contact. In the Monteagle Limestone, two major levels extend between the two coves. In the lower passages, the cave stream flows through successions of pools and riffles on sandstone and chert gravel beds (Fig. 2.32). Segments of an upper level are preserved, separated by breakdown rooms which connect the upper and lower levels (Fig. 2.33).

Near the lower entrance at Sinking Cove, flow is blocked by breakdown, producing pools up to 2 m deep (Fig. 2.34). When it leaves the cave, the stream passes through a boulder field produced by collapse of the cliff-face above the spring entrance (Fig. 2.35). Another large cave entrance nearby (Fig. 2.36) is connected to the main passage of Sinking Cove Cave, and produces springflow during periods of high discharge.

Landforms in the Canyon Walls Above the Coves

Dolines and caves are also common in the canyon walls above the coves. These are usually found at streamsinks located at major lithologic breaks. Two preferred zones are at the Raccoon Mountain/Pennington contact and the Pennington/Bangor contact.

The Pennsylvanian sandstone caprock, combining the Raccoon Mountain Formation and the Warren Point Sandstone, produces a prominent bluff above the slopes of the Pennington Formation carbonates (Fig. 2.37). While no significant surface depressions have been produced, small caves may occur where streams flow off the caprock. Still Cave and Raccoon Bluff Cave were discovered at this contact in streamsinks above Cave Cove (Fig. 2.38).

Fig. 2.32. Trunk stream passage in Sinking Cove Cave. The stream in the passage is flowing across gravels.

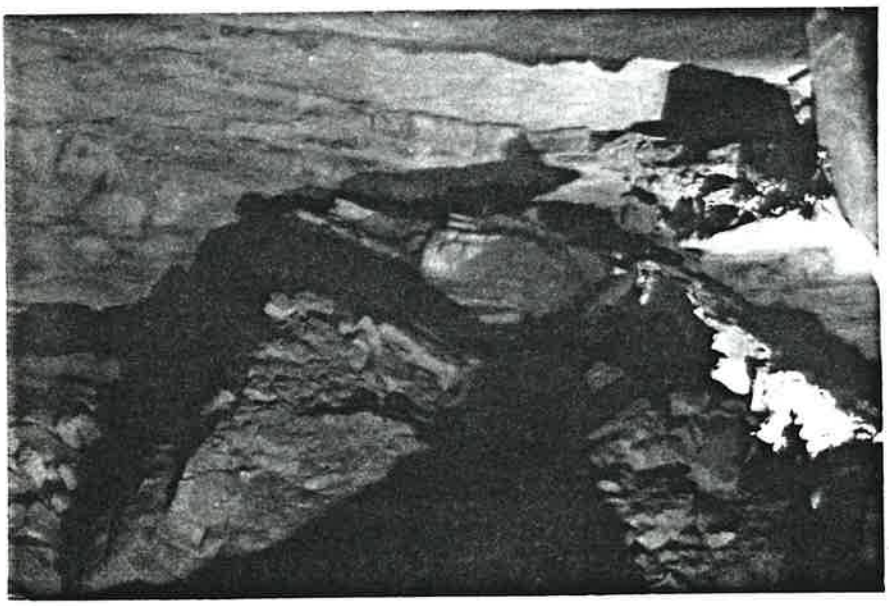

Fig. 2.33. Breakdown room connecting the two major levels of Sinking Cove Cave. Figure at lower right gives scale.

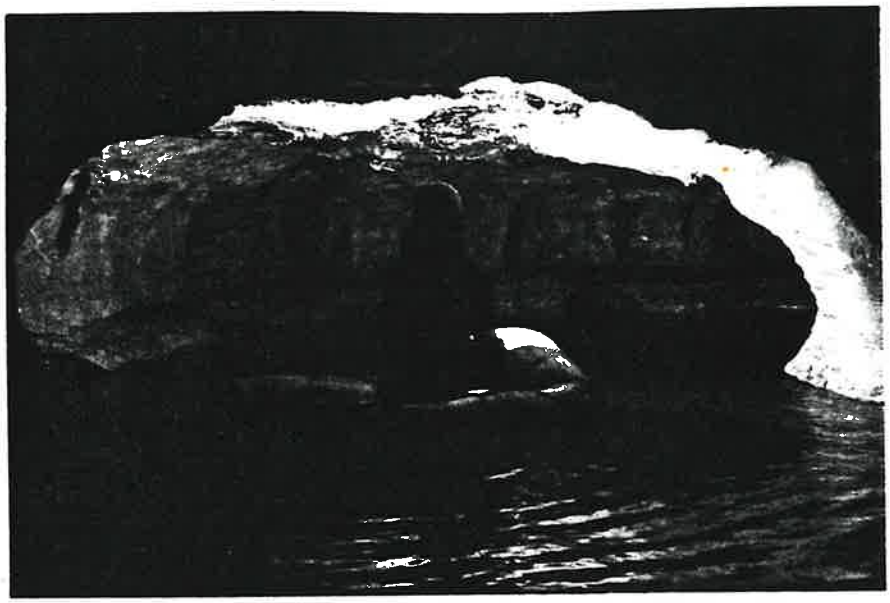

Fig. 2.34. Ponded stream immediately above SCC Spring, in Sinking Cove Cave.

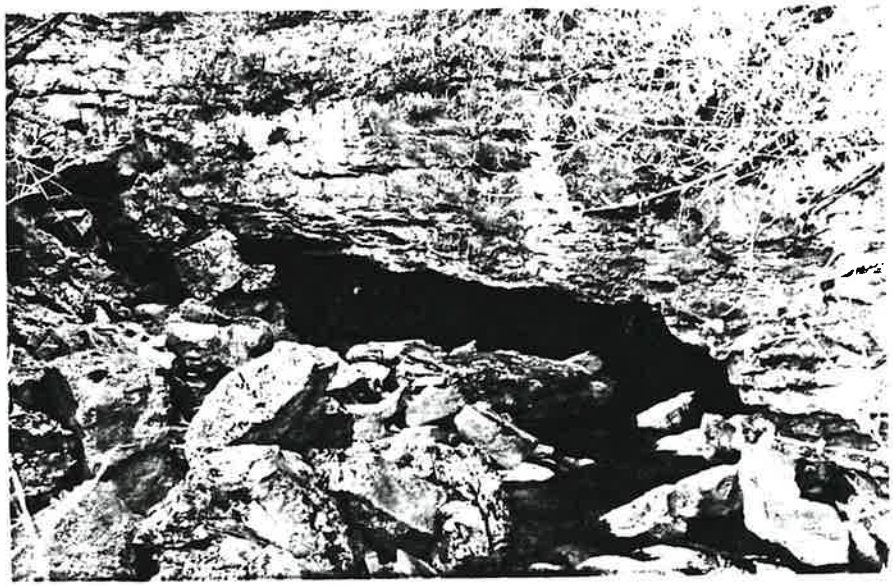

Fig. 2.35. Sinking Cove Cave Spring (SCC Spring) entrance, at the head of Sinking Cove. The limestone boulders have fallen from the cliff face above the spring.

Fig. 2.36. Relict spring entrance of Sinking Cove Cave.

Fig. 2.37. Undercut cliff in the Warren Point Sandstone, above Cave Cove.

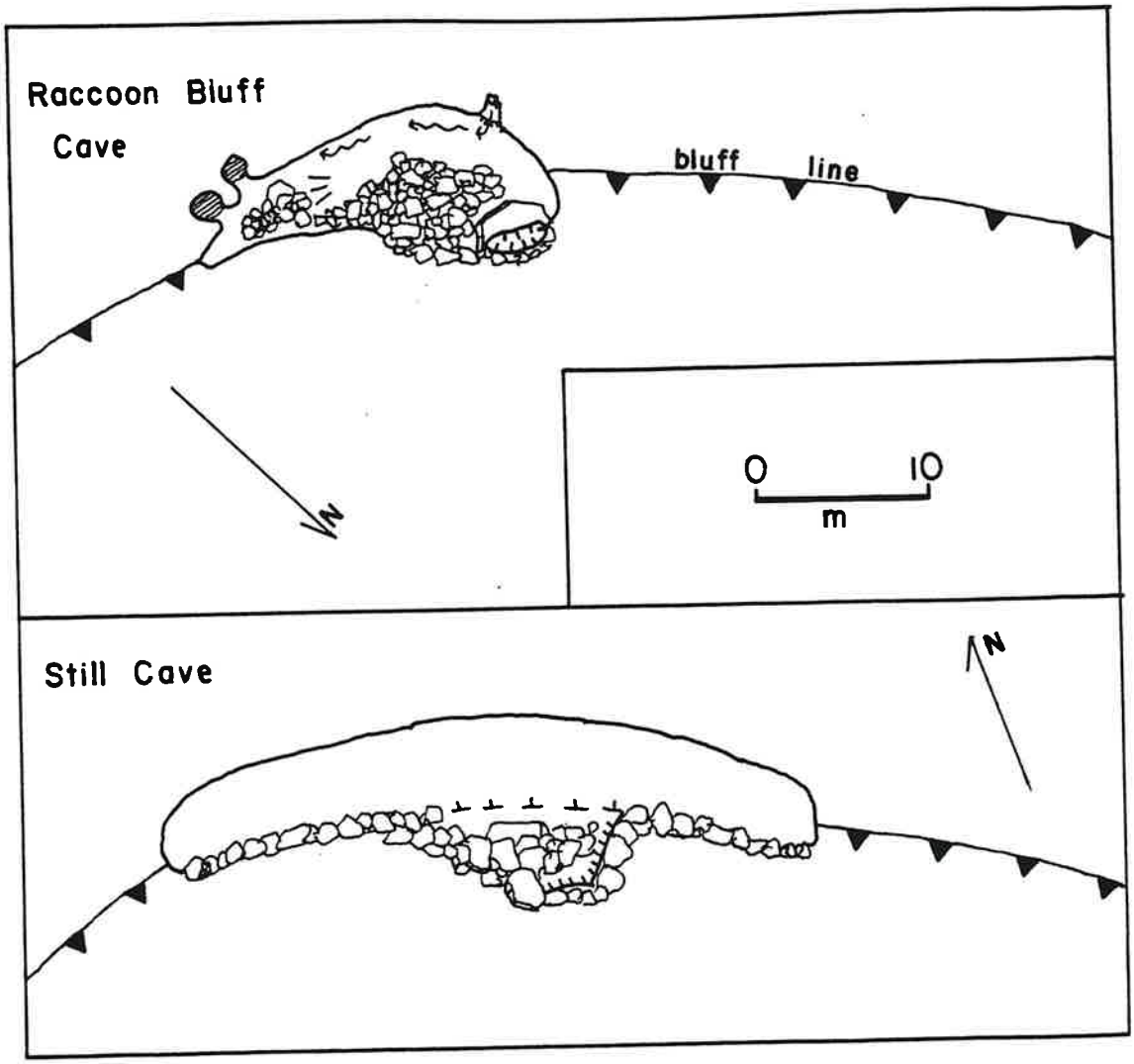

Fig. 2.38. Plans of two caves located at the Raccoon Mountain/Pennington contact above Cave Cove.

Several depressions and cave entrances are located at the Pennington/Bangor contact (390-420 m a.s.l.). Other than those described in Cave Cove (Exercise Cave and Cave Cove Cave), major streamsink cave entrances can be found in blind and dry valleys leading into Farmer Cove (Shower Cave), Wolf Cove (Wolf Cove Cave), and Sinking Cove (Boulder Entrance to Sinking Cove Cave). Collapse depressions and open vertical shafts are also common at this contact (Fig. 2.39 and 2.40).

Shower Cave is located at a streamsink in a valley leading into Farmer Cove from the southwest (Figs. 2.41 and 2.42). A 15 m shaft just inside the entrance (at 415 m a.s.l.) descends to the upper of two major levels of the cave, which is developed in limestones above and below a 2 m shale bed in the upper Bangor Limestone. A stream penetrates both levels, dropping 15 m in a series of waterfalls from the base of the entrance shaft to a 30 cm high drain in the floor of the lower level.

Wolf Cove Cave is a similar cavern development in a blind/dry valley leading into Wolf Cove from the north (#17; Fig. 2.43). From its stoped entrance at the Pennington/Bangor contact (Fig. 2.44), over 800 m of passages have been mapped, through 35 m of Bangor Limestone. Widened passages occur at two levels, separated by 10 m of narrow canyons and vertical shafts.

The upper level of the cave, roofed by calcareous sandstone, is developed in and above a 2 m bed of silty shale (the same as encountered in Shower Cave). Passage dimensions in the Footloose Passage (Figs. 2.45 and 2.46) are 4 m high by 6-8 m wide, with a flat ceiling and inward sloping ledges littered with breakdown and sand.

Fig. 2.39. Green Barrel Pit, a 15 m vertical shaft at the Pennington/Bangor contact.

Fig. 2.40. Blowhole Pit, a 13 m shaft at the Pennington/Bangor contact on Cave Cove Saddle.

Fig. 2.41. Streamsink entrance to Shower Cave. A 15 m vertical shaft is encountered 6 m behind the waterfall.

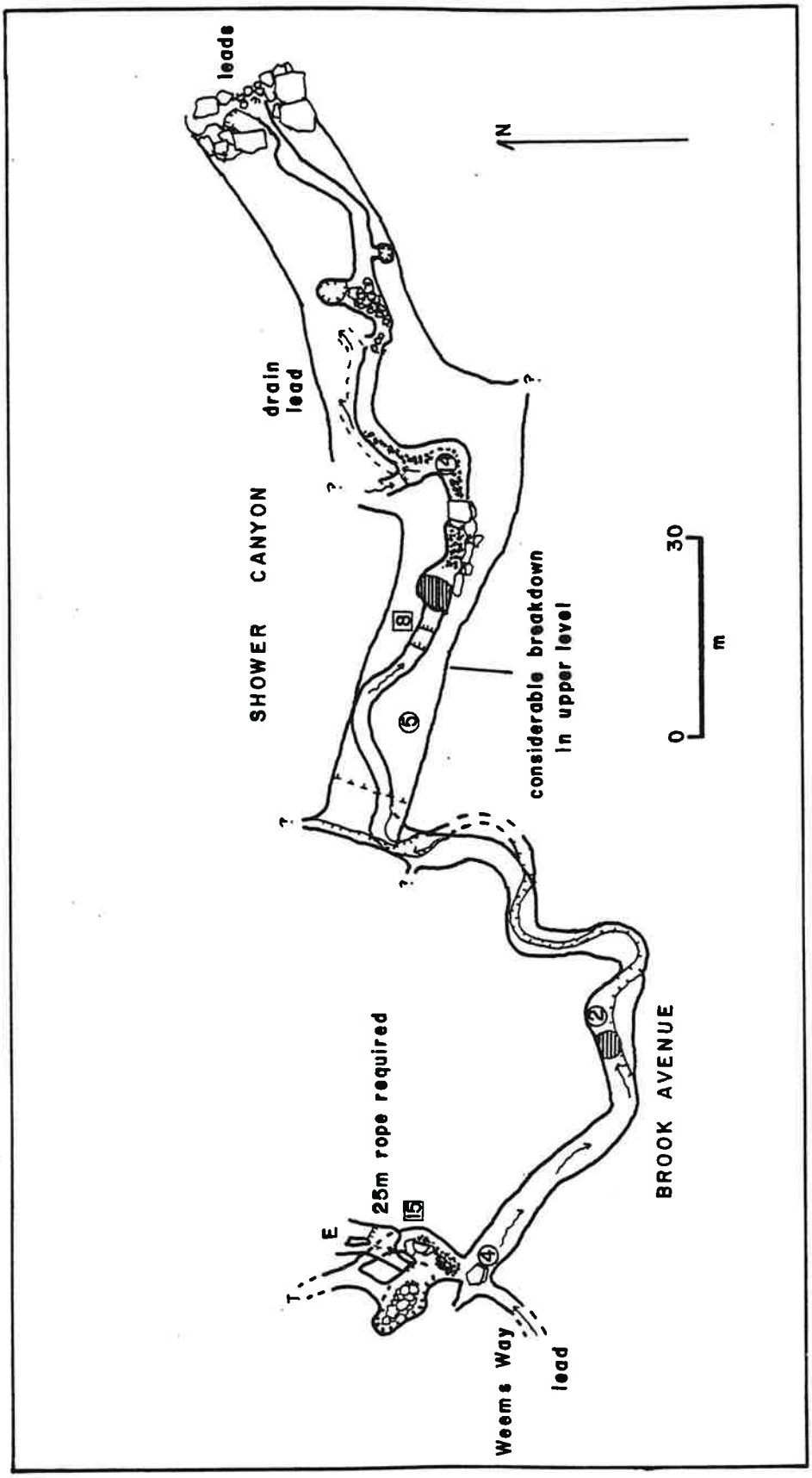

Fig. 2.42. Plan of Shower Cave.

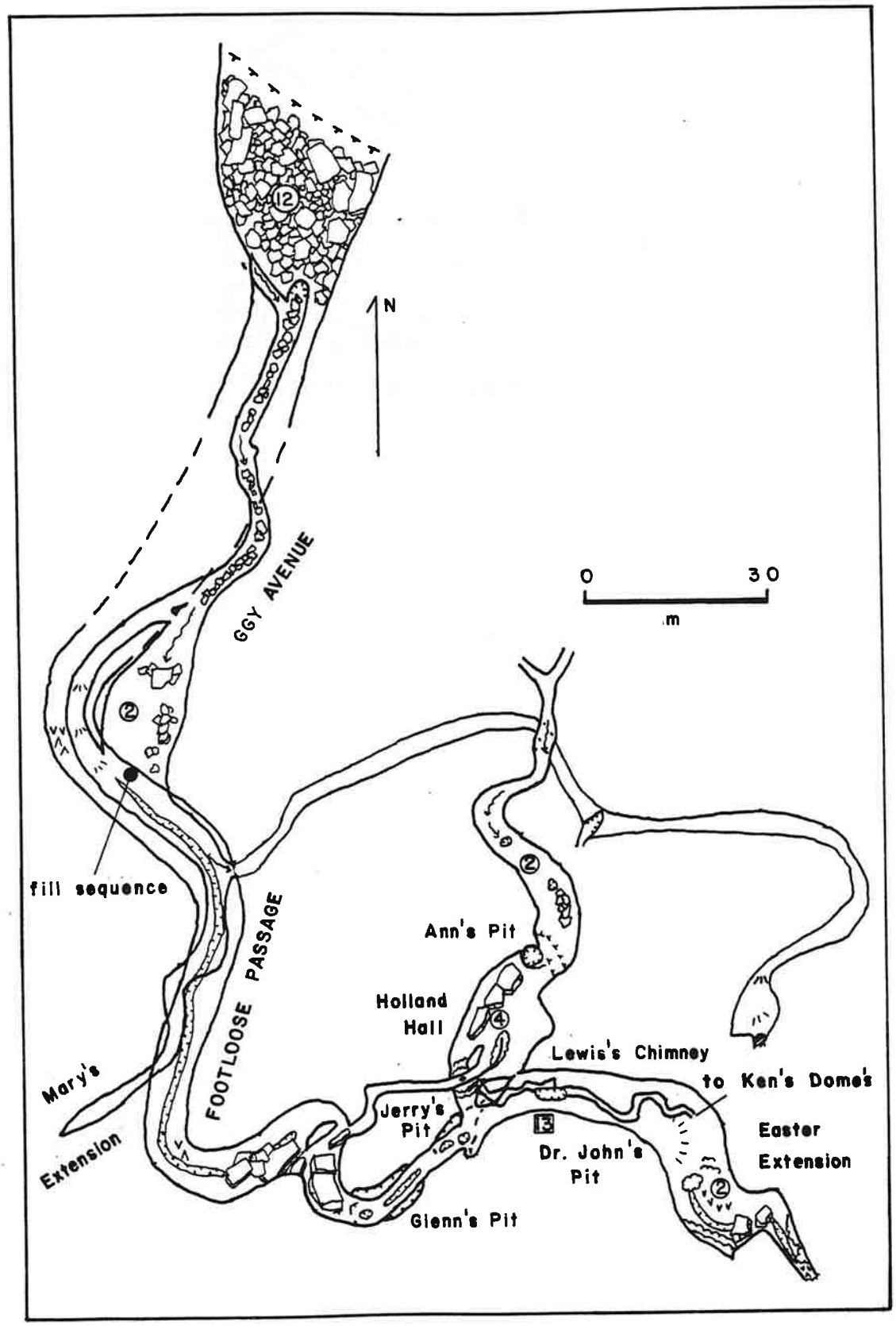

Fig. 2.43. Plan of Wolf Cove Cave.

Fig. 2.44. The entrance to Wolf Cove Cave. The entrance is in a blind valley above Wolf Cove.

Fig. 2.45. Footloose Passage in Wolf Cove Cave (upper level). Flowstone deposits are visible to the right of the photograph.

Fig. 2.46. Termination of Footloose Passage in Wolf Cove Cave. Breakdown in the background prevents access to the entrance at this level.

Directly inside the entrance, a lower level passage of the cave carries intermittent streamflow for 100 m to a stream crawl. Followed for 180 m to the lowest known room in the cave, the ponded water passage (similar to those in caves surrounding Farmer Cove) beyond indicates the proximity of the Hartselle Formation aquitard. Parts of Wolf Cave Cove have flooded in recent times, as indicated by the prevalence of washed-in organic debris in lower passages (Fig. 2.47).

The Boulder Entrance of Sinking Cove Cave is also located at the Pennington/Bangor contact. A series of vertical shafts and stream passages leads through the Bangor Limestone, Hartselle Formation, and Monteagle Limestone to the trunk passage of the cave, 130 m below this entrance.

Fig. 2.47. Organic flood debris in a lower-level passage of Wolf Cove Cave.

CHAPTER III

HYDROLOGY AND CAVERN DEVELOPMENT

In this chapter, the hydrology of the study area is examined. The present drainage system and groundwater flow conditions are analyzed from field observations and stream tracing experiments. Variations in discharge from the system are studied and related to seasonal climatic patterns. Paleohydrologic conditions are interpreted from cave evidence. Geologic controls on hydrology are discussed.

Present Hydrology

The Drainage System

Upper Sinking Cove is drained by a system of surface and subsurface streams. Subsurface flow predominates. Surface segments are typically short-lived below springs, often leading directly into streamsinks. Study of this drainage system has involved interpretation of groundwater flow patterns. Since subsurface stream segments were not always accessible, groundwater tracing techniques were adopted to determine underground flow directions.

The Use of Tracers in Groundwater Studies

Numerous studies have been made of impenetrable underground water routes using tracers (Brown et al., 1969). For example, Zötl (1957) used spore tracers in the Austrian Calcareous Alps to support his theories on the development of underground river systems. More recently, Quinlan and Rowe (1977) have made extensive use of fluorescent dyes to define

drainage patterns of the Central Kentucky Karst. The latter has been of considerable benefit for wastewater management planning in the area.

Aley and Fletcher (1976) review the various tracers which have been used in groundwater studies. These include salts, radioactive materials, fluorescent dyes, and minute biological materials. Fluorescent dyes are recommended for most applications due to their relative ease in handling and low environmental impact.

Groundwater Tracing Methods Used in this Study

A tracing method using fluorescent dye was used in this study. Experiments were set up in which dye was injected into a streamsink or at the downstream limit of exploration in cave passages. At a number of possible outlet points, packets containing activated charcoal were placed in streams to adsorb dye dissolved in the water (Fig. 3.1). After a period of time, these packets were collected and returned to the laboratory for dye elutriation and fluorometric analysis (see below). If tests indicated that the charcoal contained dye, a groundwater connection between input and output points was considered to have been established.

Rhodamine WT was chosen for use in the study. Advantages include the fact that samples can be analyzed in the laboratory with a fluorometer, allowing the use of smaller quantities than would have been necessary for visual analysis. In addition, the dye is not easily adsorbed by bed and bank materials, and fluoresces at a wavelength (582 nm) similar to that of few natural substances (Brown et al., 1969).

Fiberglas window screen was used to construct the dye collection packets, each of which contained two tablespoons of activated charcoal.

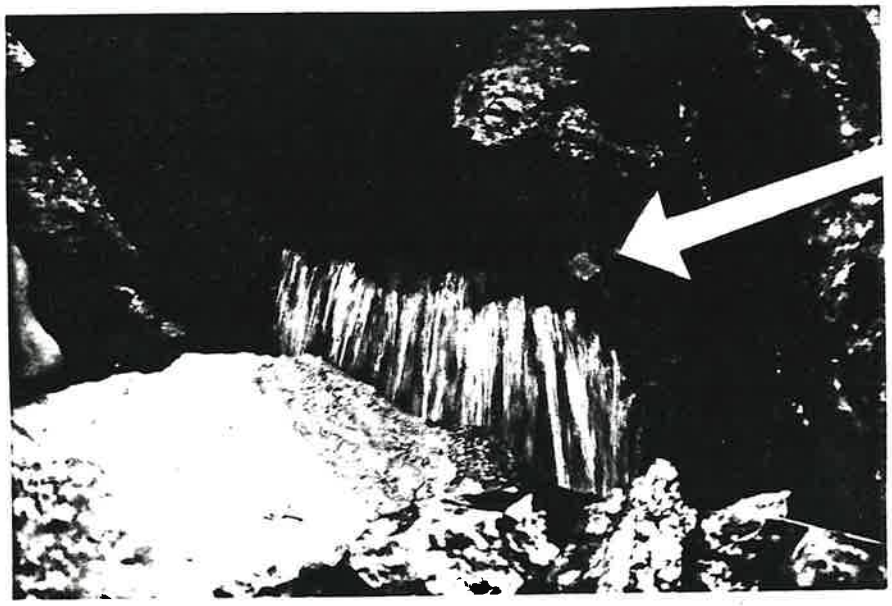

Fig. 3.1. Example of charcoal packet emplacement for dye tracing experiments (Helen Highwater Cave Spring).

These packets were placed in streams using a technique recommended by J. Quinlan (pers. comm.). Hangers to which packets could be attached were constructed of #2 stove wire, and imbedded in a concrete base. These were placed in stream beds and, if needed, secured to a tree or other stable object with nylon cord. Packets could then be positioned for optimal dye adsorption in stream currents.

A modified technique for collecting samples was used after the first four traces. Originally, samples were collected in 125 mL and 250 mL wide-mouth Nalgene bottles, which were washed thoroughly between uses. A disposable container was considered preferable to reduce the chance of contamination between experiments. Plastic bags were not used due to the danger of puncture and leakage. Thirty-five mm film canisters were chosen. Their advantages include:

1. Their size (filled 2/3 with charcoal) allows for a sufficient amount of charcoal, yet are compact for field use

2. They may be sealed securely

3. Elutriation (see below), using easily standardized chemical volumes, may be completed in the same container

4. Sufficient quantities are available free of charge to allow disposal after use

After collection, samples were returned to the laboratory for analysis. Using a technique recommended by Aley and Fletcher (1976), the charcoal samples were elutriated with ammonium hydroxide and methyl alcohol for one hour. The liquid was then filtered and analyzed with a Turner Associates Model 110 Fluorometer. Light filtered to 546 nm was used to excite the samples. Fluorescence at 590 nm, the emission wavelength of Rhodamine WT, was measured by the instrument. Known

concentrations of dye were also analyzed in order to produce a rating curve relating instrument readings to dye concentrations in parts per billion.

Concentrations of dye as low as .01 ppb (parts per billion) can be measured using the Turner fluorometer. For analysis with charcoal packets, however, equivalent concentrations this low are not reliable, since minute quantities of naturally fluorescing materials may produce readings. Packets placed at springs prior to dye injections often fluoresced to an equivalent of 0.5 ppb. In this study, equivalent concentrations of 1 ppb or less were considered 'negative' traces. Equivalent concentrations between 1 and 2 ppb were considered 'possible positive' traces. Concentrations greater than 2 ppb were considered 'positive' traces. In interpretations it must be remembered that although a 'positive' trace should, barring contamination, establish a connection, a 'negative' trace (or even a zero reading) cannot negate the possibility of a connection.

Groundwater Tracing Experiments

Trace #1: Cave Cove Sink at Exercise Cave to Eight Potential Outputs

Charcoal was placed at eight potential outputs before dye injection (see Fig. 3.2):

1. The stream flowing through Cave Cove Cave (A)
2. The ponded water body in lower-level Cave Cove Cave (B)
3. Farmer Cove Spring (D)
4. The stream flowing through Farmer Cove Cave (E)
5. The stream flowing into Upper Sinking Cove Cave (J) (includes flow from Helen Highwater and Bill's Caves)

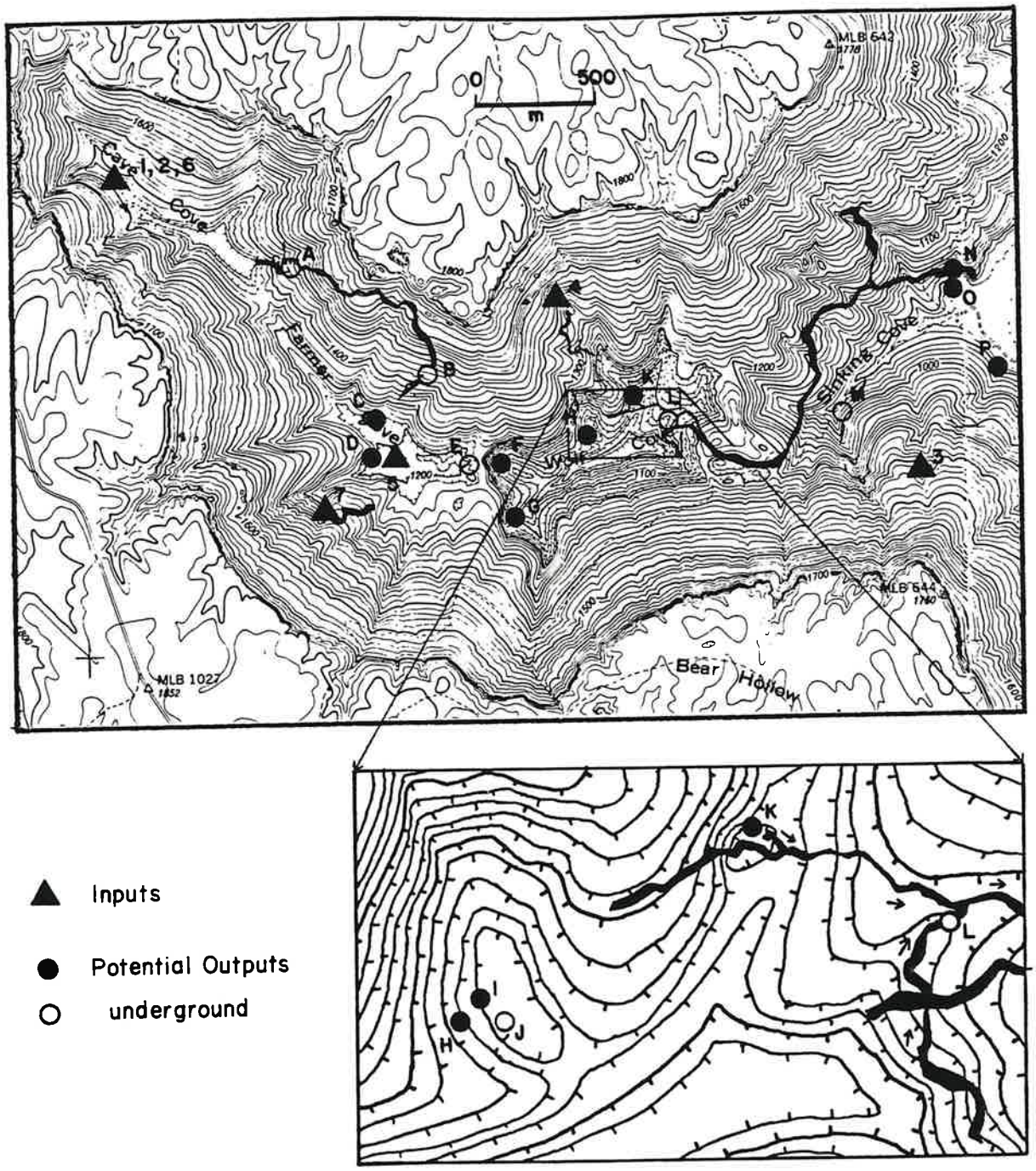

Fig. 3.2. Dye input and potential output locations for stream tracing experiments. A portion of Wolf Cove is enlarged. Site descriptions are given in the text (also see Tables 3.1 and 3.2).

6. The stream flowing through Sinking Cove Cave, upstream from the confluence with the Waterfall/Xylophone Cave tributary (L)

7. SCC (Sinking Cove Cave) Spring (N)

8. A spring in the boulder field below SCC Spring (O)

Five hundred millilitres of dye was injected into the streamsink at 1710 hr on 27 June 1980 (Table 3.1). Water samples were collected at SCC Spring on a regular basis over the next 3 days, in order to estimate a flow-through time. Charcoal was collected from other points on 30 June.

Results are given in Table 3.2. Positive traces were indicated for Upper Sinking Cove Cave and the trunk stream in Sinking Cove Cave near the Wolf Cove entrance. A possible positive trace was indicated for the stream in Farmer Cove Cave (E). Maximum readings for SCC Spring, 0.5 ppb, were insufficient to establish a flow-through time.

Negative traces were indicated for points in Cave Cove Cave (A and B) and for Farmer Cove Spring (D).

Trace #2: Cave Cove Sink to Springs near Helen Highwater Cave

Upper Sinking Cove Cave is fed by two springs, Helen Highwater Cave (H) and Bill's Cave (I), both located directly above. In order to determine which of these was the actual spring outlet in trace #1, another was planned.

Charcoal was placed at the two springs, as well as in Upper Sinking Cove Cave. Five hundred millilitres of dye was again injected at Cave Cove Sink on 4 July; charcoal was collected 2 days later. Traces were positive to all three points.

Table 3.1. Water tracing experiments in Upper Sinking Cove, Franklin Co., Tenn.

No.*	Dye Input	Dye Volume (mL)	Injection Time	Date (1980)	Date Packets Collected
1	Cave Cove Sink	500	1710	6/27	6/30
2	Cave Cove Sink	500	1200	7/04	7/06
3	Green Barrel Pit	250	1900	8/18	8/20-21
4	Wolf Cove Cave stream	500	1715	8/21	8/23
5	Farmer Cove stream	500	1200	12/13	12/14&21
6	Cave Cove Sink	1000	1145	12/29	12/30-31
7	Shower Cave	250	1700	6/06 (1981)	6/07

*See Fig. 3.2

Table 3.2. Results of Water Traces in Upper Sinking Cove, Franklin Co., Tenn.

Outlet	Tracing Experiment (see Table 3.1). Results given in parts per billion. 1	2	3	4	5	6	7
A Cave Cove Cave stream	0						
B Cave Cove Cave - ponded lower level	0						
C Estavelle in Farmer Cove Spring						0.7	
D Farmer Cove Spring	0						
E Farmer Cove Cave	1.1						
F (north) Springs in west wall							6.0
G (south) of Wolf Cove							1.0
H Helen Highwater Cave		8		44.2	15(12/21)	17(12/30) 75(12/31)	1.0
I Bill's Cave		14					
J Upper Sinking Cove Cave	90.6	10		0.8	15(12/14) 17(12/21)		
K Thorn Cave				132.6			
L SCC - trunk passage under Wolf Cove	11.8			0	373(12/21)	111	
M Ashlee Cave			0				
N SCC Spring	0.5		23.8 (22.1)			1.5(12/30) 4.5(12/31)	
O Spring at edge of boulder field (near SCC Spring)	0.5						
P Green Spring			2700.0				

*designations on map (Fig 3.2).

Trace #3: Green Barrel Pit to Ashlee Cave, Sinking Cove Cave, and Green Spring

Charcoal was placed in Ashlee Cave (M), SCC Spring (N), and Green Spring (P). Two hundred fifty millilitres of dye was injected at 1900 hr on 18 August 1980 into the waterfall entering Green Barrel Pit (see Fig. 2.13). Charcoal was collected 20-21 August.

A strong positive trace was indicated for Green Spring (Fig. 3.3), located in a hillside across from SCC Spring. Dye-colored pools below the spring were noted on 20 August, becoming more intense by the next morning. Ashlee Cave received no dye as of 1930 hr on 20 August. The positive trace to SCC Spring (collected at 1200 hr on 21 August) was not expected, since no likely stream inputs are known.

Trace #4: Streamsink above Wolf Cove Cave to Helen Highwater Cave, Xylophone Cave, and Sinking Cove Cave

Charcoal was placed at Helen Highwater Cave (H), Upper Sinking Cove Cave (J), Xylophone Cave (K), the trunk stream in Sinking Cove Cave upstream from Xylophone Cave tributary (L), and SCC Spring (N). Five hundred millilitres of dye was injected at 1715 hr on 21 August 1980 into a streamsink above Wolf Cove Cave. During wetter periods, this stream flows through the cave. Charcoal was collected 2 days later.

A positive trace was indicated for Helen Highwater Cave, but not for Upper Sinking Cove Cave directly downstream. Since charcoal collection from Helen Highwater was completed within 10 minutes of collection from the other cave, contamination must be suspected.

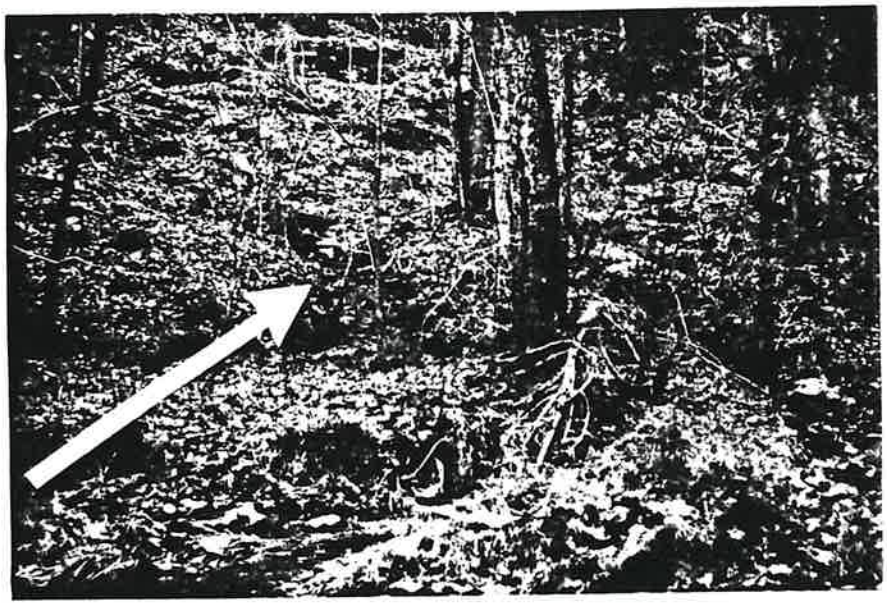

Fig. 3.3. Green Spring. This is one of a group of small springs located at the base of the slopes forming the western margin of Sinking Cove.

A strong positive trace was indicated for Xylophone Cave. No dye was adsorbed in upstream Sinking Cove Cave, but concentrations were again recorded for SCC Spring.

Trace #5: Farmer Cove Creek to Helen Highwater Cave, Upper Sinking Cove Cave, and Sinking Cove Cave

Charcoal was placed in Upper Sinking Cove Cave (J) at 1200 hr on 13 December 1980. Five hundred millilitres of dye was injected at the same time in the stream flowing from Farmer Cove Spring, which sinks gradually into the floor of the cove. The first charcoal installed was collected the following day, and new charcoal placed in Helen Highwater Cave (H), Upper Sinking Cove Cave (J), and Sinking Cove Cave (L). This charcoal was collected one week later.

Positive traces were indicated for all points. The 15 ppb value for Upper Sinking Cove Cave one day after dye injection suggests a peak concentration flow-through time of less than 24 hours. Considerably more dye was adsorbed in Sinking Cove Cave than was indicated for the Helen Highwater/Upper Sinking Cove Cave resurgence.

Trace #6: Cave Cove Sink to Farmer Cove Estavelle, Helen Highwater Cave, and Sinking Cove Cave

A repeat of trace #1 was attempted with 1000 mL of dye. Discharge was similar (approximately 28 L/sec at SCC Spring), representing moderate flow conditions. Charcoal was placed at Farmer Cove Estavelle (C), Helen Highwater Cave (H), and Sinking Cove Cave (L and N). Dye was injected at the streamsink at 1145 hr on 29 December 1980. Charcoal was removed from Helen Highwater Cave and Sinking Cove Cave springs on the 30th and from all springs on the 31st.

When Helen Highwater Cave spring was visited at 0930 hr on the 30th, no dye was visible. By 0940 hr, dye became apparent, producing a distinctive pink coloration in the water. A 22-hour flow-through time was thus indicated. Dye adsorption values from charcoal packets support this observation.

Significant quantities of dye were not adsorbed at SCC Spring for 30 hours after dye injection. A new packet of charcoal placed at this spring at 1745 hr on the 30th, however, had retained an equivalent of 4.5 ppb by 0945 the next morning, some 30 to 46 hours after dye injection. Insufficient field time was available for further collection at this spring. Peak concentrations may have occurred after the charcoal was removed.

No dye was adsorbed in Farmer Cove Estavelle (C).

Trace #7: Shower Cave to Springs in Wolf Cave

Packets were placed at two springs in the west wall of Wolf Cave (F and G), as well as at Helen Highwater Cave (H). Two hundred fifty millilitres of dye was injected at 1700 hr on 6 June 1981 at the farthest point of exploration of the stream flowing through Shower Cave. Following heavy rains, discharge was high. The next morning, at 1000 hr, the charcoal packets were colleted.

Only the trace to F, a spring emerging on the Hartselle Formation in the west wall of Wolf Cave, was positive (6 ppb equivalent).

An Outline of the Present Drainage System of Upper Sinking Cove

Based on field observations and on evidence from groundwater tracing (Fig. 3.4), the drainage of the study area can be described as a

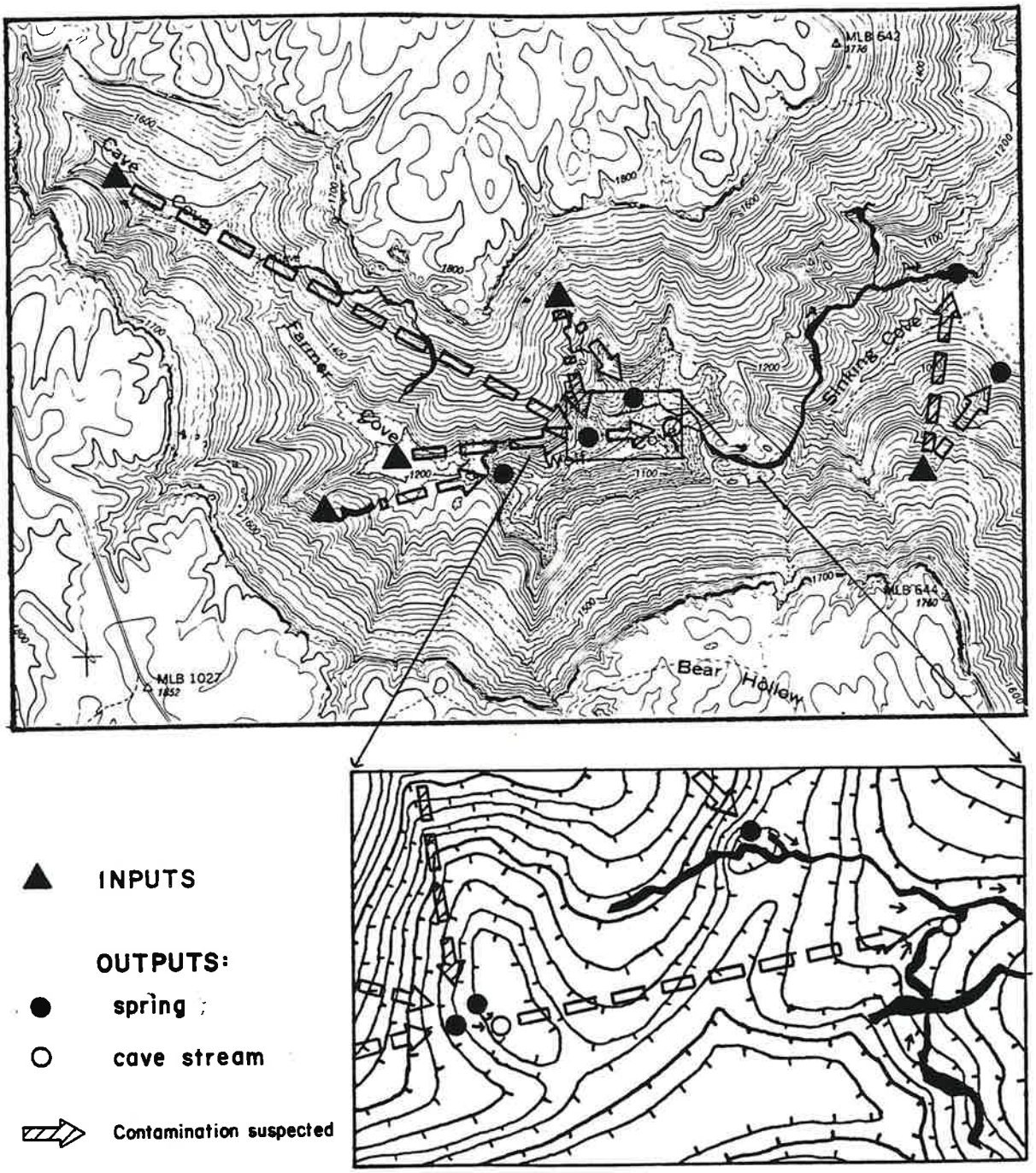

Fig. 3.4. Groundwater flow directions in Upper Sinking Cove as determined through stream tracing experiments.

multiple-aquifer system of tributaries leading into a central trunk channel. Surface and subsurface segments make up the system.

The trunk channel identified begins as a surface stream on the plateau above Cave Cove. This stream, Cave Cove Creek, occupies a blind valley and eventually sinks in a collapse doline at Exercise Cave, in the floor of Cave Cove. Dye traces indicate a resurgence in Wolf Cove, 2 km downvalley at Helen Highwater Cave. A short surface stream segment leads into a ponor, Upper Sinking Cove Cave (frontispiece). Traced to a major stream passage in Sinking Cove Cave, the same water may be followed for 2 km to its final resurgence at Sinking Cove Cave Spring.

Tributary components of the system also consist of surface and cave stream elements. Caves carrying significant tributary streamflow include Cave Cove Cave, Shower Cave, Wolf Cove Cave, Waterfall Cave, and Ashlee Cave. Sinking Cove Cave also includes major tributary passages.

Underground tributaries appear to be independent; i.e., water does not tend to cross from one to another as in a single-aquifer system. In some areas, however, distributaries occur, especially where streams intersect major shale zones. Thus, for example, water sinking at Cave Cove Sink resurges at two springs in Wolf Cove.

Groundwater Flow Conditions

Vadose Groundwater Flow

Examination of caves and springs in the study area (Chapter II) indicates a prevalence of vadose flow conditions. Cave streams, like surface streams, generally have detectable gradients through alternating

pools and riffles on sandstone and chert gravel beds. While not all springs are able to be explored upstream, airflow is perceptible at most, suggesting continuous exposure to the atmosphere in upstream passages.

Rapid groundwater flow rates may be used to identify free-flow conditions. These rates can be estimated from flow-through times in groundwater tracing experiments. Trace #6, from Cave Cove Sink to Helen Highwater Cave and Sinking Cove Cave (29-31 December 1980), gave reasonably reliable data for flow-through times along the trunk water route, under moderate discharge conditions. Dye was first observed at Helen Highwater Cave 22 hours after emplacement in Cave Cove (peak concentrations occurred within the next several hours). Dye took a minimum of 8-14 hours more to reach SCC Spring.

Using a correction factor[1], 1.60 times the overland distance of 2050 m., the underground stream distance from Cave Cove Sink to Helen Highwater Cave is approximately 3280 m. The flow-through time, 22 hours, gives a groundwater flow rate of 149 m/hr. Calculated for the lower half of the trunk channel, from Helen Highwater Cave to SCC Spring, an in-cave distance of 2800 m (1750 m overland), the groundwater flow rate is 200-350 m/hr. Both derived flow rates indicate free-flow conditions.

---

[1]A representative factor was obtained from known cave distances in the study area. The trunk stream passage of Sinking Cove Cave, for instance, extends for 2130 m between the upper and lower ends of the cave, an overland distance of 1400 m. In Cave Cove Cave, a 1320 m long stream passage extends for 790 m overland. The average of correction factors derived from each of these caves, 1.52 and 1.67, respectively, is 1.60. This figure is used to roughly estimate unknown cave stream distances from overland distances in the study area.

Groundwater flow rates in the trunk channel are expected to be greater than those in smaller channels. An example of a much smaller channel is that between Green Barrel Pit and its outlet in Sinking Cove, Green Spring. Discharge from this spring is usually less than one litre per second. Dye injected into Green Barrel Pit, at a distance of 530 m overland, took approximately 48 hours to reach Green Spring. Given a corrected stream distance of 848 m, the groundwater flow rate, 18 m/hr, is much less than found in the trunk stream. Free-flowing vadose groundwater is, however, still indicated.

Paraphreatic Groundwater Flow

While free groundwater flow through the vadose zone appears to predominate in Upper Sinking Cove, areas of restricted groundwater movement exist. In caves near the bottom of Farmer Cove, for instance, ponded water bodies are found which produce sumps in cave passages. Similarly, at about the same elevation in Cave Cove Cave (360 m), lower-level passages (under the north wall of Farmer Cove) are flooded. These flooded caves may result from the presence of the 14 m of shales in the Hartselle Formation, located just beneath the floor of Farmer Cove.

Conditions of restricted flow which have similarities with phreatic flow, but are limited spatially (do not relate to a true watertable), are classified as paraphreatic. In the study area, paraphreatic flow conditions are generally limited to Farmer Cove, but flooded passages have also been found in the bottom of Wolf Cove Cave and Exercise Cave.

Seasonal Flow Variations

The impact of discharge variations on karst processes may be significant. Solutional processes are intensified during periods of high flow, and it may be that the bulk of erosion occurs during floods. Seasonal climatic patterns are partly responsible for these discharge events.

Discharge at Sinking Cove Cave Spring

The discharge from Sinking Cove Cave Spring, the main hydrologic outlet for the study area, was studied during parts of June, August, and September 1980, in conjunction with stream chemistry sampling (see Chapter IV). Direct discharge measurements and stage records were used to document changes in discharge from the system.

Discharge was measured using a Gurley flowmeter system, combining velocity readings from the flowmeter with surveyed cross-sectional areas. Choosing an appropriate site for measurements, however, proved difficult. In the boulder field below SCC Spring, several springs emerge. No one spring represents the total flow. A stage recorder was set up downstream of the point at which the flow from all of these springs join, in hopes of measuring the total flow. A rating curve was produced, relating discharge measurements to stage (Fig. 3.5a), thus allowing discharge to be calculated from measurements of stage.

A problem became apparent in the above analysis. As shown in the rating curve, discharge rapidly decreases with only slight changes in stage. It appears that extrapolated discharge reaches zero before stage does so. This is also seen when discharge is related to cross-sectional

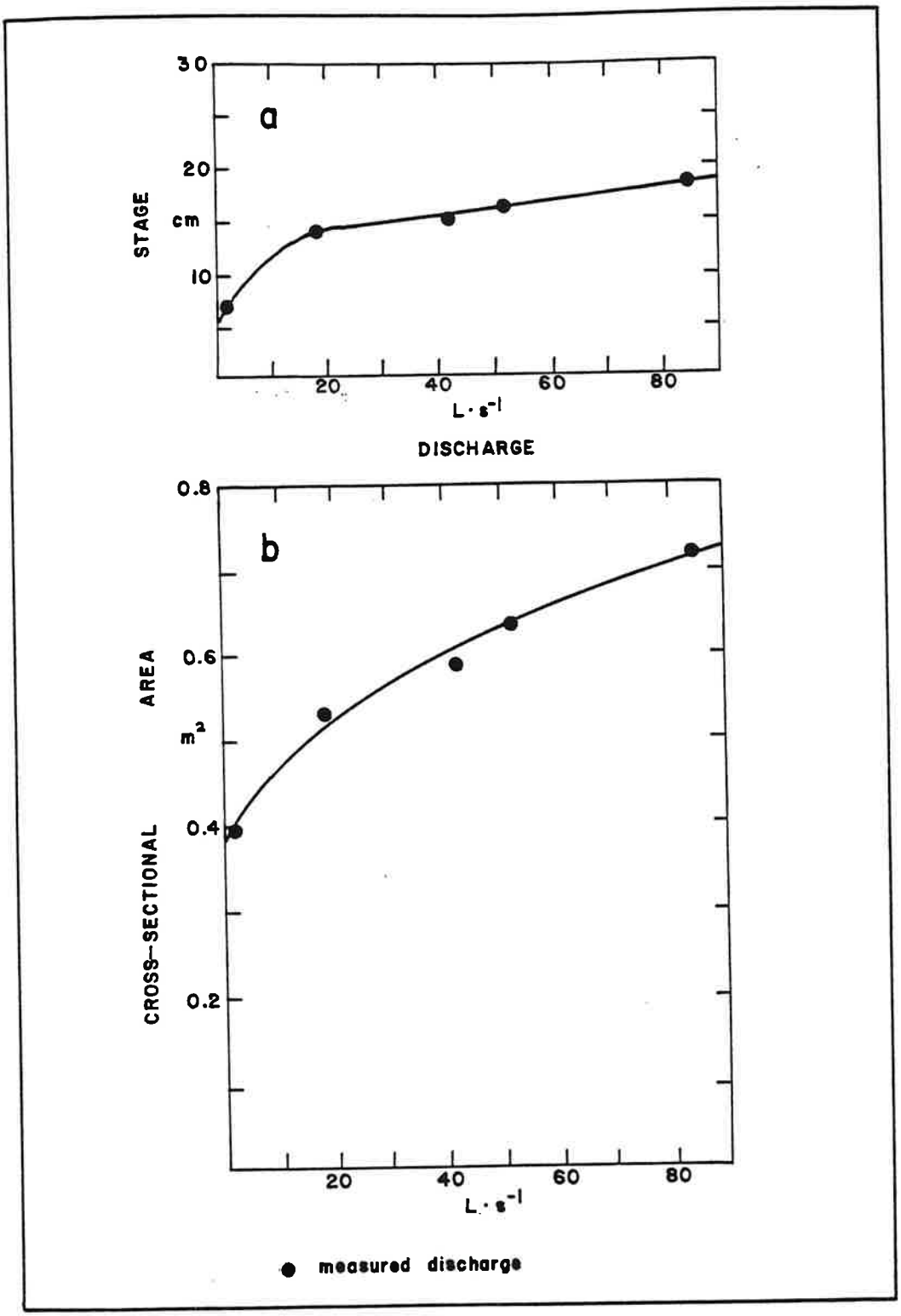

Fig. 3.5. Stage and discharge below Sinking Cove Cave Spring.

area (Fig. 3.5b). The extrapolated curve seems to indicate a cross-sectional area of 0.38 m^2 (over half that at peak discharge recorded) at a discharge of zero.

This may be explained by loss of flow to underground systems along the length in which discharge is being measured. This assessment is further supported by discrepancies between discharge measured at the stage recorder and at SCC Spring upstream. On 15 June measured discharge at the stage recorder was 26.3 L/sec. Two days later, with identical stage at the base station, measured discharge at SCC Spring was 36.0 L/sec. These results are surprising since SCC Spring is only one of at least three which combine to flow past the stage recorder.

Because of these measurement problems, an estimate of the runoff and thus discharge of the drainage basin was derived using a water budgeting method developed by Thornthwaite and Mather (1955). Daily records of precipitation and temperature were obtained from the Tennessee Valley Authority for stations near the study area (January 1979 - March 1981). From these values, monthly estimates of potential evapotranspiration and actual exapotranspiration (AET) were derived (Fig. 3.6; ~~Appendix B~~). Assuming a soil storage capacity of 100 mm, budgeting of water needs and supplies allowed estimates to be made of monthly soil moisture fluctuations, water deficits, and water surpluses. Assuming that a given percent[1] of surplus water is available for runoff each month, monthly runoff figures (in mm) were derived.

---

[1]For small drainage basins, relatively high runoff percentages are recommended. Seventy percent was used in this study.

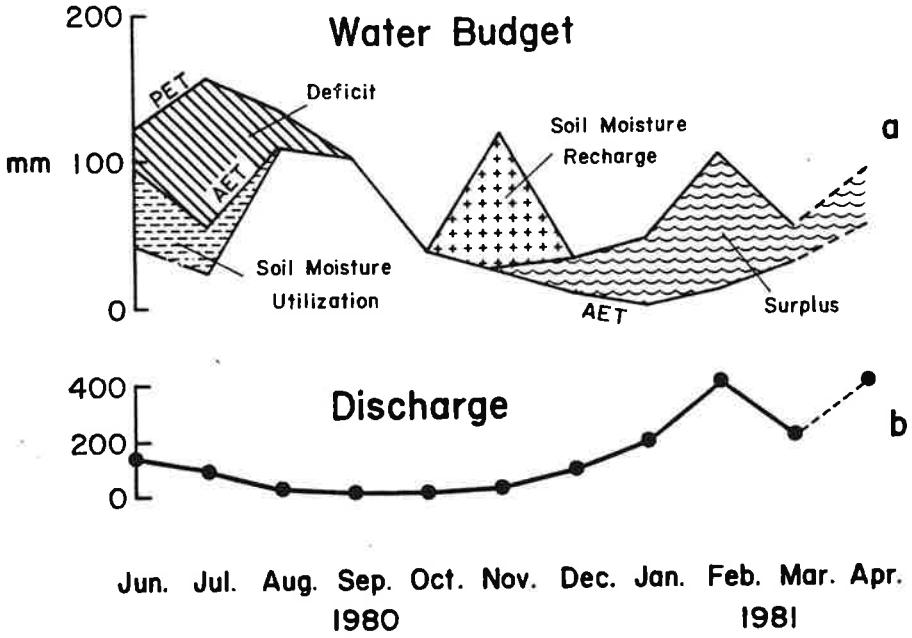

Fig. 3.6. Water budget curves and estimated drainage basin discharge from June 1980 to April 1981.

Mean monthly discharge values (in m^3/sec) for the study area were derived by multiplying runoff (in mm) by the estimated drainage area ($13.5 \times 10^5 m^2$), and dividing by 2.592×10^6 sec/month (Fig. 3.6b). The computed results were then compared with measured flows. In general, measured discharge at SCC Spring and the base station represented 20-25% of the computed total flow in June, August, and December (e.g., discharge measured at SCC Spring 30 December 1980 was 26.1 L/sec; computed discharge was approximately 130 L/sec). Considerable flow is apparently lost to lower systems.

Similar flow-loss situations were noted at other springs in the study area. Measured flows at springs appear to represent only a portion of the total flow from upstream drainage basins. Reliable estimates of the magnitude of tributary flow inputs could thus not be made.

Seasonal Discharge Trends and Floods

Observations from June 1980 to April 1981 indicate seasonal trends in stream discharge. Maximum seasonal precipitation occurred in winter 1980-81, producing a marked increase in discharge in February. Long-term climatic records for the area indicate that on average maximum precipitation occurs in winter as it did in 1980-81.

One result of the precipitation regime is that floods are common in the months of February, March, and April, verified by local residents. In 1979 and 1980, floods occurred in March. In March 1979, cave explorers were trapped in Sinking Cove Cave as the cave stream rose to the low ceiling of the passage just above the spring entrance. According to reports, not only was the lower portion of this cave flooded, but

so was much of the floor of Sinking Cove (R. Buice, W. Chamberlin, pers. comm.).

One year later, after 122 mm rainfall on March 19 and 20, flooding was even more extensive. Local residents considered this flood the worst in at least 20, and perhaps 50 years. Attempts to visit Upper Sinking Cove at this time were prevented by swollen streams downvalley from SCC Spring. Only the spring at the head of Little Crow Creek, which drains Sinking Cove itself, could be reached. Photographs of this spring before and during the flood (Fig. 3.7-3.9) attest to its magnitude.

Observation was thus limited to the aftermath of the flood. Flood debris in Farmer Cove indicated that this depression had been inundated to a depth of 10 m (Fig. 3.10). Debris on the walls of the lower passages of Cave Cove Cave indicates that water levels in the cave rose at least 14 m. Since Farmer Cove Estavelle is believed to be an overflow outlet for Cave Cove Cave, the flooding of Farmer Cove probably resulted from a combination of surface and springflow into Farmer Cove with input from Cave Cove, through the cave.

Paleohydrology

Clues about the nature of past hydrologic systems in Upper Sinking Cove are preserved in its caves. Caves have been found which apparently once served as drainage conduits, but lost their source of water as a result of subterranean stream piracy upstream. Evidence about the nature of past flow conditions may also be seen in characteristic passage morphologies and depositional features.

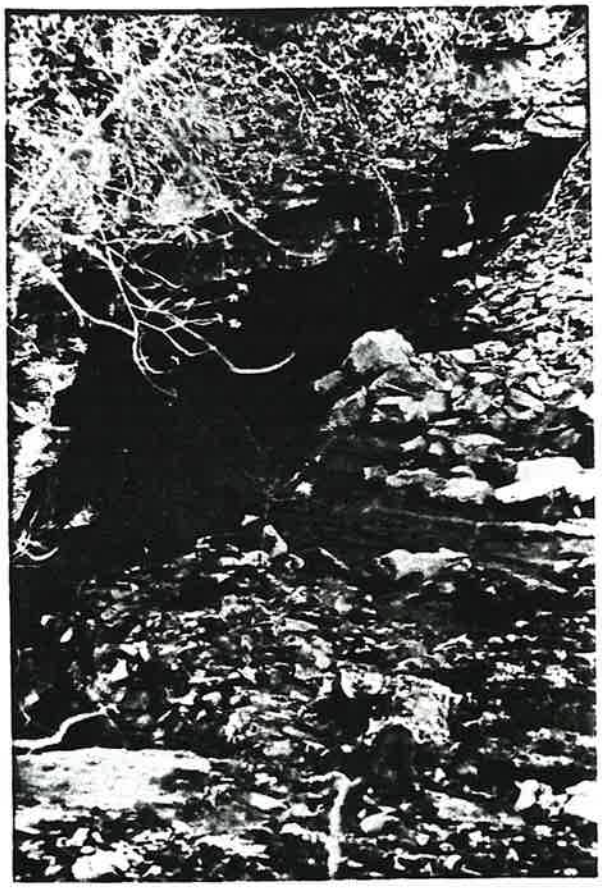

Fig. 3.7. Spring at the head of Little Crow Creek (drains Sinking Cove), under normal flow conditions. View from the south.

Fig. 3.8. Spring at the head of Little Crow Creek, under flood conditions, 20 March 1980. View from the north.

Fig. 3.9. Outflow downstream of Little Crow Creek spring, under flood conditions. The standing waves are approximately 1.0 m high.

Fig. 3.10. Part of the floor of Farmer Cove, photographed a few weeks after the March 1980 flood. Debris left by the flood reached the level indicated by the arrow.

Relict Features of Past Drainage Systems

Inactive subsurface drainage routes are sometimes preserved as relict cave passages. Cave Cove Cave, for example, appears to be a relict drainage conduit for Cave Cove. Its entrance (see Fig. 2.15) is situated at the end of a presently dry streambed. Two hundred metres inside, the entrance passage intersects the caves currently active stream passage. A ceiling channel in the main passage downstream of the intersection appears to have been a former extension of the entrance passage. The source of flow for this passage may have been cut off when Cave Cove Creek was pirated underground 720 m upvalley at Exercise Cave.

Another example of changes in underground drainage over time is Suicide Cellar Cave, in Farmer Cove, which may once have been a downvalley extension of Cave Cove Cave. Subterranean stream piracy appears to have beheaded Suicide Cellar Cave, leaving it as a detached remnant of a former trunk drainage system which extended from Cave Cove across what is now Farmer Cove.

Evidence of former, now abandoned, drainage routes is also present in Wolf Cove and Sinking Cove. Thorn Cave may at one time have been part of the Sinking Cove Cave System, but was separated by the development of the blind valley in the lowest part of the floor of Wolf Cove. The relict spring entrance at Sinking Cove Cave Spring is further evidence of past changes in underground drainage routes.

Groundwater Flow Conditions in the Past

The character and distribution of relict caves suggests that a vadose, multiple-aquifer drainage system existed in the past. Sinuous

passages with scalloped walls and eroded sediment fills indicative of vadose flow are common, while honeycomb and anastomosing passages indicative of paraphreatic flow occur in limestones underlain by aquitards. Relict cave passage gradients almost always indicate vadose flow.

Ancient deposits in caves are also indicative of past changes in streamflow activity. In some relict cave passages, sequences of stream-laid deposits recorded changes in the function of the passage as lower stream passages were developed and absorbed the flow. In other passages, alternations between periods of active streamflow and relatively dry conditions were suggested by the presence of redissolved calcite deposits.

In the main passage of Cave Cove Cave, for example, are redissolved speleothems which indicate a recurrent phase of streamflow activity near the ceiling of the passage. Most of these calcite deposits are small stalactites (20-30 cm in length) and are 2.5-3 m above the cave floor. Aggradation of stream sediments might explain the apparent renewal of streamflow at this level in the passage.

One large flowstone deposit in this passage appears to record two calcite depositional phases. A redissolved older deposit is partially covered by an unaffected flowstone which extends 2 m from the south wall of the passage. Deposition apparently occurred on top of stream sediments which have since eroded, leaving the flowstone suspended 1.8 m above the cave floor. Clastic stream gravels remain attached to the bottom surface of the feature (Fig. 3.11).

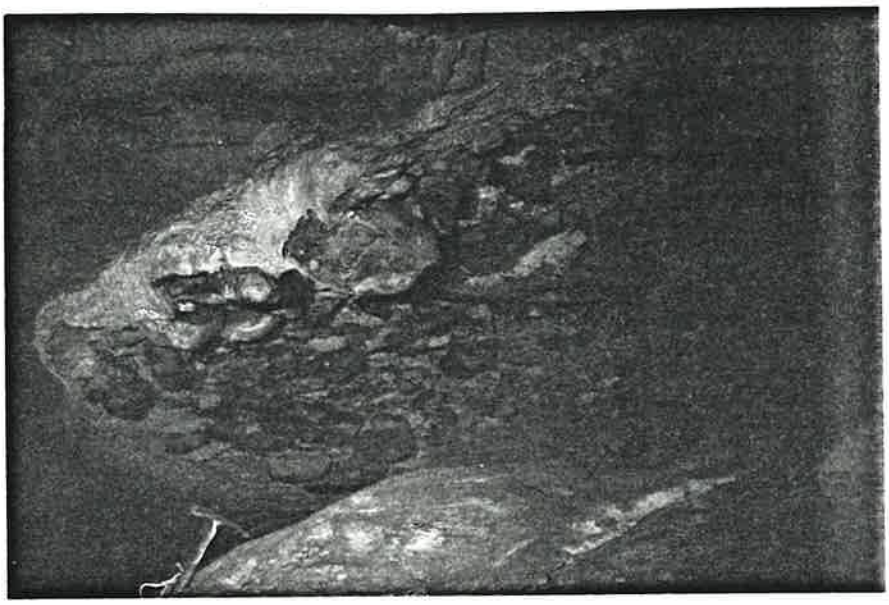

Fig. 3.11. Underside of a relict flowstone, suspended above the floor of Cave Cove Cave. Sandstone cobbles are imbedded.

Deposits in Wolf Cove Cave also record a history of flow changes. A sediment sequence in Footloose Passage, resting on a ledge of silty shale, may have been deposited under conditions of diminishing stream-flow, probably resulting from stream piracy as lower passages developed. Streamlaid gravels are overlain by cross-bedded sands and a flowstone cover (Fig. 3.12). Subsequent collapse into lower passages exposed the sequence in the upper walls of the passage.

Near the lower entrance of Sinking Cove Cave, gours 1-2 m high appear to be relict features (Fig. 3.13). At no time during the study period was any flow observed. Nearby are stalactites, stalagmites, and flow-stones (some of which remain active). Considerable re-solution of these deposits has occurred (Fig. 3.14), and may be a result of an increase in flooding of this passage.

Geology, Hydrology, and Cavern Development

Lithologic Controls

The elevations of springs in the study area are closely related to the elevations of aquitards. Five springs were observed between 455 and 465 m a.s.l., associated with a shale bed at 450 m in the Pennington Formation. At 405-420 m a.s.l., four springs are associated with the dolomitic limestones and shale partings near the base of the Pennington. Four springs occur in Wolf Cove on the Hartselle Formation, at 345 m a.s.l. Two other springs are related to the 2 m shale bed at 320 m a.s.l. in the Monteagle Limestone. Finally, in Sinking Cove, several springs occur between 260 m and 270 m a.s.l., on chert beds of the lower Monteagle and upper St. Louis Limestones. The only spring in Upper Sinking Cove not located at an aquitard is Farmer Cove Spring.

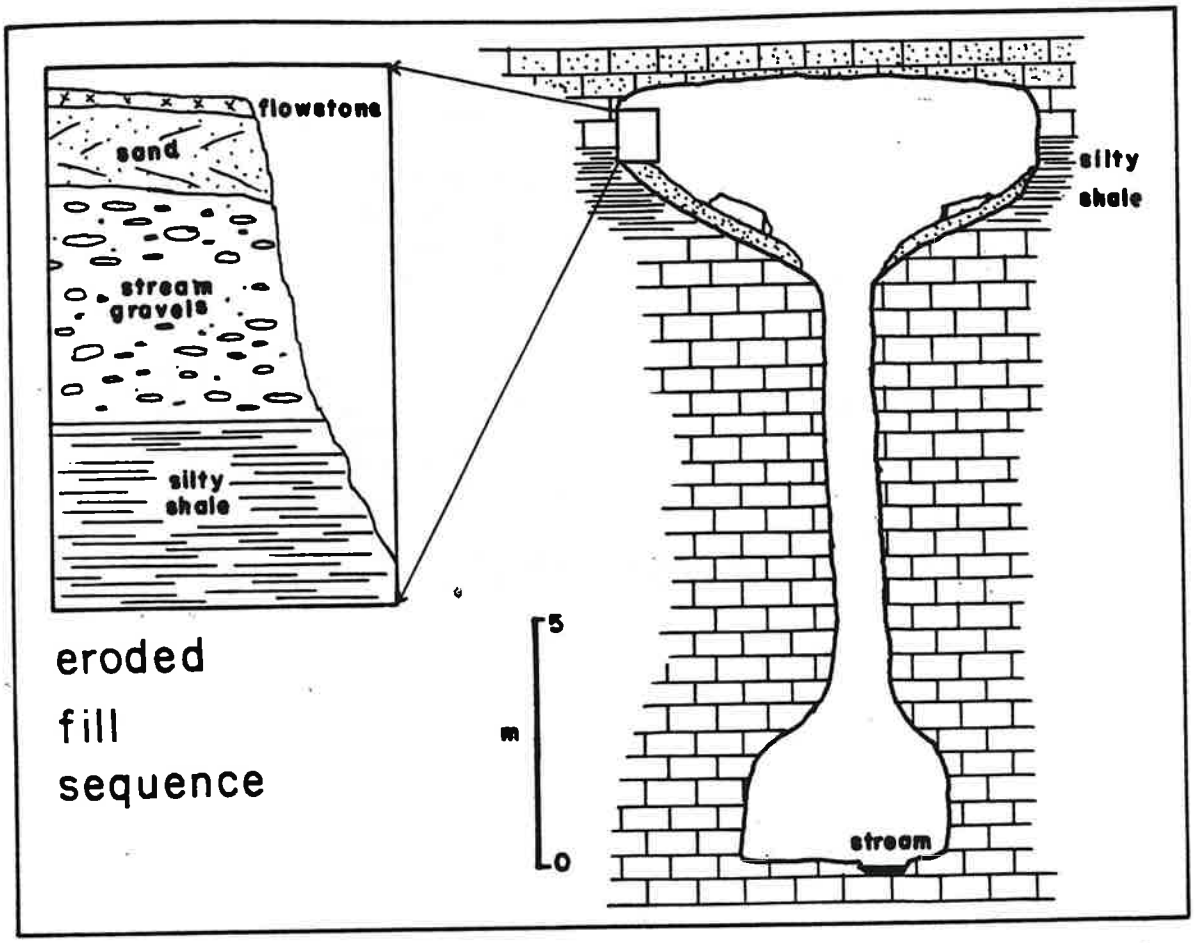

Fig. 3.12. Location of an eroded fill sequence in a typical cross-section of Wolf Cove Cave.

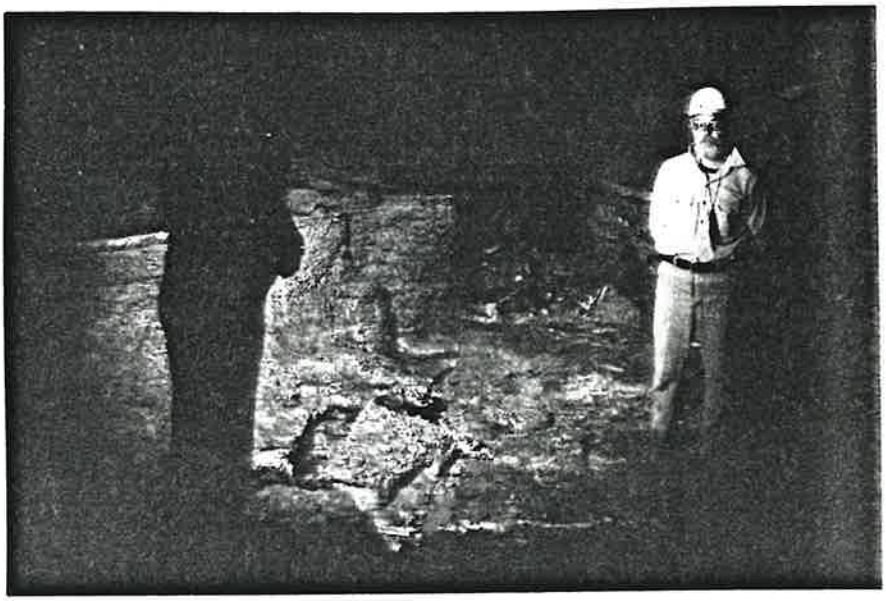

Fig. 3.13. Relict gours in Sinking Cove Cave.

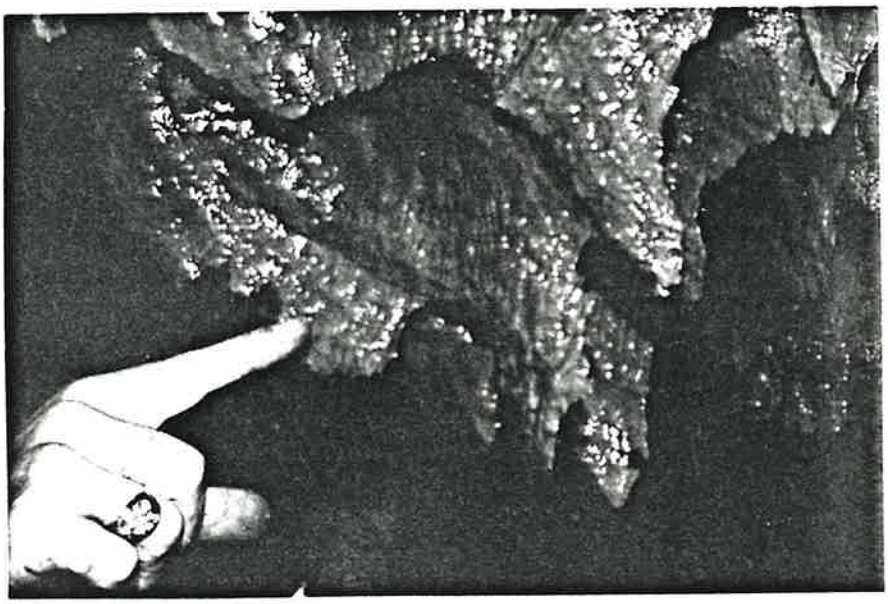

Fig. 3.14. Redissolved speleothems in Sinking Cove Cave.

Streamsink locations are frequently determined by changes in lithology. The Pennington/Bangor contact is a good example of this as no surface streams extend beyond this contact zone. Other major areas of streamsinks include the top of the Pennington Formation, below the caprock, and the top of the Monteagle Limestone, below the Hartselle Formation.

Locations of in-cave water bodies under paraphreatic flow conditions are generally limited to areas directly above aquitards. The presence of flooded cave passages above the Hartselle Formation in Farmer Cove is one instance.

Relict caves which indicate past paraphreatic flow conditions are also associated with aquitards. Anastomoses observed in Wolf Cove Cave and Shower Cave, for example, are in limestones directly above the 2 m shale bed in the Bangor at 382 m a.s.l.

Two major base levels are evident in the study area, one at shales in the Hartselle Formation, the other at cherts on the Monteagle and St. Louis Limestones. The effect of these may be seen in a longitudinal profile of the study area which shows the most important caves (Fig. 3.15).

Structural Controls

The influence of joints and bedding planes on the paleohydrology of the study area can be seen in cave passages. Some passages are preferentially widened along these structural features. Former bedding plane anastomoses and joint-aligned passages are commonly preserved as ceiling channels. The importance of bedding planes cannot always be distinguished from the effects of variations in bedrock lithology. If joints are preferentially selected for passage development, this will be

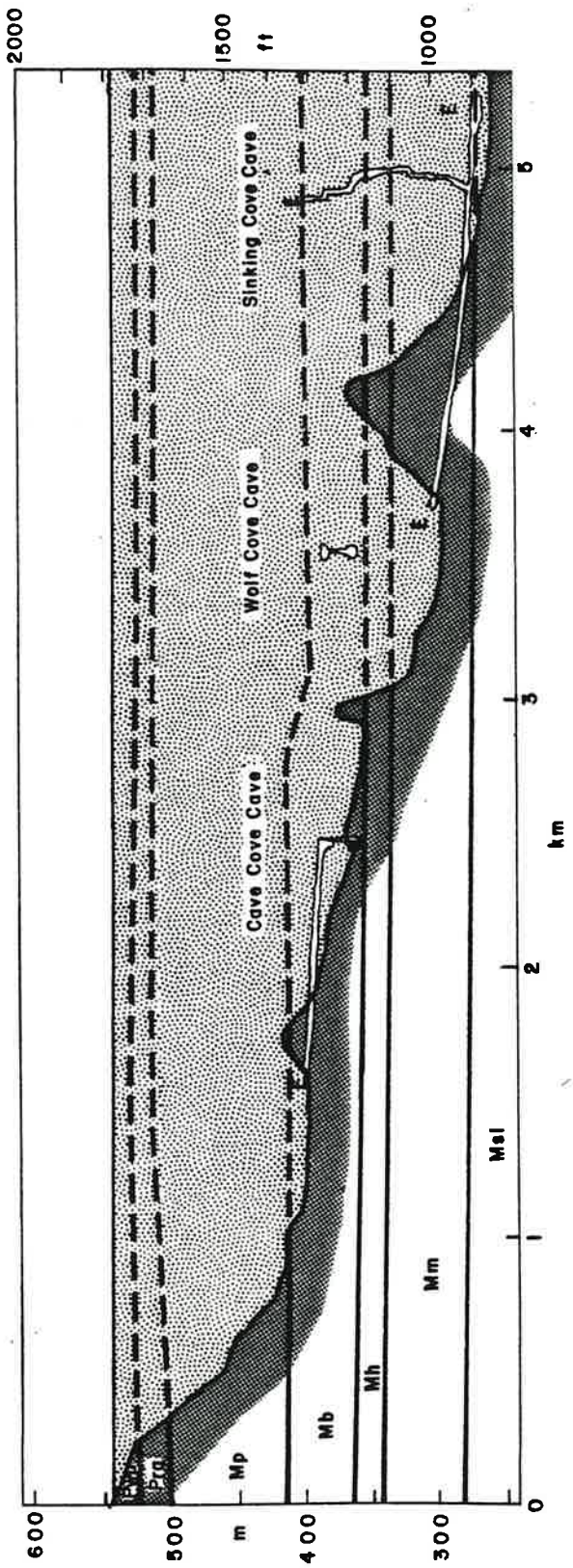

Fig. 3.15. Diagram showing the longitudinal cross-section of the study area, measured along the central axes of the major depressions (lower part of figure). The plateau surface (upper part of figure), the stratigraphy, and major caves are also shown. See Table 2.1 and Figure 2.3 for definitions of stratigraphic units (P_{wp}, Pra, Mp, etc.).

reflected in higher frequencies of passage orientations near joint orientations. If no orientational controls are active, a uniform distribution is expected. A sinuous or meandering habit in cave passages may produce a uniform orientation distribution.

To test the control of joints in study area caves, orientations of passages were measured from cave maps. A total of 138 orientations were measured from passages in Sinking Cove Cave (96), Wolf Cove Cave (18), and Cave Cove Cave (24). These were grouped for each cave into 18 ten-degree intervals from 270° to 90°, and displayed in rose diagrams (Fig. 3.16). Cave passage orientation distributions from Sinking Cove Cave and Cave Cove Cave exhibit concentrations near 315° and 55°. As noted in Chapter II, joint orientation distributions are also bimodal, but with concentrations near 295° and 35°.

The significance of peaks in orientation data has been analyzed by Sawatzky (1977) for lineaments on Landsat imagery. A significance value is obtained for each class frequency in relation to an expected frequency, defined by the mean (u). Given that:

f = no. of azimuths per smoothing intervals

N = total no. of measurements

p = smoothing interval/180°.

Then

$$P_f = \frac{N!}{f!(N-f)!} \times pf(1-p)^{N-f}$$

Three possibilities exist

1. f is less than u. Then

$$SV \text{ (significance value)} = 1 - \frac{\sum_{n=0}^{f} Pn}{\sum_{n=0}^{u} Pn} \times 100$$

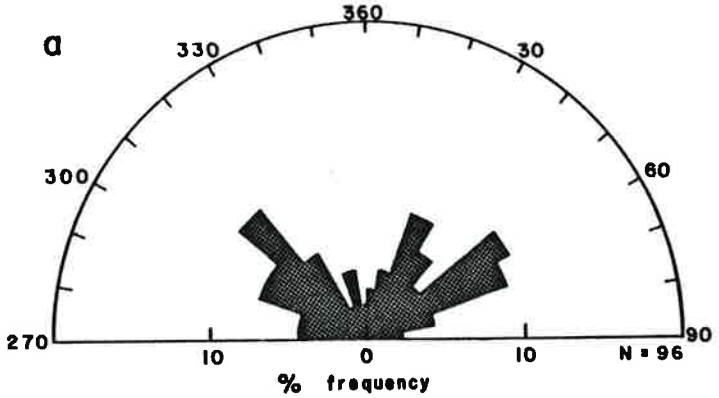

Sinking Cove Cave Passages

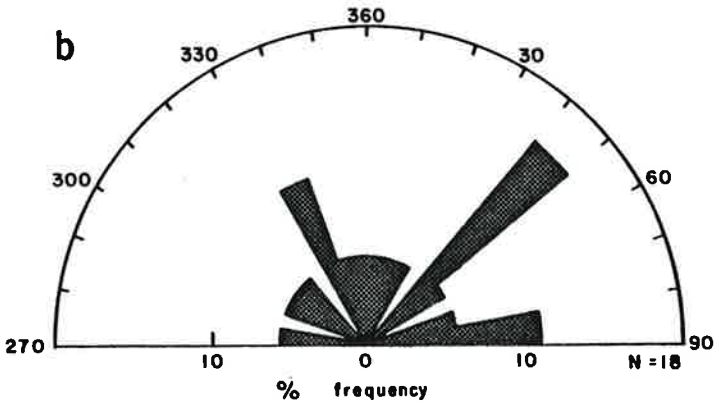

Wolf Cove Cave Passages

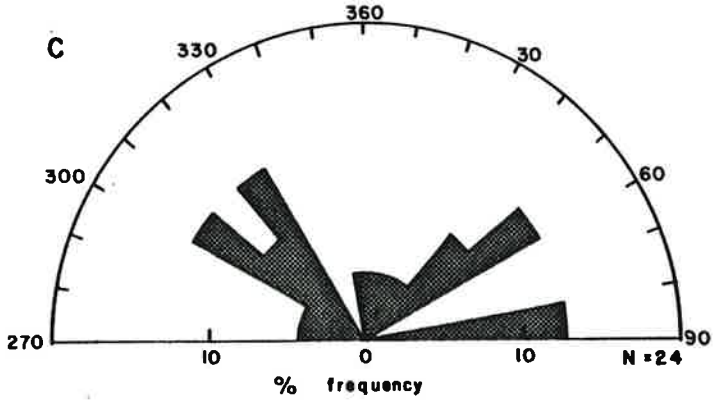

Cave Cove Cave Passages

Fig. 3.16. Cave passage orientations of selected caves in Upper Sinking Cove.

2. f is greater than u. Then

$$SV = 1 - \frac{\sum_{n=f}^{N} Pn}{\sum_{n=u}^{N} Pn} \times 100$$

3. f is equal to u. Either formula yields zero SV. Based on the author's experience, values over 90 are considered significant. Values increase with greater dispersion from the expected value, so classes with either low or high frequencies may be significant.

A FORTRAN program, TREND (C. H. Sun, 1981), using the above formulas, was used to analyze the cave passage and joint orientation data. Orientations were grouped in 10°, 20°, and 30° increments from 270° to 90°. Significant classes are shown in Table 3.3.

Using 10° increments, four significant classes, all high-frequency, are indicated for joint orientations. Sinking Cove Cave has two significant classes, but none corresponding to those of joint orientations. Cave Cove Cave and Wolf Cove Cave passages produce no significant classes.

Using 20° increments, six significant classes are indicated for joint orientations. One of these (350°-9.9°) is also significant for Sinking Cove Cave passage orientations, and another (330°-349.9°) for Cave Cove Cave orientations. Both are low-frequency classes. No significant classes are indicated for Wolf Cove Cave passages.

Three significant classes are indicated for joint orientations using 30° increments. One of these (330°-359.9°), again a low-frequency class, is also significant for Sinking Cove Cave passage orientations.

Table 3.3. Significant orientation classes: joints and cave passages in Upper Sinking Cove.

Joints	Cave passages		
	Sinking Cove C.	Cave Cove C.	Wolf Cove C.
Interval = 10° :			
290-299.9 +			
300-309.9 +			
	310-319.9 +	None	None
020-029.9 +			
030-039.9 +			
	050-059.9 +		
Interval = 20°:			
290-309.9 +			
310-329.9 -			
330-349.9 -		330-349.9 -	
350-009.9 -	350-009.9 -		None
030-049.9 +			
	050-069.9 +		
070-089.9 -			
Interval = 30°:			
	300-329.9 +	300-329.9 +	
330-359.9 -	330-359.9 +		None
030-059.9 +			
060-089.9 -			

\+ High-frequency classes.

\- Low-frequency classes.

No similarities exist with Cave Cove Cave significant classes. Wolf Cove Cave passages again show no significant trends.

The presence of coincident significant classes in joint and cave passage orientations indicates a significant degree of structural control in the development of Sinking Cove and Cave Cove Caves. Bimodal peak frequencies for cave passages tend to occur 10° to 20° clockwise from joint orientation peaks. The presence of other orientational controls is suspected.

The two tendencies of cave passages noted above, toward non-uniformity from joint control or toward uniformity from a sinuous habit, are thus exemplified to varying degrees among caves in the study area. All caves exhibit joint-controlled passages and sinuous passages. In Sinking Cove Cave and Cave Cove Cave, significant numbers of joint-controlled passages exist. Passages in Wolf Cove Cave, however, exhibit a greater degree of uniformity.

Conclusions: The Hydrology of Upper Sinking Cove

The hydrology of the study area may be described as a karst drainage system dominated by subsurface flow through vadose caves. Surface flow is generally limited spatially to areas underlain by aquitards and surface alluvium, or temporally to periods of excessive discharge when conduit systems are overloaded and water backs up into surface depressions. The present drainage system has evolved from relict systems with similar characteristics.

CHAPTER IV

SOLUTIONAL DENUDATION OF UPPER SINKING COVE

In this chapter, solutional denudation processes active in Upper Sinking Cove are studied by examining the chemistry of waters in various parts of the drainage system, at different times of the year. Spatial and seasonal patterns in water chemistry and soil CO_2 levels are analyzed. Solutional denudation in the study area is quantified (1) on the basis of the water chemistry data, and (2) by measuring solutional erosion of rock tablets placed at various sites in Upper Sinking Cove.

Water Chemistry

The chemistry of water in the study area was examined through a combination of field, laboratory, and statistical analyses. Nine chemical variables were measured in samples collected from June 1980 through April 1981. Using these variables, the chemical activities of the most common positive and negative ions dissolved from limestone (Ca^{2+}, Mg^{2+}, and CO_3^{2-}) were estimated.

Measurements of water temperature, pH, electrical conductivity, and alkalinity (as HCO_3^-) were made in the field. Water samples (250 or 500 mL) were collected for laboratory analysis. A Sargent-Welch pH meter, calibrated with buffers at 7 and 4 pH, was used for pH and alkalinity measurements. Alkalinity was determined by titration of a

20 mL sample of stream water with .01N HCl to an endpoint between 3 and 4 pH. Alkalinity, in equivalents per litre, was calculated using the equation:

$$Alk(eq/L) = \frac{VaCa - Hf(Va + Vs)}{Vs}$$

where

Va = volume of acid used (mL)

Ca = concentration of acid used (eq/L) = .01 eq/L

Hf = final H^+ concentration of solution ($Hf = 10^{-pH}$)

Vs = sample volume (mL) = 20 mL

Conductivity, in micromhos, was measured with a YSI Salinity-Conductivity-Temperature meter. Conductivity is a measure of ionic strength and was used as a field indicator to total hardness. Where possible, readings were completed at the stream site. In order to protect the instruments, however, cave waters were analyzed at the surface.

In the laboratory, water samples were titrated for total and calcium hardness, using Hellige reagents.[1] The Versene method was used to determine calcium and magnesium concentrations. Fifty millitres water samples were used for each titration. Hardness in parts per million (mg/L) - $CaCO_3$ equivalent (ppm*) was calculated by multiplying the titrating solution (Versene) volume used to reach the end-point (in mL) by 20. All titrations were repeated until two values were obtained which differed by no more than 2 ppm*. Titration results represent an average of these two values.

---

[1] Hellige, Inc., Garden City, NY. Versene was used with borax sulfide and indicators for total hardness; and with sodium hydroxide and indicators for calcium hardness.

Elemental analysis of a few samples was used to determine concentrations of 20 elements, including calcium and magnesium. These samples were collected in 50 mL sample bottles. A few drops of 20% HNO_3 were added to each sample to prevent biologic interference. Samples were analyzed in the Plasma Emission Spectrometry Laboratory at the Institute of Ecology, University of Georgia.

Saturation indices with respect to calcite (SI_C) and dolomite (SI_D), equilibrium partial pressures of carbon dioxide (as -log PCO_2), and bicarbonate ion concentrations in water samples were derived using a FORTRAN program, TOMCHEM (Wigley, 1971). Input variables to the program were pH, alkalinity, temperature, and calcium and magnesium hardness. Activities of individual ions in solution were computed according to:

$$a_i = f_i m_i$$

where

a_i = the activity of the individual ion

f_i = the activity coefficient of the ion, estimated by an iterative process, using molar concentrations of all cations and anions (CO_3^{2-} concentrations are estimated from alkalinity and pH values) and water temperature

m_i = the molar concentration of the individual ion

Saturation indices represent the thermodynamic state of a solution relative to equilibrium with a solid-phase mineral. The saturation index for calcite, for example, is given by

$$SI_C = \log\left(\frac{IAP}{K_C}\right)$$

where

IAP = the ion activity product, $a_{Ca}^{2+} \times a_{CO_3}^{2-}$

K_c = the equilibrium constant for $CaCO_3$

If at equilibrium, K_c = IAP, and the ratio will be unity, giving SI_C = 0. If IAP is less than K_c, saturation has not been reached, and is indicated by a negative SI_C. If the sample is supersaturated, SI_C will be positive.

Alkalinity and pH measurements were used for computation of the activity of CO_3^{2-}. These were also used to estimate PCO_2 levels at equilibrium with a theoretical gas phase, according to Henry's law.

TOMCHEM also computes a charge balance error value, comparing concentrations of positive and negative ions. Input from the study area typically produced positive error. This probably results from the presence of unmeasured sulfate ions (SO_4^{2-}), commonly derived from shale minerals.

Five variables, temperature, pH, total hardness, SI_C, and log PCO_2, are used to describe samples. Due to their close correlations with total hardness and SI_C, respectively, conductivity and SI_D are not needed to characterize samples. They are, however, included in the tables for comparison.

A description of the 39 water sampling sites is given in Table 4.1. These may be identified on topographic maps in Figures 4.1, 4.3 and 4.6.

Water Samples Collected 15-30 June 1980

A base camp was set up 150 m downstream of SCC Spring on 15 June 1980. A stage recorder was assembled for streamflow studies (Chapter III), and a sampling program initiated. Samples were collected daily from the

Table 4.1 Water Chemistry Sampling Sites, Upper Sinking Cove

Site	Elevation (m asl)	Geologic Formation	Description
T1	535	Pwp	stream flowing on the plateau surface, upstream from the caprock escarpment at Still Cave, at the head of Cave Cove
T2	490	Mp	First resurgence of trunk stream (Cave Cove Creek) below Still Cave
T3	460	Mp	Lower resurgence of Cave Cove Creek
T4	440	Mp	Cave Cove Creek flowing over shales
T5	425	Mp	Cave Cove Creek immediately above confluence with a major surface tributary in headward Cave Cove
T6	415	Mp	Cave Cove Creek immediately above Cave Cove Sink at Exercise Cave
T7	320	Mm	Cave Cove Creek resurgence in Wolf Cove, at Helen Highwater Cave
T8	300	Mm	Cave Cove Creek in Sinking Cove Cave, under Wolf Cove
T9	270	Mm	Cave Cove Creek final resurgence in Sinking Cove: SCC Spring
B1	260	Msl	Cave Cove Creek in boulder field
B2	260	Msl	Cave Cove Creek at base camp, 150 m downstream from SCC Spring
K1	400	Mp	spring above Green Barrel Pit, above the Pennington/Bangor contact
K2	260	Msl	Green Spring, outlet for Green Barrel Pit, in Sinking Cove
K3	290	Mm	stream flowing through Ashlee Cave
K4	400	Mp	spring near the Boulder Entrance to Sinking Cove Cave, above the Pennington/Bangor contact

Table 4.1 (continued)

Site	Elevation (m asl)	Geologic Formation	Description
K5	275	Mm	Boulder Entrance tributary at confluence with Cave Cove Creek, in Sinking Cove Cave
K6	260	Msl	spring near base camp, at edge of boulder field
W1	525	Pra/Mp	stream flowing off caprock to the north of Wolf Cove
W2	425	Mp	streamsink above Wolf Cove Cave
W5	355	Mb/Mh	Waterfall Cave spring
W6	305	Mm	Thorn Cave spring (downstream from W5)
W7	300	Mm	Waterfall/Thorn tributary in Sinking Cove Cave
W8	455	Mp	spring in the canyon wall to the south of Wolf Cove
F1	365	Mb	Farmer Cove Spring
F2	365	Mb	Farmer Cove Creek (downstream from F1)
F3	355	Mb	stream flowing through Farmer Cove Cave
F4	355	Mb	Farmer Cove Estavelle (standing water in a small flooded cave near passages of Cave Cove Cave
C1	355	Mb	ponded water in lower-level Cave Cove Cave
V1	425	Mp	Lower Pennington Cave spring, in headward Cave Cove
P2	555	Pwp	Robin's Pond on plateau top

Table 4.1 (continued)

Site	Elevation (m asl)	Geologic Formation	Description
Sinking Cove Cave:			
D1	(SCC)	Mm	dripwater under Wolf Cove
D2	(SCC)	Mm	dripwater under Wolf Cove saddle
D3	(SCC)	Mm	dripwater
D4	(SCC)	Mm	dripwater
D5	(SCC)	Mm	dripwater in first breakdown room (no calcite deposits associated)
D6	(SCC)	Mm	dripwater
D7	(SCC)	Mm	dripwater
D8	(SCC)	Mm	dripwater
S4	(SCC)	Mm	gour pool near D4

stream at the base camp, or from SCC Spring, in order to measure time-related chemical variations. Samples were also collected from 16 other locations distributed throughout the study area including one sample of dripwater from Sinking Cove Cave (Table 4.2; Fig. 4.1).

Average characteristics of samples collected during the June period were:

Temperature = 14.9°C

pH = 7.5

Total hardness = 91.9 ppm*

SI_C = -1.45

Log PCO_2 = -2.72 (-3.18, if P2 is excluded)

Elevation = 361 m

Temperature varied from 12.5°C in Cave Cove Cave to 24.6°C in Robin's Pond (P2). No water from springs or cave streams was warmer than 14.9°C. Except for the relatively acid waters above the caprock, pH values were between 7.5 and 8.0. Total hardness in springs and streams varied from 3 ppm* in a stream flowing from the caprock (W1) to 137 ppm* at Green Spring (K2), in Sinking Cove. The dripwater sample from Sinking Cove Cave had the highest hardness of any sample collected during the study: 292 ppm*. Waters in streams and springs were all undersaturated, with SI_C varying from -7.70 on the caprock (W1) up to -0.43 at SCC Spring. The only saturated sample was the Sinking Cove Cave dripwater. The lowest and highest PCO_2 values were associated with waters on the plateau surface. The highest (-1.66) was derived from Robin's Pond, but may reflect lowering of pH by organic acids.

Table 4.2 Selected Water Chemistry Sampling Results, Upper Sinking Cove, 15-30 June, 1980

Site	Date (6/80)	Temperature (°C)	pH	TH (ppm*)	Conductivity (μmhos)	SI_C	SI_D	log PCO_2
T6	26	16.7	7.8	53	88	-1.20	2.88	-3.46
T7	25	14.3	7.8	115	140	-0.61	-1.72	-3.14
T8	19	13.3	7.8	122	160	-0.51	-1.61	-3.06
T9	17	13.0	7.9	126	144	-0.43	-1.34	-3.16
B2	16	13.9	8.0	125	143	-0.35	-1.21	-3.30
K2	15	13.1	7.7	137	160	-0.63	-1.68	-2.98
K3	16	13.2	7.8	148	170	-0.45	-1.31	-3.03
K5	19	13.2	7.8	122	137	-0.56	-1.52	-3.06
K6	16	13.3	8.0	120	148	-0.37	-1.29	-3.31
W1	18	18.3	5.4	3	8	-7.70	-15.09	-3.63
W5	18	14.0	7.6	77	97	-1.13	-2.80	-3.10
W8	15	13.3	7.5	58	70	-1.43	-3.49	-3.09
F1	26	13.7	7.9	100	125	-0.69	-1.87	-3.35
F2	26	16.9	7.9	99	131	-0.61	-1.74	-3.33
V1	26	14.9	7.5	46	64	-1.64	-3.78	-3.22
C1	27	12.5	8.0	109	238	-0.44	-1.27	-3.28
P2	18	24.6	5.6	6	13	-4.77	-9.54	-1.66
D8	19	13.5	7.9	292	352	+0.19	-0.02	-2.85

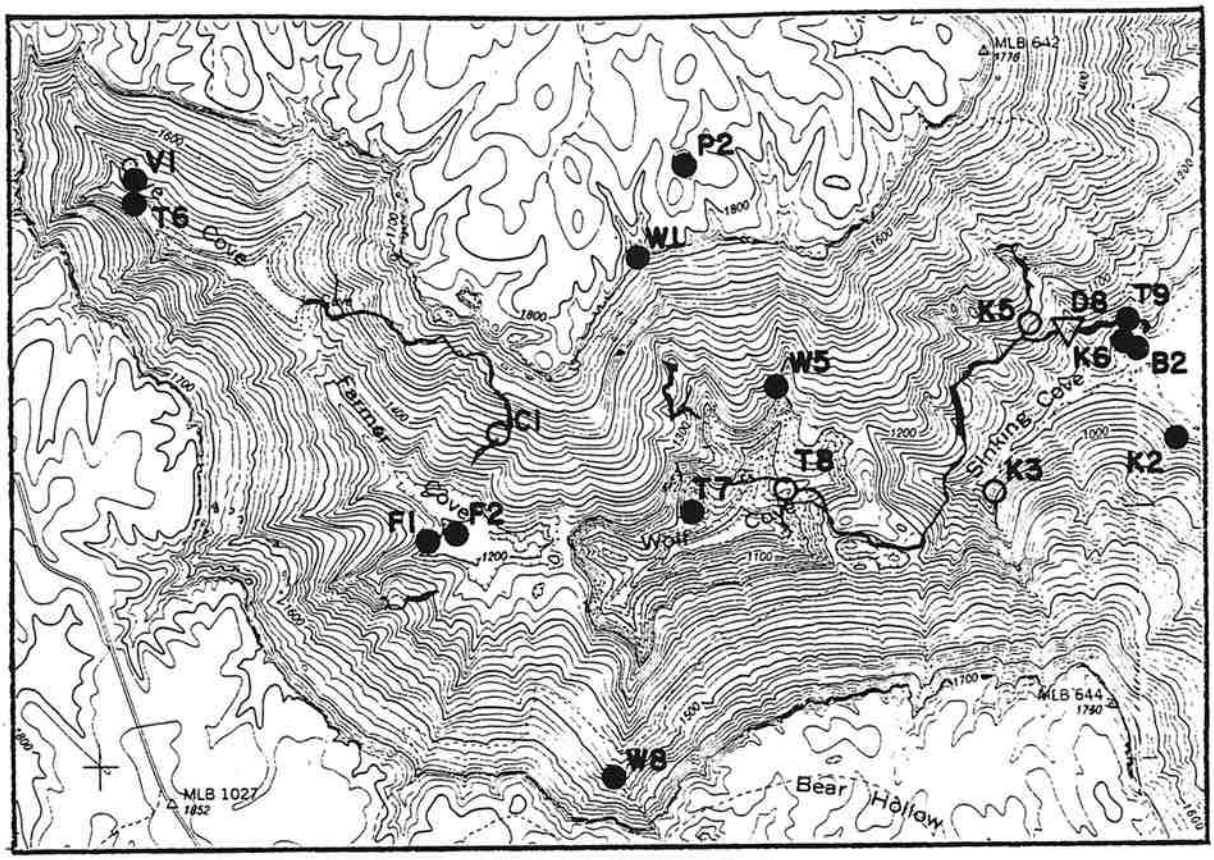

● Surface Streams and Springs

○ Cave Streams

▽ Cave Dripwaters

Fig. 4.1. Water chemistry sampling sites, June 1980. See Table 4.1 for site descriptions.

Water Samples Collected 12-23 August 1980

A new sampling program was initiated on 12 August 1980. As discharge from SCC Spring had stabilized at low flow, emphasis was placed on spatially distributed sampling. Knowledge gained of the drainage system from stream traces in June was used to select sampling locations. Nine sites along the trunk stream from the caprock above Cave Cove to SCC Spring were sampled. Seventeen other locations, including 7 dripwaters in Sinking Cove Cave (D1-D7), were also sampled (Fig. 4.2). Results are given in Table 4.3.

Average characteristics of samples (excluding cave dripwaters) collected during August were:

Temperature = 15.8°C

pH = 7.5

Total hardness = 91.8 ppm*

SI_C = -1.33

Log PCO_2 = -2.92

Elevation = 374 m

Spatial variations in water chemistry in August were similar to those in June (Table 4.3). Water temperatures were higher overall, and ranged from 13.0°C in Ashlee Cave to 20.8°C in Cave Cove Creek, immediately above Exercise Cave. pH again ranged between 7.5 and 8.0, except for the caprock stream sample (T1: pH = 5.4). Total hardness varied from 5 ppm* in the caprock stream to 146 ppm* at Green Spring (Fig. 4.3). Samples wereagain undersaturated, but six of the seven sites sampled in both June and August were closer to saturation in June. There was no systematic pattern to log PCO_2 variations.

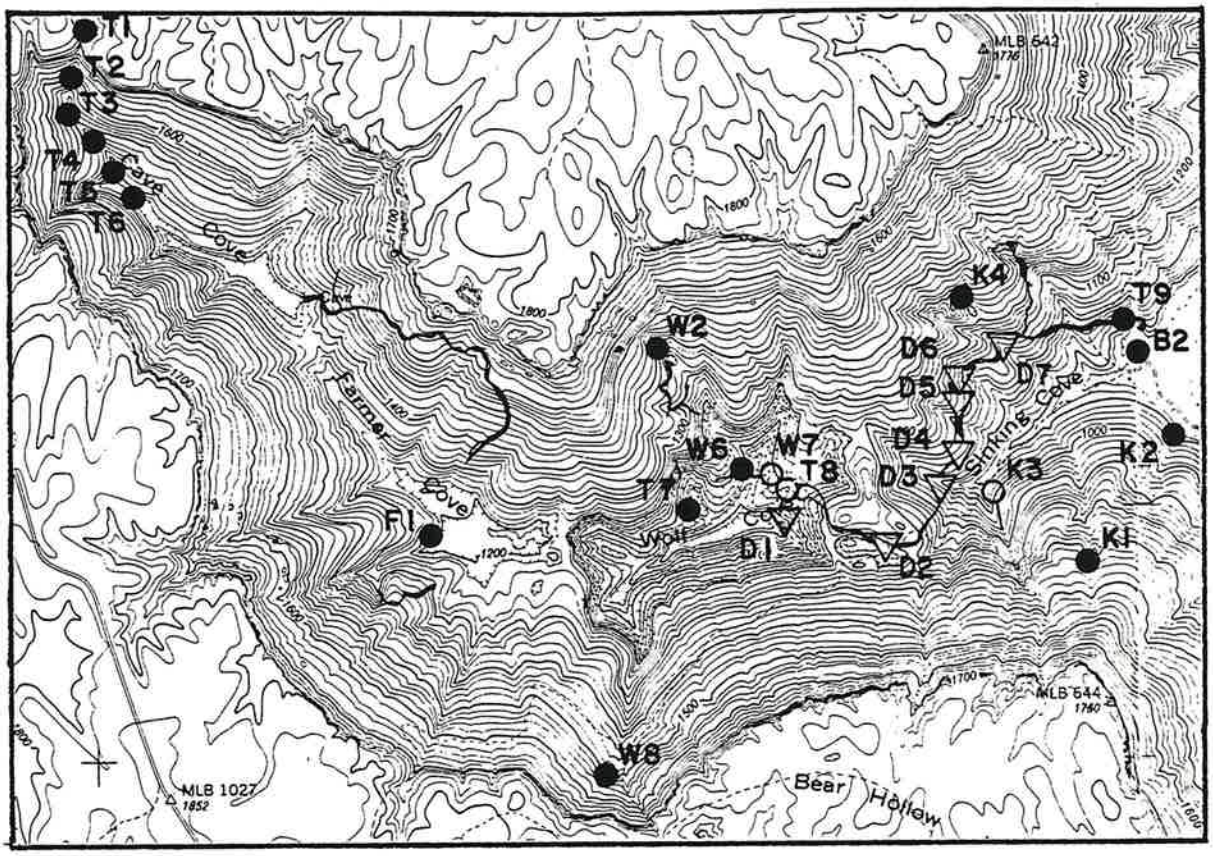

● Surface Streams and Springs

○ Cave Streams

▽ Cave Dripwaters

Fig. 4.2. Water chemistry sampling sites, August 1980. See Table 4.1 for site descriptions.

Table 4.3 Selected Water Chemistry Sampling Results, Upper Sinking Cove, 12-23 August 1980

Site	Date (8/80)	Temperature (°C)	pH	TH (ppm*)	Conductivity (μmhos)	SI_C	SI_D	log PCO_2
T1	14	20.1	5.4	5	10	-7.66	-14.78	-3.62
T2	14	16.9	7.3	32	48	-2.12	-4.90	-3.20
T3	14	17.0	7.7	53	82	-1.25	-3.08	-3.33
T4	14	18.7	7.8	54	93	-1.01	-2.66	-3.34
T5	14	17.3	8.0	68	107	-0.59	-1.66	-3.35
T6	14	20.8	7.9	76	127	-0.64	-1.76	-3.30
T7	15	13.7	7.7	131	171	-0.61	-1.67	-2.96
T8	15	13.3	7.7	140	190	-0.57	-1.68	-2.96
T9	15	13.6	7.7	134	179	-0.58	-1.63	-2.94
B2	13	13.5	7.9	122	148	-0.42	-1.40	-3.02
B2	19	15.5	8.1	126	191	-0.05	-0.59	-3.22
K1	18	14.0	7.6	118	214	-0.75	-1.84	-2.84
K2	18	16.0	7.6	146	207	-0.66	-1.74	-2.89
K3	18	13.0	7.3	142	207	-0.94	-2.21	-2.47
K4	21	14.9	7.4	110	170	-0.98	-2.33	-2.66
W2	21	16.5	7.2	60	99	-1.69	-3.90	-2.80
W6	21	16.7	7.7	86	133	-0.91	-2.38	-3.17
W7	19	14.8	7.4	108	179	-1.00	-2.53	-2.72
W8	20	14.0	7.2	58	92	-1.65	-4.15	-2.76
F1	20	14.0	7.3	94	143	-1.21	-2.92	-2.65

Table 4.3 (continued)

Site	Date (8/80)	Temperature (°C)	pH	TH (ppm*)	Conductivity (μmhos)	SI_C	SI_D	log PCO_2
D1	19	12.7	7.6	175	233	-0.42	-1.52	-2.71
D2	19	14.0	7.5	128	132	-0.70	-1.98	-2.67
D3	19	13.0	7.8	148	360	-0.37	-1.30	-2.98
D4	22	13.2	7.7	160	210	-0.35	-1.40	-2.82
D5	22	12.7	7.4	104	149	-1.07	-2.83	-2.76
D6	22	12.9	7.5	160	230	-0.61	-1.73	-2.64
D7	22	13.0	7.6	169	380	-0.41	-1.38	-2.67
S4	22	13.7	7.3	105	141	-1.13	-2.81	-2.62

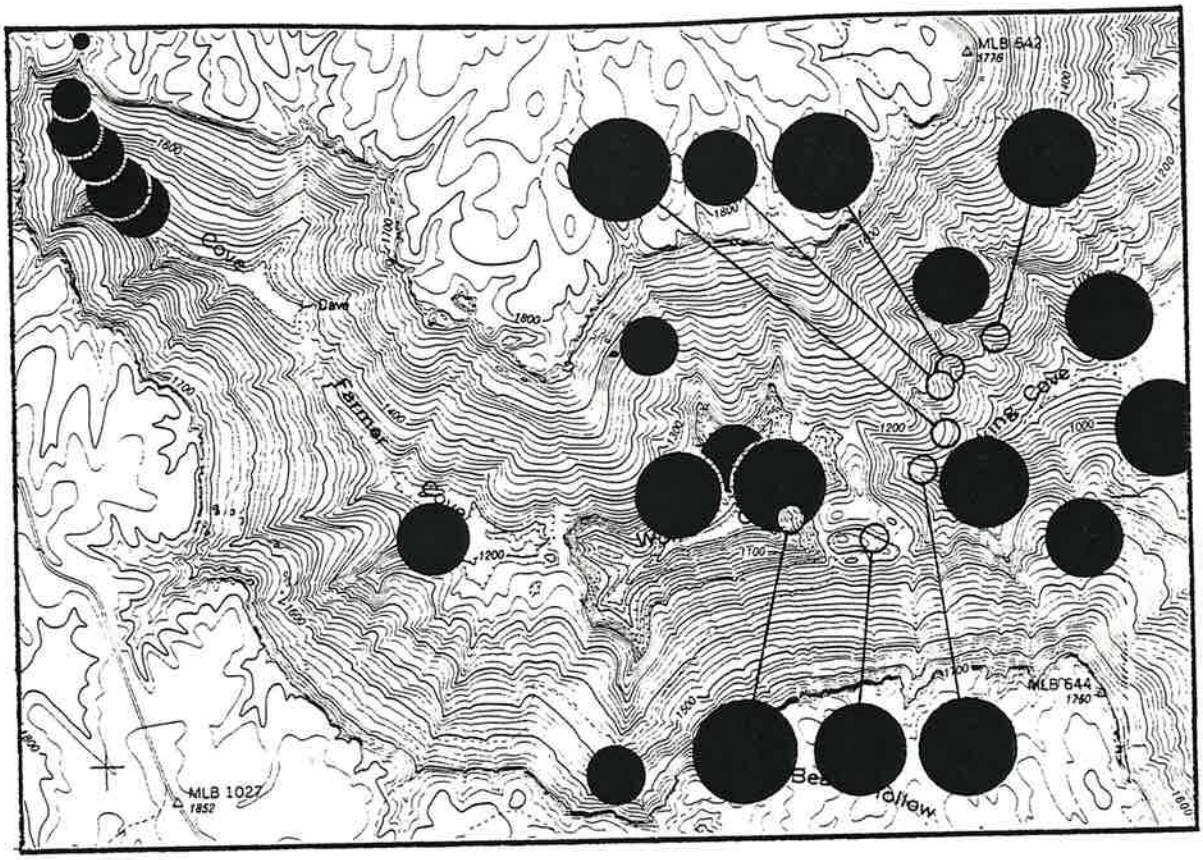

Fig. 4.3. Total hardness of water samples collected during August 1980.

The seven Sinking Cove Cave dripwaters sampled in August had higher hardness, were nearer saturation, and had higher log PCO_2 values (mean TH = 149 ppm*; SI_C = -0.56; log PCO_2 = -2.75) than stream and spring waters. Calcite deposits were associated with most dripwater sites. An exception was D5, located at the edge of a large breakdown room. Its low hardness and saturation index values (TH = 104 ppm*; SI_C = -1.07) suggest that it may be dominated by conduit (rather than diffuse) inputs. A report from W. Chamberlin (pers. comm.) may support this interpretation: During the flood of March 1979 which trapped Chamberlin and other explorers in the cave for two days, this normally insignificant dripwater input was producing a heavy waterfall, thus indicating conduit recharge along this drainage route.

The picture of the major elements of the drainage system provided by the water tracing experiments allowed an analysis to be made of the changes in chemistry of water as it moved through the system (Fig. 4.4). While a surface stream on the plateau, Cave Cove Creek (T1) had low pH (5.4), low hardness (5 ppm*), and was highly undersaturated (SI_C = -7.66). Log PCO_2 was close to atmospheric levels (-3.62). After flowing from the plateau and through Still Cave, it resurges (T2: elevation 490m a.s.l.), 45 m below T1. At this point pH (7.3), total hardness (32 ppm*), SI_C (-2.12), and log PCO_2 (-3.20) had all increased. As Cave Cove Creek flowed through successive sinks and springs to the floor of Cave Cove, pH increased rapidly to a relatively stable level (7.7) by T3 (460 m a.s.l.) as did log PCO_2 (-3.33). SI_C was stabilized by T5 (SI_C = -0.59), at 425 m a.s.l. (T5), 120 m upstream from the major streamsink at Exercise Cave. Hardness increased steadily to 76 ppm* by T6 (415 m a.s.l.), immediately above this sink (pH = 7.9; SI_C = -0.64; log PCO_2 = -3.30).

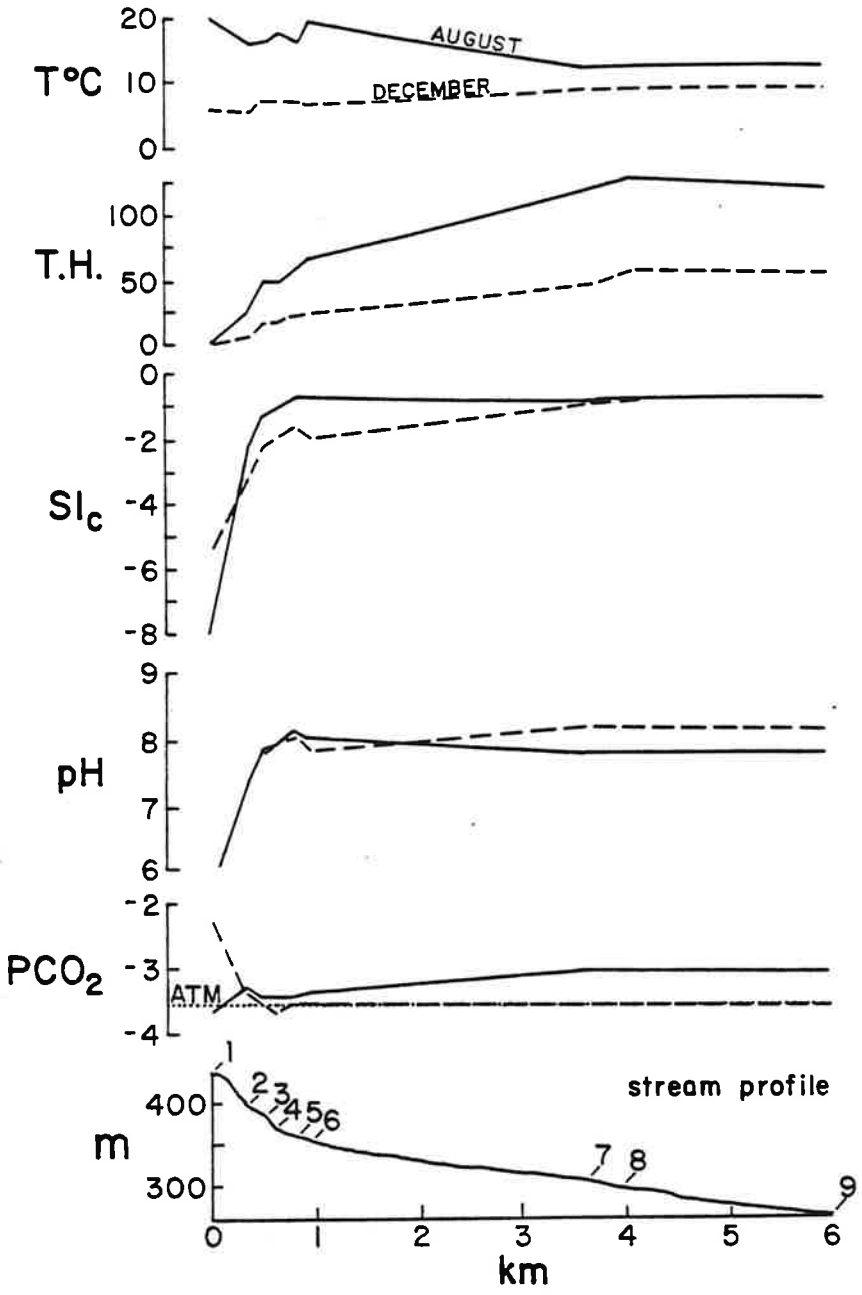

Fig. 4.4. Changes in water chemistry along the trunk stream from the head of Cave Cove to SCC Spring. August and December results are compared.

Between Cave Cove and Wolf Cove, inputs include diffuse percolation water from the floor of Farmer Cove as well as conduit inputs, one of which is Farmer Cove Creek (the output of Farmer Cove Spring). Although access could not be gained to the trunk stream as it flowed under Farmer Cove, the chemical characteristics of diffuse inputs to this stream would be similar to those of Sinking Cove Cave dripwaters, which were typically high in dissolved ions and close to saturation (excluding D5, average dripwater had: pH = 7.6; TH = 157 ppm*; SI_C = 0.48; log PCO_2 = -2.73). Farmer Cove Creek, determined by stream tracing experiments to be a tributary input above Wolf Cove, probably had little effect on the water chemistry of the trunk drainage stream.[1] The overall effect of these inputs was to increase total hardness between Cave Cove Sink and Helen Highwater Cave (Wolf Cove) from 76 to 131 ppm*, with little increase in SI_C (-0.64 to -0.61).

Between Helen Highwater Cave (T7) and SCC Spring (T9), several conduit inputs are known to join the system. Water from Shower Cave (not sampled), Wolf Cove Cave (W2 and W6), Waterfall Cave (W6), the Boulder Entrance tributary (K4, K5), and other sources (W8 and possibly K3) are incorporated into the trunk stream. These inputs include those which had higher than expected hardness (K4 residual = +29 ppm*) and those with lower than expected hardness (W6 residual = -37 ppm*). Diffuse

---

[1] Linear regression models relating total hardness and SI_C to site elevation (see below) were used to predict the chemical characteristics of streams at given elevations. Data from Farmer Cove Spring and locations along the trunk channel were fairly well predicted by the models (e.g., residuals from regression for Farmer Cove Spring data were -2 ppm* in total hardness and -0.27 in SI_C). At its confluence with the trunk stream, Farmer Cove Creek probably had similar chemistry.

dripwaters contributed little hydrologic input and probably had no significant effect on the chemistry of the trunk flow through Sinking Cove Cave. The net effect of all inputs was to produce little change in hardness of SI_C between T7 and T9 (TH: 131 to 134 ppm*; SI_C: -0.61 to -0.58).[1]

Water Samples Collected 29 September - 1 October 1980

Upper Sinking Cove was examined in late September after heavy rains which did not produce flooding in the area. Eleven samples (Appendix B) were collected at SCC Spring.

Discharge rose from 51.5 L/sec on the 29th to 84.7 L/sec on the 30th. Rain ended on the evening of the 30th and discharge dropped to 18.4 L/sec by the next day. Water temperature was between 13.0 and 13.3°C. pH ranged from 7.6 to 7.9, with an average of 7.7. Total hardness varied somewhat with discharge, ranging from 123 ppm* (at 18.4 L/sec) to 142 ppm* (at 84.7 L/sec). SI_C and log PCO_2 exhibited little systematic variation, and averaged -0.58 and -2.94, respectively.

Water Samples Collected 22-23 and 29-31 December 1980

Sampling of the nine sites along the trunk stream (T1-T9) was repeated in December. Fourteen other samples were collected, including two dripwaters from Sinking Cove Cave (Fig. 4.5). Results are given in Table 4.4. Three samples were collected for elemental analysis. These results are given in Table 4.5.

---

[1] Stabilization of SI_C beyond Cave Cove Sink may in fact represent attainment of saturation in the trunk stream. A consistent measurement error may account for negative derived SI_C values.

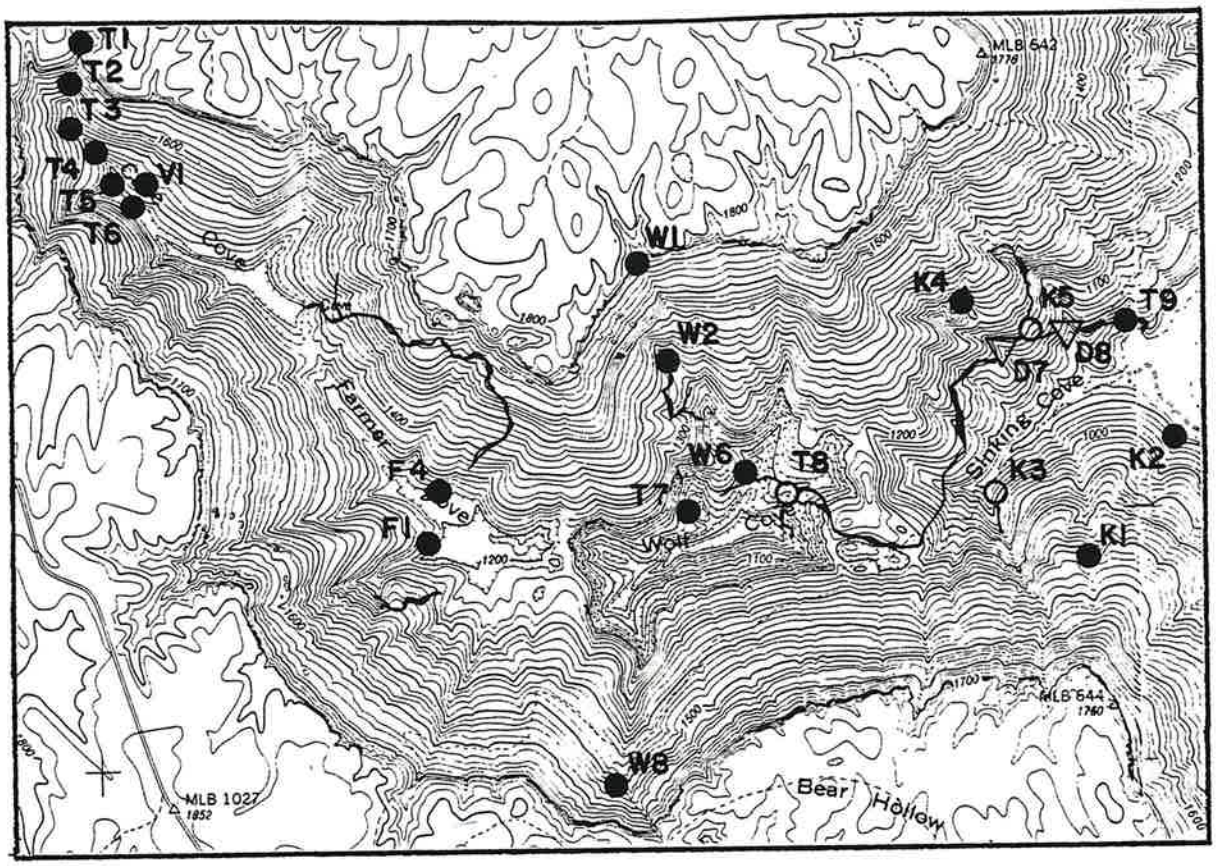

● Surface Streams and Springs

○ Cave Streams

▽ Cave Dripwaters

Fig. 4.5. Water chemistry sampling sites, December 1980. See Table 4.1 for site descriptions.

Table 4.4 Selected Water Chemistry Sampling Results, Upper Sinking Cove, December 1980

Site	Date (12/80)	Temperature (°C)	pH	TH (ppm*)	Conductivity (μmhos)	SI_C	SI_D	log PCO_2
T1	23	6.3	5.7	6	10	-5.38	-10.64	-2.07
T2	23	6.0	7.2	10	18	-3.15	-6.73	-3.30
T3	23	8.0	7.6	20	32	-2.17	-4.78	-3.45
T4	23	8.0	7.8	23	34	-1.83	-4.18	-3.59
T5	23	8.0	7.9	31	43	-1.45	-3.28	-3.49
T6	23	7.6	7.7	29	43	-1.81	-4.09	-3.45
T7	31	10.0	8.1	55	82	-0.76	-2.02	-3.50
T8	31	10.0	8.1	67	91	-0.63	-1.75	-3.45
T9	30	10.1	8.2	68	95	-0.52	-1.54	-3.55
K1	30	9.8	8.1	44	61	-0.98	-2.39	-3.62
K2	30	10.1	8.2	68	99	-0.52	-1.54	-3.55
K3	30	10.2	8.1	105	151	-0.33	-1.03	-3.30
K4	31	10.0	7.8	64	60	-1.39	-2.63	-3.34
K5	30	11.9	7.5	59	88	-1.29	-2.99	-2.88
W1	22	4.0	5.7	5	12	-5.12	-10.02	-1.65
W2	22	8.7	8.2	28	41	-1.20	-2.76	-3.81
W6	31	9.0	8.1	43	57	-0.96	-2.47	-3.60
W8	31	8.2	8.1	35	47	-1.20	-2.97	-3.74
F1	29	9.7	7.8	55	78	-1.02	-2.58	-3.17
F4	29	10.1	7.4	56	78	-1.41	-3.37	-2.77
V1	29	8.4	8.0	26	36	-1.57	-3.55	-3.76
D7	30	10.0	7.5	149	200	-0.52	-1.63	-2.47
D8	30	10.0	8.0	201	260	+0.10	-0.19	-2.92

Table 4.5 Elemental Analysis of Three Samples, Upper Sinking Cove, 29-31 December*

Element	T6	T7	T9
Ca	18.944	40.480	48.895
Mg	4.538	9.970	12.597
Si	6.500	6.618	6.963
K	2.931	3.871	2.931
Na	2.922	3.203	3.323
Al	0.528	0.513	1.054
Zn	0.159	0.553	0.248
P	---	0.314	0.222
B	0.133	0.098	0.114
Sr	0.037	0.090	0.121
Fe	0.050	0.039	0.047
Ni	0.041	0.068	0.033
Cr	0.028	0.051	0.016
Cu	0.014	0.014	0.013
Mn	0.004	0.008	0.015
Pb	0.010	0.017	0.007
Ba	0.009	0.012	0.011
Co	0.006	0.005	0.005
Cd	0.002	0.002	0.001
Mo	---	---	---
Total	36.856	65.915	76.618

*Results given in parts per million, $CaCO_3$ equivalent.

Average characteristics of samples collected during December 1980 were:

Temperature = 8.8°C

pH = 7.7

Total Hardness = 43.2 ppm*

SI_C = -1.65

Log PCO_2 = -2.72 (strongly influenced by 2 high readings at T1 and W1)

Elevation = 387m

Except for the expected reversal of temperature trends (temperature increased with lower elevation, due to greater in-cave streamflow), the spatial tendencies of December water chemistry variables were similar to those noted in August. Temperature and hardness (Fig. 4.6) values were generally lower, and ranged from 4.0°C and 5.7 ppm* in a caprock stream (W1) to 10.2°C and 105 ppm* in Ashlee Cave (K3). Most samples were less saturated than in August.

Compared with summer readings, cave dripwaters were lower in hardness (149 and 201 ppm*, as compared with 169 and 292 ppm* at similar sites in summer), but differed little with respect to other variables.

Samples collected along the trunk channel exhibited changes similar to those noted in August (see Fig. 4.4). Both pH and SI_C, however, had steady increases from 5.7 to 8.2 and from -5.38 to -0.52, respectively, between T1 and T9. To contrast, in summer, SI_C had reached -0.59 before sinking in Cave Cove. Total hardness again exhibited a regular increase, though reaching only 68 ppm* at site T9.

Elemental sample data revealed solutes other than calcium and magnesium which were present in the waters of Upper Sinking Cove. Of

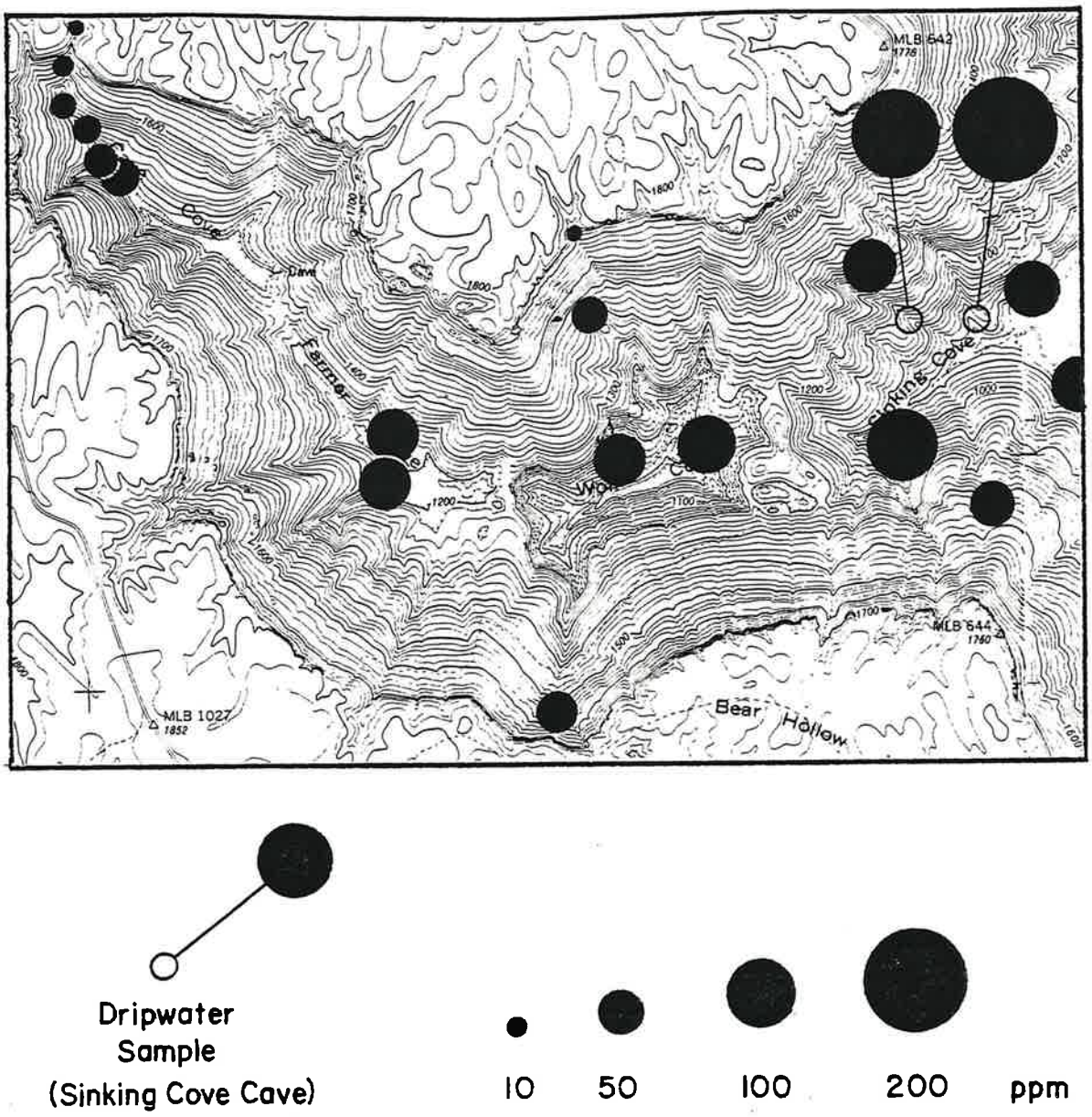

Fig. 4.6. Total hardness of water samples collected during December 1980.

the other elements evaluated, the important silicate mineral constituents (silica, potassium, sodium, and aluminum) had the highest concentrations. These did not, however, tend to exhibit regular increases from T6 to T9 as occurred with calcium and magnesium. The concentration levels of these elements were probably reached much earlier, on the caprock where water was sufficiently aggressive to dissolve silicate minerals. Ca^{2+} and Mg^{2+} concentrations in these analyses presented 81.0, 92.5, and 90.3% of total hardness evaluations from concurrent samples at T6, T7, and T9, respectively.

Water Samples Collected 25-26 April 1981

Four samples were collected in April 1981 for seasonal comparisons. Three samples were collected from points along the trunk drainage streams, and one from a tributary (Farmer Cove Spring). Results are given in Table 4.6.

Temperature ranged from 1.20° C at Farmer Cove Spring to 12.9 at Helen Highwater Cave, with an average of 12.5° C. pH varied little, ranging from 7.8 at Cave Cove Sink to 8.2 at SCC Spring. Total hardness was, as expected, lowest at Cave Cove Sink (28 ppm*) and highest at SCC Spring (64 ppm*). Similarly, SI_C increased from -1.61 at Cave Cove Sink to -0.64 at SCC Spring, with a value of -0.83 at Farmer Cove Spring (average SI_C = -0.99). Log PCO_2 varied little among the locations sampled, and had an average value of -3.46.

Geologic/Topographic Context of Spatial Variations in Water Chemistry

Stream chemistry data were compared with two topographically-derived variables. The first, 'depth', is the difference between caprock

Table 4.6 Selected Water Chemistry Sampling Results, Upper Sinking Cove, 25-26 April 1981

Site	Date (4/81)	Temperature (°C)	pH	TH (ppm*)	Conductivity (μmhos)	SI_C	SI_D	log PCO_2
T6	25	12.5	7.8	28	38	-1.61	-3.60	-3.51
T7	26	12.9	8.0	51	71	-0.88	-2.20	-3.44
T9	26	12.6	8.1	64	68	-0.64	-1.75	-3.49
F1	25	12.0	8.0	57	87	-0.83	-2.05	-3.40

elevation and site elevations, and is a measure of the rock thickness penetrated by the stream above the site. The second, 'drainage distance', is the straight-line distance from the site to the closest upstream topographic divide; it is a surrogate for relative hydrologic input (the difficulties encountered in the estimation of tributary discharge inputs are discussed in Chapter III). For tributaries, the drainage distance was measured directly up canyon sides on topographic maps. In the case of the trunk channel, the drainage route was known from stream traces; its drainage distance was thus measured in a succession of three straight lines from SCC Spring to the plateau surface at the head of Cave Cove.

In June, water increased in pH, total hardness, and SI_C as it dropped through successive layers of limestone. Correlation/regression analyses (Table 4.7) showed strong positive relationships between depth (the dependent variable) and total hardness (linear) and SI_C (exponential). The inverse relationship of temperature with depth is because surface flow (with higher temperatures than subsurface flow in June) is less common at lower elevations in the study area. Log PCO_2 appeared to be unrelated to either of the two topographic variables.

No apparent relationship between chemistry and drainage distance was noticed in June, August, or December (Tables 4.8 and 4.9). Vertical movement of water through a thickness of limestone appeared to be more effective in explaining water chemistry. The highest correlations were between depth and total hardness and SI_C. Assuming that drainage distance is a reasonable surrogate for hydrologic input, this analysis shows

Table 4.7 Correlation/Regression Analysis for Water Chemistry and Topographic Variables,* Upper Sinking Cove, June 1980

Dependent Variable	Independent Variable (see text): Depth (560 m-site elevation)	Independent Variable (see text): Drainage Distance
Temperature	Y = 20.007 - 0.026X r = -0.771 S.L. = 0.0002	r = 0.5057 not significant to 0.01
pH	Y = 6.12 + 0.007X r = 0.803 S.L. = 0.0002	r = 0.4056 not significant to 0.01
Total Hardness	Y = -1.722 + 0.472X r = 0.9554 S.L. less than 0.0001	r = 0.5057 not significant to 0.01
SI_C	$Y = -5.2102e^{-0.0087X}$ r = -(-0.9044)** S.L. less than 0.0001	r = 0.3905 not significant to 0.01
log PCO_2	r = -0.3119 not significant to 0.01	r = -0.1751 not significant to 0.01

*Analysis of linear and non-linear (exponential) relationships were used. Relationships giving the highest correlation coefficient are reported. S.L. = significance level.

**This represents a positive correlation. Transformation to natural logarithms required the use of $-SI_C$, to remove negative numbers.

Table 4.8 Correlation/Regression Analysis for Water Chemistry and Topographic Variables,* Upper Sinking Cove, August 1980

Dependent Variable	Independent Variable (see text) Depth (560 m-site elevation)	Drainage Distance
Temperature	Y = 18.778 - 0.016X r = -0.5923 S.L. = 0.0075	r = -0.3692 not significant to 0.01
pH	r = 0.4772 not significant to 0.01	r = 0.3457 not significant to 0.01
Total Hardness	Y = 9.0037 + 0.446X r = 0.9112 S.L. less than 0.0001	Y = 65.67 + 0.0013X r = 0.5757 S.L. = 0.0099
SI_C	$Y = -2.8569e^{-0.00568X}$ r = -(-0.7351)** S.L. = 0.0003	$Y = 1.518e^{-0.0002X}$ r = -(-0.5895)** S.L. = 0.0079
log PCO_2	r = -0.5236 not significant to 0.01	r = 0.0475 not significant to 0.01

*See note in Table 4.7; does not include dripwater samples.

**positive correlations

Table 4.9 Correlation/Regression Analysis for Water Chemistry and Topographic Variables* Upper Sinking Cove, December 1980

Dependent Variable	Independent Variable (see text) Depth (560 m-site elevation)	Drainage Distance
Temperature	Y = 5.627 + 0.018X r = -0.8574 S.L. less than 0.0001	r = 0.3949 not significant to 0.01
pH	Y = 6.733 + 0.0055X r = 0.6461 S.L. = 0.0016	r = 0.3214 not significant to 0.01
Total Hardness	Y = -2.242 + 0.263X r = 0.8723 S.L. less than 0.0001	r = 0.4653 not significant to 0.01
SI_C	$Y = -4.5728e^{-0.0073X}$ r = -(-0.8798)** S.L. less than 0.0001	r = -(-0.5093) not significant to 0.01
log PCO_2	r = -0.3773 not significant to 0.01	r = -0.1733 not significant to 0.01

*See note in Table 4.7; does not include dripwater samples.

**positive correlations

that hydrologic input was ineffective controlling spatial variations in water chemistry. Thickness of limestone contacted by streams, regardless of their size, appeared to be of much greater importance.

Seasonal Variations in Water Chemistry and Discharge

Four sites were sampled in June, August, December, and April, in order to examine seasonal variations in water chemistry. Three of these, Cave Cove Sink at Exercise Cave (T6), Helen Highwater Cave spring (T7), and SCC Spring (T9), are located along the trunk stream, and represent Cave Cove, Wolf Cove, and Sinking Cove exposures. A fourth, Farmer Cove Spring (F1), is part of a major tributary to the system.

Fig. 4.7 shows variations in temperature, total hardness, pH, SI_C and log PCO_2 at these four sites as well as monthly air temperature means, during the four sampling periods. As expected, the seasonal trend in water temperature followed that of air temperature, but at springs (T7, T9, and F1) seasonal differences were less marked. Total hardness exhibited a definite seasonal trend, reaching a maximum at all four sites during the summer months, especially in August. A similar trend was exhibited in log PCO_2. A strong seasonal trend in SI_C was apparent at Cave Cove Sink (T6), with a peak in August; seasonal trends were not apparent downstream. Farmer Cove Spring, in contrast, was most highly undersaturated in August. Except for Cave Cove Sink, pH exhibited a distinct seasonal trend with peaks during the winter and spring sampling periods.

Average discharges from Upper Sinking Cove during the four sampling periods were estimated from direct measurements and water-budget studies

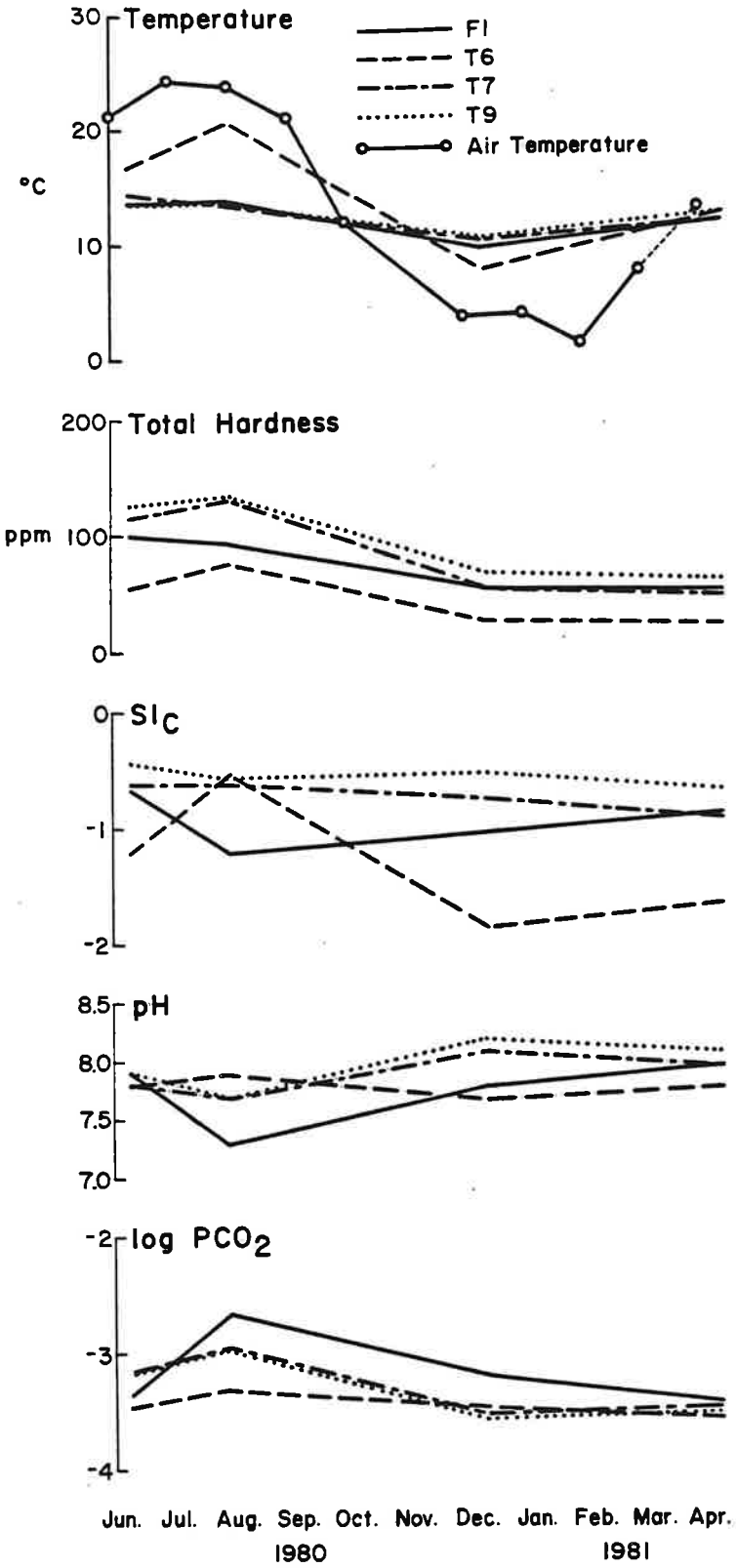

Fig. 4.7. Seasonal changes in water chemistry at four sites in Upper Sinking Cove, June 1980 to April 1981.

to be

June	118 L/sec
August	10 L/sec
December	117 L/sec
April	350 L/sec

Discharge decreased from June to August, and drought conditions were experienced into early fall. Partial groundwater recharge in late fall caused an increase in discharge by late December, building it up to June levels. Further increases during the winter months led to a peak in February, and generally high discharge continued into April.

Patterns of total hardness and SI_C did not closely reflect this pattern, especially in a comparison of June and December results. If discharge was the primary controlling factor, hardness values would be expected to be similar in these two periods, as discharge levels were nearly the same. Hardness in June, however, was nearly twice that in December, at all four sites.

Measurements made in late September at SCC Spring (see Appendix B) suggest that peaks in total hardness and log PCO_2 occurred in early fall (30 September at T9: TH = 138 ppm*; log PCO_2 = -2.86). Since pH was also relatively low (7.6), factors affecting the soil/water CO_2 chemical system may have been responsible for these changes.

Soil Air Measurements

Measurements of CO_2 concentrations in soil air were made during the course of the study. The Dräger system, consisting of a calibrated pump and CO_2-sensitive measurement tubes, was used in combination with a Miotke probe inserted to varying depths in the soil.

Readings were made at 10 sites during June 1980 (Fig. 4.8; Table 4.10). These ranged from 0.20% (log $^{P}CO_2$ = -2.7) in well-drained loam on the plateau surface to 1.7% (-1.77) in organic clay-rich alluvium in Farmer Cove.

Only two readings were made during December because of equipment difficulties. CO_2 at Site 3, on the plateau surface, dropped from 0.56% (-2.25) in June to 0.32% (-2.49) in December. CO_2 at Site 8, near Hunter's Camp on the south slopes near the base camp in Sinking Cove, was also lower (1.25% in June to 0.53% in December).

Six measurements of CO_2 were made in April 1981 (Table 4.11). Four of these, on slopes and in alluvium in Farmer Cove, showed CO_2 levels at approximately one percent (log PCO_2 = -2.00). The other two measurements, on the plateau surface and in the alluvial floor of Wolf Cove, had half this concentration. At sites where measurements had also been made in summer 1980, CO_2 was lower in April 1981. Site 9, in Wolf Cove alluvium, was down from 0.74% (-2.13) in summer to 0.50% (-2.30) in April. Site 10, in Farmer Cove alluvium, was down from 1.7% (-1.77) to 1.0% (-2.00). At Hunter's Camp on the south slopes of Sinking Cove, CO_2 was up from the past December (0.53 to 1.10%, or -2.28 to -1.95), but not up to summer levels (June PCO_2 = 1.25%, or -1.90).

The above results indicate a seasonal variation in soil CO_2 concentrations, which is probably related to seasonal cycles in biogenic CO_2 production. Although no readings were made in September due to water-saturated soil conditions, it is expected that these would have exhibited the highest CO_2 concentrations, as indicated by low pH, high PCO_2, and high total hardness of water during this period.

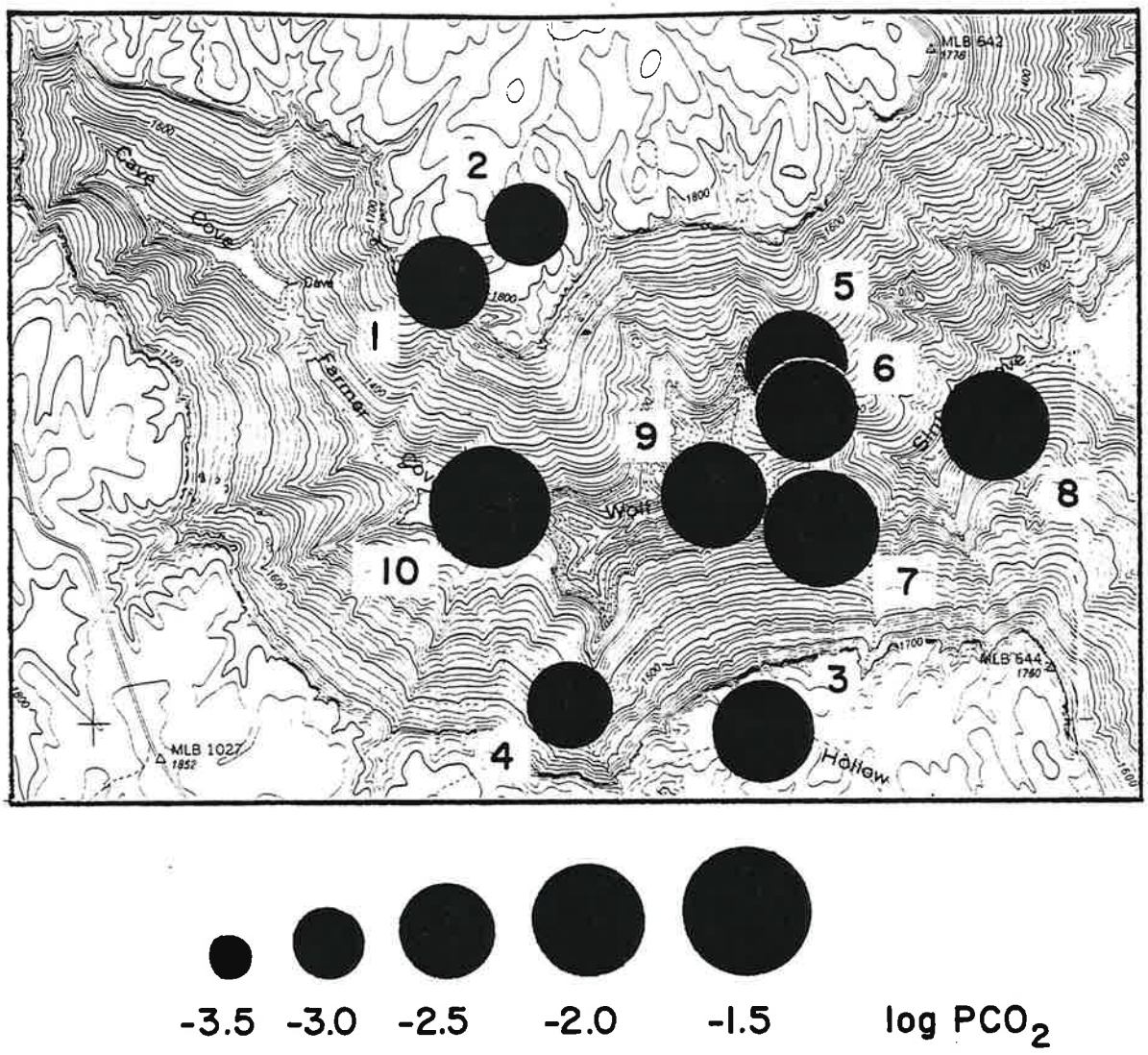

Fig. 4.8. Soil CO_2 levels, June 1980 (see Table 4.10 for site descriptions).

Table 4.10 CO_2 Concentrations in Soil Air, June 1980

Site	Description	CO_2 concentration %	log PCO_2
1	Caprock depression--moist, organic clay-rich soil	0.35	-2.46
2	Plateau surface--well-drained loam	0.20	-2.70
3	Plateau surface--well-drained loam	0.56	-2.25
4	South canyon slope--well-drained loam	0.27	-2.58
5	North canyon slopes--well-drained loam	0.67	-2.17
6	Wolf Cove saddle--well-drained loam	0.54	-2.27
7	Small depression on saddle--moist, organic soil, under wet conditions	1.30	-1.89
8	South slopes at low elevation--well-drained loam Hunter's Camp	1.25	-1.90
9	Alluvium in floor of Wolf Cove--organic	0.74	-2.13
10	Alluvium in Farmer Cove--organic, clay-rich	1.70	-1.77

Table 4.11 CO_2 Concentrations in Soil Air, April 1981

Site	Description	CO_2 concentration %	CO_2 concentration log PCO_2
8	South slopes at low elevation--well-drained loam Hunter's Camp	1.1	-1.95
9	Alluvium in floor of Wolf Cove--organic	0.5	-2.30
10	Alluvium in floor of Farmer Cove--organic, clay-rich	1.0	-2.00
11	Alluvium in floor of Farmer Cove near Farmer Cove Spring--organic, clay-rich	1.0	-2.00
12	South canyon slopes--well-drained, rocky	1.0	-2.00
13	Plateau surface--well-drained loam	0.44	-2.36

Comparison of Results with Global Soil CO_2 Models

Global climatic models of soil CO_2 and the chemical evolution of carbonate groundwater have been proposed (Drake and Wigley (1975), Harmon et al. (1975)). Strong positive linear relationships have been found by these workers between water temperature and PCO_2 concentrations in soil air and saturated spring and well waters. Saturated waters followed the relationship

$$\log PCO_2 = -3.16 + 0.07\ T\ (\text{in } °C)$$

This theoretical PCO_2 value resulted from an initial soil PCO_2 given by

$$\log PCO_2 = -1.97 + 0.04\ T \text{ (Drake and Wigley, 1975).}$$

Using a mean water temperature (at SCC Spring) for the study period, 11.6° C, application of the temperature-PCO_2 models above leads to an expected theoretical log PCO_2 in saturated groundwater of -2.23, and in soil air, -1.51. Although average derived groundwater values obtained in Upper Sinking Cove differ greatly from the above prediction (average log PCO_2 = -3.19); the assumption in the model of saturated waters is not held in this case. Soil CO_2 values, however, are also overestimated by the model. The average June reading (growing season) from Upper Sinking Cove is -2.12, 0.61 lower than predicted by the temperature model.

A model using annual actual evapotranspiration (AET) as predictor (Brook et al., in press) gives closer results. According to this model, soil PCO_2 is predicted by

$$\log PCO_2 = -3.47 + 2.09(1-e^{(-.00172AET)}).$$

Incorporating the annual AET value for Upper Sinking Cove, 767 mm,

obtained by water-budget analysis of average temperature and precipitation values, log PCO_2 is predicted to be -1.93, with a positive error of 0.19.

The soil CO_2 system in Upper Sinking Cove is thus well predicted by its climate. As waters are generally undersaturated, however, groundwater PCO_2 models which assume saturation cannot be tested. In most of these models, distinction is made between open- and closed-system CO_2 evolution. When limestone dissolution occurs in the soil zone, allowing constant replenishment of CO_2 for production of carbonic acid, this is referred to as open-system evolution. Closed system evolution occurs in an aquifer, sealed from CO_2 sources, where only the originally diffused CO_2 is available: theoretical groundwater PCO_2 values are easily interpreted in this case. In Upper Sinking Cove, solution likely occurs both in the soil zone and in cave passages exposed to the atmosphere. Solution in the soil zone is clearly open system CO_2 evolution. Solution in cave passages is limited to the original CO_2 from soil air diffusion, as in closed system evolution, but suffers from the release of carbon dioxide into low-PCO_2 cave air. Theoretical groundwater log PCO_2 values are therefore lower than might be expected from climatic models, even if saturation had been reached.

Erosion Measurement using Rock Tablets

Trudgill (1975) outlined a method in which relative rates of erosion could be measured using rock tablets placed in the field for extended periods. Erosional weight-loss of tablets over this period may then be compared among environments in which the tablets were placed (e.g., streams, soils).

Rock tablets were produced by slicing 2.5 cm cores of Bangor Limestone (from a sample collected at a road-cut near the study area) into 0.7 cm-thick pieces with a water-cooled cutter. These were then smoothed and standardized on a rock grinding plate. Each was washed in distilled water and alcohol, then dried at 105° C for 24 hours. The weights of tablets (approximately 10 g each) were recorded to a precision of 0.0001 g, with a Sartorius Balance (Table 4.12). Tablets were sealed in packets constructed of fiberglas window screen and 200 lb. test nylon string. Labels were attached to a length of string used to secure the tablets.

Twenty tablets were placed at sites throughout Upper Sinking Cove (including soils, streams, caves, and springs) in June 1980. Seventeen[1] of these were recovered in December, six months after emplacement. Recovered tablets were washed and dried again, then weighed to determine erosional weight-loss, as percent of the original weight (Table 4.12). Figure 4.9 shows the distribution of tablet placements and erosional weight losses.

Tablets recovered from soils in December included two from sites on the plateau surface (4 and 7), one from a depression on the plateau (1), one from Wolf Cove Saddle (8), two from the canyon slopes (2 and 5), two from alluvium in depression floors (3 and 6), and one from mud in Farmer Cove Swamp (10). All but one of these had an erosional weight-loss of less than one percent; most tablets lost less than 0.5%. The exception was the tablet placed in Farmer Cove Swamp (10), which suffered over 2% weight-loss.

---

[1]Three were not recovered: one buried in soil on Wolf Cove Saddle, one under the waterfall at Cave Cove Sink, and one on bare sandstone.

Table 4.12 Erosional Weight-Loss in Rock Tablets, Upper Sinking Cove, June to December 1980

		original weight (g)	after 6 months (g)	percent weight loss
Tablets placed in soils				
1	at 60 cm depth in moist, organic, clay-rich soil in caprock depression floor	10.2408	10.2161	0.2412
2	at 20 cm depth on north canyon slopes in clay-rich rocky loam	10.4691	10.4433	0.2464
3	at 20 cm depth in organic alluvium in Farmer Cove floor	10.5089	10.4822	0.2541
4	at 20 cm depth in loose, well-drained loam on plateau surface	10.1828	10.1521	0.3015
5	at 20 cm depth in clay-rich loam on south canyon slopes	10.5958	10.5576	0.3605
6	at 20 cm depth in loose, organic alluvium in Wolf Cove floor	10.7356	10.6934	0.3931
7	at 20 cm depth in well-drained loam on plateau surface	10.3614	10.3134	0.4633
8	at 10 cm depth in clay-rich, organic soil in saddle depression floor	10.4732	10.4229	0.4803
9	at 30 cm depth in same location	10.7225	10.6579	0.6025
Tablet placed in swamp				
10	at 30 cm depth in Farmer Cove swamp mud	10.3213	10.0989	2.1548

Table 4.12 (continued)

		original weight (g)	after 6 months (g)	percent weight loss
Tablets placed in water bodies				
11	in 20 cm waterfall in stream flowing through Ashlee Cave	10.9629	10.9429	0.1824
12	in ponded water upstream of SCC Spring	10.8276	10.7979	0.2743
13	in riffles 420 m upstream of SCC Spring (Sinking Cove Cave)	10.4347	10.3946	0.3843
14	in riffles near upstream end of Sinking Cove Cave, under Wolf Cove	10.6266	10.5786	0.4517
15	in Robin's Pond (was out of water when recovered)	9.9691	9.7926	1.7705
16	in sand-bedded stream in Farmer Cove Cave (was buried in sand when recovered)	11.1493	10.9065	2.1777
17	in stream flowing off the plateau surface above Wolf Cove Cave	10.3327	9.4737	8.3134

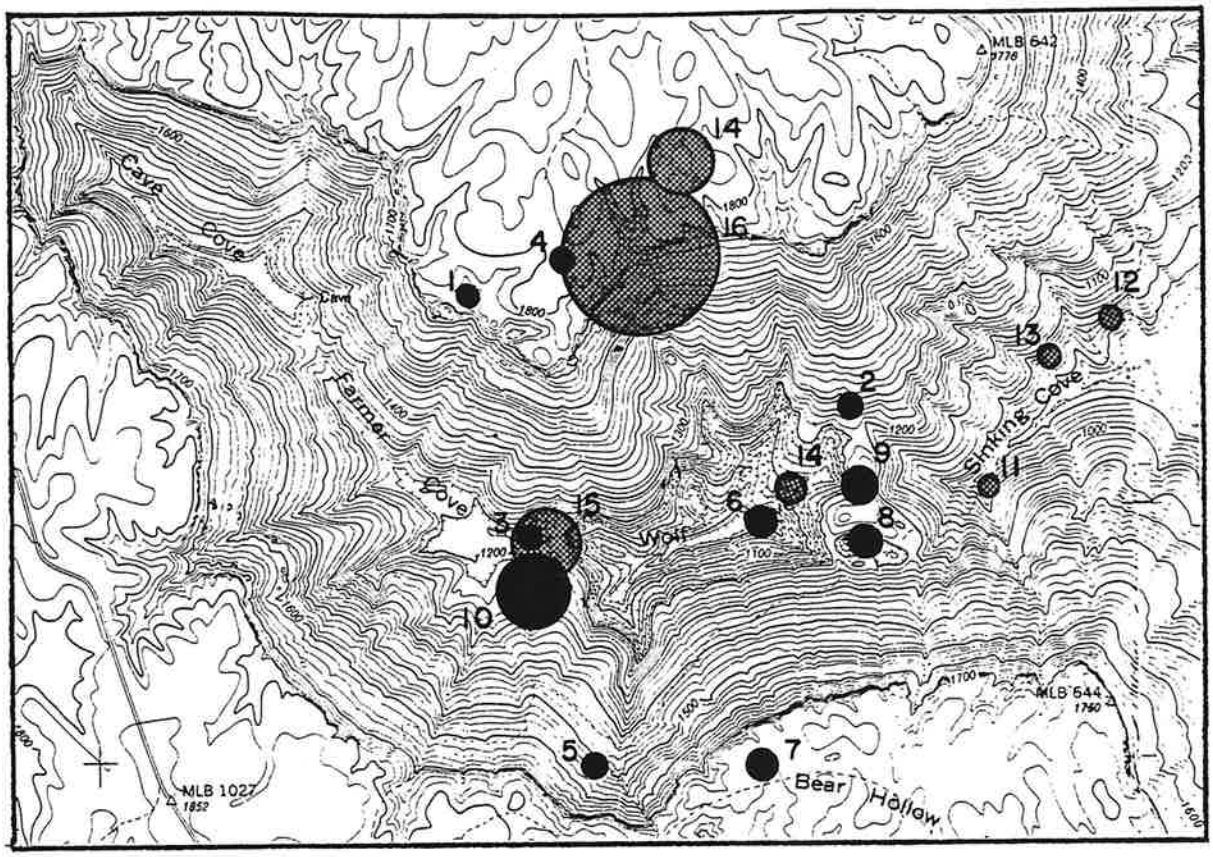

Tablets Placed:

in water

in soil

Percent Weight Loss

0.2 0.5 1.0 2.0 4.0 8.0

Fig. 4.9. Rock tablet weight-loss over a six month period, June-December 1980.

Six tablets were recovered from water bodies. Erosional weight-loss ranged from less than 0.2% in Ashlee Cave to over 8% in a stream flowing off the plateau surface (17). Tablets placed in Sinking Cove Cave (12, 13, and 14) displayed progressively greater weight-loss upstream: the least (0.27%) in ponded water just upstream of SCC Spring, increasing to 0.38% in riffles upstream of the Boulder Entrance tributary, and the greatest (0.45%) in riffles under Wolf Cove. Tablets in Farmer Cove Cave and Robin's Pond were found out of water when collected. In spite of this, each incurred weight losses of approximately 2%.

The results indicate a great deal of systematic variation in tablets placed in water, but less so in soils. The presence of water may be a factor in sub-soil weathering: tablet 10 placed in continuously moist swamp mud suffered the greatest weight-loss of tablets placed in soils. For water to be effective, however, it must be chemically aggressive. This fact is clearly shown in the results of tablets placed in streams: little limestone was dissolved in waters with relatively low aggressivity (downstream Sinking Cove Cave and Ashlee Cave), but considerable weight-loss occurred in tablets placed in streams known to be aggressive (e.g., streams flowing off the plateau surface).

Though the packet material did not prevent mechanical erosion by sand-sized particles, the results suggest that corrasion was less important then corrosion. The stream in which the greatest tablet weight-loss occurred was of smaller size and less turbulent than the stream segment in Sinking Cove Cave, where tablet #13 suffered a weight loss less than 5% of the former. Both streams have sand in bed materials.

Discussion

Solutional denudation in Upper Sinking Cove is affected by hydrologic, geologic, and biologic factors. The presence of water is a prerequisite to limestone solution. Though the specific effect of short-term discharge variations could not be isolated in this study, it is likely that such considerations are important.

Geologically, the study area may be divided into two solutional environments: the caprock and the underlying carbonates. Before leaving the caprock, streams are low in hardness and are highly aggressive. As carbonates are encountered along a stream's route from the plateau surface to final springs in the east of the study area; hardness progressively increases and aggressivity decreases. Geologic variations below the caprock appear to be less important to water chemistry than the total thickness of carbonate rock penetrated.

Biologic factors, such as the production of CO_2 in soil air, are important seasonal controls of solution. The results of this study suggest that seasonal cycles of CO_2 production, with a peak during summer and perhaps fall, result in a similar cycle of limestone solution, as reflected in the chemistry of waters sampled at various times of the year.

Spring chemistry analyses have been used in the interpretation of flow systems above springs (Shuster and White, 1971). The predominance of conduit flow conditions is indicated for springs in the study area. Seasonal variations are pronounced and saturation is never reached. Even dripwaters, which exhibit less seasonal variation in hardness, were atypical of purely diffuse flow systems. Conduit flow thus may also play a part in cave dripwater sources.

Estimation of Karst Denudation Rates in the Study Area

Results of solution chemistry studies can be used to estimate a steady-state karst denudation rate. Using average total hardness and discharge values for SCC Spring, solutional denudation, according to Douglas (1964), is given by:

$$X = \frac{TQ}{AD}$$

where

T = 97 mg/L (average June and December total hardness at SCC Spring)

Q = 7.87 x 10^6 m^3/year (estimated annual discharge from the system)

A = 13.5 x 10^6 m^2 (estimated drainage area)

D = 2.77 g/ml (average density of 22 rock samples from the study area)

A denudation rate derived from these figures is 20.4 mm/1000 years (or m^3/km^2/year). If corrected for the fact that only 40% of the estimated drainage area is underlain by limestone, solutional denudation of the limestone portion is 51.0 mm/1000 years. This rate assumes the average hardness for SCC Spring during the study period, 97 mg/L, and the estimated discharge, 7.87 x 10^6 m^3/year, are representative of average conditions.

The total discharge estimate given above, 7.87 x 10^6 m^3/year, based upon measurements and water budget analyses for 1980-81, equates with a runoff of 583 mm/year. This value is considerably lower than the average annual runoff figure, 783 mm, derived by subtracting annual actual evapotranspiration (767 mm) from average annual precipitation (1550 mm). Using this higher runoff estimate, and assuming no change in

average total hardness at SCC Spring, increases the average denudation rate estimate to 68.5 mm/1000 years.

Rock tablet weight-loss experiments provide another measure of denudation, which in this case seems to support the above estimate. Conversion must be made from weight-loss per six-month period to erosion rate, in mm/1000 years. A flat limestone surface, having the same area as the surface area of a tablet (15.71 cm^2) must be considered. Below this surface will be a thickness of unexposed limestone defined by the volume of the tablet (3.68 cm^3) to be .234 cm. An eight percent weight-loss can then be directly converted to an eroded thickness of 0.0187 cm. Multiplying by 2000 gives a denudation rate of 374 mm/1000 years. An average weight-loss, 3.6%, from three representative surface and cave streams (in Sinking Cove Cave, Farmer Cove Cave, and a surface stream near the caprock) gives an average erosion rate for streams of 169 mm/1000 years. An average weight-loss for tablets placed in soils is 0.37%, giving a soil denudation rate of 17 mm/1000 years. In actuality, it is expected that solution rates in the soil zone are higher than this, since solution continues into limestone below the uppermost 20-60 cm in which tablets could be placed.

With these estimates, it can easily be seen how an overall denudation rate (based on conditions during the study period) of 51 mm/1000 years could result from some combination of a subsoil solution rate somewhat above 17 mm/1000 years and a streambed (surface and subsurface) solution rate of 169 mm/1000 years.

The above estimates are for solutional denudation. Actual erosion rates must also take into consideration non-karstic erosion processes,

such as fluvial erosion and mass wasting, which may be highly significant during floods.

The average karst denudation rate obtained in this study, 68.5 mm/1000 years ($m^3/km^2/year$), may be compared with results obtained elsewhere. Smith and Atkinson (1976) report 107 erosion rates published by workers in tropical, temperate, and arctic/alpine areas of the world. Frequency distributions of these results are shown in Fig. 4.10. Denudational conditions in Upper Sinking Cove appear to be typical of temperate karsts, which have a mean erosion rate of 56.9 $m^3/km^2/year$. To date, however, no suitable mathematical models relating denudation rate to climatic or geologic variables are available in the literature.

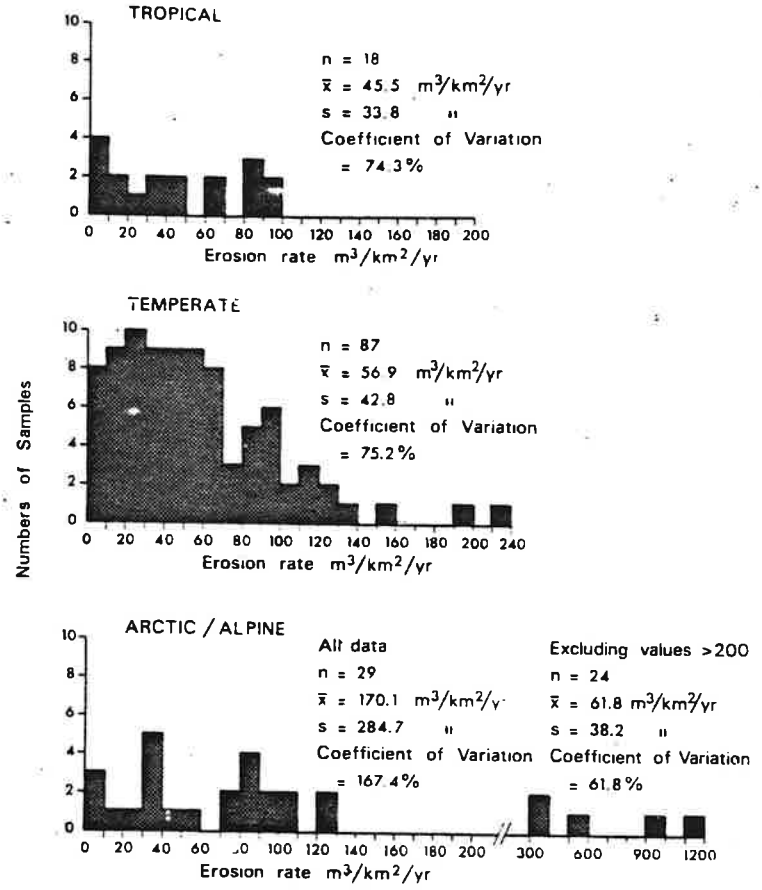

Fig. 4.10. Frequency distributions of denudation rates from published studies of karst areas. After Smith and Atkinson (1976).

CHAPTER V

SUMMARY AND DISCUSSION

The preceding chapters have outlined the hydrological and denudational conditions of Upper Sinking Cove. The results are summarized below and a model for karst landform development, based upon these results, is presented.

A multiple-aquifer karst hydrologic system, with minor surface components, is organized into a central trunk channel, which has been traced from the head of Cave Cove to Sinking Cove Cave Spring, and a network of independent tributaries. Geologic controls are responsible for the localized production of paraphreatic flow conditions, surface resurgences, and erosional base levels above aquitards, and the preference for joints in groundwater routing. Evidence from caves indicates that the present hydrologic system has evolved from similar systems in the past. Vadose conduit flow conditions appear to dominate cave developmental histories, except above aquitards, where paraphreatic flow has played a role.

Results of the studies of solution chemistry also indicate that the present drainage is through an open conduit karst drainage system. Total hardness in streams is highly variable seasonally, with a peak in the summer months related to a similar seasonal pattern of biogenic CO_2 production in soils. The thickness of limestone bedrock penetrated by a stream appears to play a more important role than stream size in the chemical evolution of waters in Upper Sinking Cove. Total hardness

and SI_C, for example, are directly correlated in all seasons with the vertical distance between the sampling location and the caprock surface.

Solutional denudation of the study area is taking place in two environments: subsoil and subaqueous. An average karst denudation rate of 68.5 m^3/km^2/year (51 m^3/km^2/year during 1980-81) has been estimated from the results of process studies. This rate arises from a combination of subsoil denudation, which is fairly consistent spatially, and subaqueous denudation, which is highly variable spatially and related to the chemical aggressivity of water.

Karst Landform Development in Upper Sinking Cove

Crawford's (1978) model of slope retreat and cavern development along the Cumberland Plateau escarpment was reviewed in Chapter II. From work conducted in Upper Sinking Cove, it is apparent that most aspects of the Crawford model can be applied to this area, but that in some respects landscape evolution does not fit with Crawford's ideas. Similarities and problems will now be discussed and then a revised model, applicable to conditions in Upper Sinking Cove, will be presented as an evolutionary history of the area.

Important elements of Crawford's model are that resistant beds produce erosional base levels, and that vertical shafts occur where streams penetrate these beds. In Upper Sinking Cove, shale sequences act as aquitards to which upstream cave passages are graded. Vertical shafts are frequently found where streams penetrate these aquitards; surface streamsinks tend to occur here.

Groundwater flow conditions in Upper Sinking Cove are in most cases as predicted by Crawford's model: vadose conduit flow. Caves show no evidence of past developments at or below a watertable. Not considered in the 1978 model, however, are paraphreatic flow conditions. The fact that paraphreatic flow occurs in Upper Sinking Cove, but possibly not in other parts of the Cumberland Plateau escarpment, may be because of the extremely thick shale sequence of the Hartselle Formation in this area.

Streams entering cave passages at swallets are the most important source of aggressive water for cavern enlargement in Crawford's model. This was also indicated in Upper Sinking Cove. In all locations, water entering caves at streamsinks was found to be chemically aggressive to limestone; this was true even for sinks in the Monteagle Limestone (e.g., at the streamsink in Wolf Cove, where water from Xylophone Cave flows into Sinking Cove Cave, SI_C remained below -0.9 in August and December, 1980). The role of percolation water in dissolving limestone at the regolith/bedrock interface, presented in Crawford's model, was also demonstrated in Upper Sinking Cove by the results of rock tablet solution studies: tablets placed in soils lost 0.25 to 0.60% of their original weight over a six-month period. Also predicted by the model, diffuse inputs (represented by cave dripwaters) were near saturation, and thus were unimportant for cave passage enlargement.

If Crawford's model is correct, the depressions of Upper Sinking Cove should have developed as solution valleys behind the escarpment as a result of a local thickening of the Bangor Limestone. The Pennington/Bangor contact in Farmer Cove is in fact 10-20 m higher than at other locations which agrees with Crawford's model. The presence of

multiple depressions, however, requires other causes such as local variations in fracture intensity. Subterranean stream piracy is favored where joints are relatively well-developed.

From its inception as a caprock valley system to the karst drainage system active today, the Upper Sinking Cove region must have passed through a series of developmental stages. Assuming that the karst processes that are active today were also active in the past, this history can be reconstructed from (i) the characteristics of the present drainage system, and (ii) evidence of past drainage features preserved in relict caves.

The first stage in Fig. 5.1 depicts a surface stream flowing off the receding caprock and across the carbonates below. Aggressive water encountering these beds has begun to seep underground, widening joints and bedding planes. Seepage is favored in the Bangor Limestone especially in areas of relatively high joint frequency.

In Stage II, the caprock has receded further, and subterranean stream piracy has resulted in the development of a blind valley at the present location of Wolf Cove. The streamsink is near the Pennington/Bangor contact and may be similar to the present analog in Cave Cove, at Exercise Cave. Penetration of the Hartselle Formation has not yet occurred, and a spring emerges downvalley on this aquitard. The floor of Sinking Cove is still distant. The advance of this alluviated floor, underlain by cherts of the upper St. Louis Limestone, follows the development of the depressions in Upper Sinking Cove.

In Stage III, Farmer Cove and Cave Cove are initiated. A major blind valley terminates in Cave Cove at the Pennington/Bangor contact, and drains through Cave Cove Cave underneath an incipient Farmer Cove

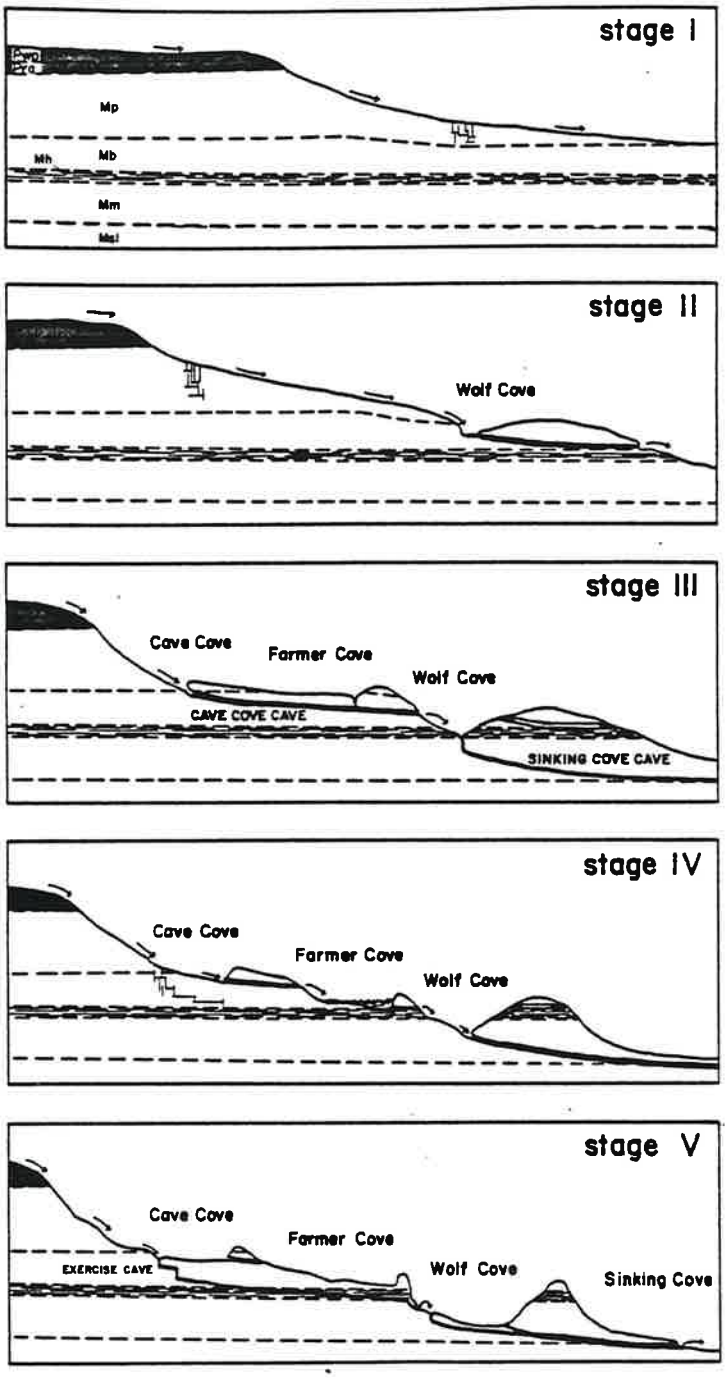

Fig. 5.1. Five stages of karst landform development in Upper Sinking Cove. Explanation given in text.

to a resurgence in Wolf Cove. A dry valley is left at the location of what is now Farmer Cove. In Wolf Cove, Sinking Cove Cave begins to enlarge as the Hartselle Formation is penetrated.

In Stage IV, Wolf Cove has penetrated the Hartselle Formation as Sinking Cove Cave develops into a major drainage conduit. Rapid downcutting results as the drainage channel is adjusted to the new erosional base level at the floor of Sinking Cove. Upvalley, Farmer Cove has collapsed through passages of Cave Cove Cave. Downstream blockage of drainage routes from the depression results in surface ponding; and alluviation occurs across the floor of Farmer Cove.

In Stage V, the present situation, Farmer Cove is about to penetrate the Hartselle Formation. Drainage conduits are still poorly developed, however, and surface flooding is common. Aggressive waters entering Cave Cove have taken a new route: they sink now at Exercise Cave, at the headward end of the cove. At some point between this new streamsink and the spring in Wolf Cove, the Hartselle Formation is penetrated by the conduit.

Future developments will see the expansion of Wolf Cove and Sinking Cove along the route of Sinking Cove Cave leading to the eventual coalescence of the two coves. Farmer Cove and Cave Cove should evolve in a similar manner. As old depressions deepen, expand, and coalesce, they will be replaced by new depressions farther up the canyon. The outcome of these developments will be to extend the canyon into the plateau and to bring about the headward expansion of Sinking Cove.

Appendix A Cave Map Symbols

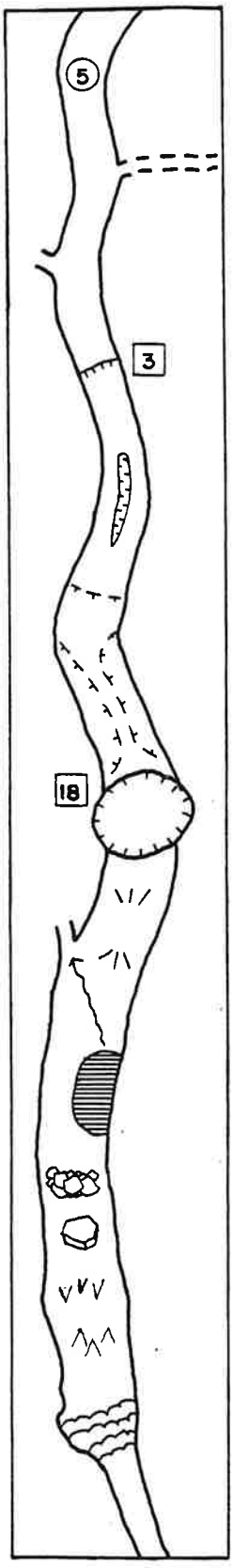

Surveyed Cave Passage: passage height in meters

Unsurveyed Cave Passage

Lead

Abrupt Drop in Floor: hachures point to lower floor

Canyon in Floor

Abrupt Drop in Ceiling: hachures point to lower ceiling

Ceiling Channel

Vertical Shaft

Slope in Floor: lines diverge downslope

Stream

Ponded Water

Breakdown

Stalactites

Stalagmites

Flowstone

Appendix B Water Chemistry Changes at SCC Spring, Summer to Early Fall 1980

Site	Date	T° C	pH	TH ppm*	Conductivity µmhos	SI_C	SI_D	log PCO_2	Discharge L/sec
T9	6/15	13.0	7.9	120	146	-0.47	-1.47	-3.20	19.8
B2	6/15	14.2	7.9	122	130	-0.40	-1.31	-3.15	19.8
B2	6/16	13.9	8.0	125	143	-0.35	-1.21	-3.30	18.4
T9	6/17	13.0	7.9	126	144	-0.43	-1.34	-3.16	19.8
T9	6/18	13.0	7.9	126	143	-0.43	-1.35	-3.16	19.8
T9	6/19	13.2	8.0	122	150	-0.30	-1.14	-3.23	18.4
T9	6/20	13.3	7.8	128	142	-0.53	-1.58	-3.08	17.0
T9	6/22	13.7	7.8	130	147	-0.47	-1.43	-3.03	12.7
B2	6/24	14.1	7.9	130	153	-0.37	-1.26	-3.14	13.6
B2	6/24	14.3	7.8	126	153	-0.55	-1.64	-3.12	14.2
B2	6/24	13.8	7.8	127	153	-0.52	-1.58	-3.08	16.1
B2	6/25	13.7	7.9	127	152	-0.39	-1.26	-3.13	48.7
B2	6/25	13.8	7.8	127	153	-0.53	-1.56	-3.08	51.0
B2	6/25	13.9	7.9	124	151	-0.45	-1.40	-3.19	53.8
B2	6/25	13.9	7.9	126	153	-0.45	-1.42	-3.21	52.4
B2	6/25	14.8	7.9	126	152	-0.45	-1.39	-3.22	51.5
B2	6/25	14.7	7.9	126	149	-0.46	-1.39	-3.22	48.1
B2	6/25	14.0	7.9	128	140	-0.45	-1.38	-3.21	31.1
B2	6/26	14.0	7.9	128	149	-0.45	-1.45	-3.20	18.4
T9	6/29	13.9	7.9	110	196	-0.43	-1.33	-3.12	~ 56

continued

continued - Appendix B

T9	6/30	13.9	7.9	103	139	-0.51	-1.55	-3.19	≈ 52
T9	6/30	14.0	7.8	101	131	-0.64	-1.82	-3.12	≈ 48
T9	8/15	13.6	7.7	134	179	-0.58	-1.63	-2.94	2.5
B2	8/13	13.5	7.9	122	148	-0.42	-1.40	-3.02	2.8
B2	8/19	15.5	8.1	126	191	-0.05	-0.59	-3.22	3.1
B1	9/29	13.2	7.8	135	310	-0.53	-1.60	-3.11	55.2
B1	9/29	13.0	7.9	136	210	-0.33	-1.22	-3.11	51.5
B1	9/30	13.0	7.8	141	213	-0.45	-1.40	-3.03	73.6
B1	9/30	13.3	7.7	142	202	-0.54	-1.59	-2.93	84.7
T9	9/30	13.2	7.6	138	198	-0.67	-1.90	-2.86	84.7
B1	9/30	13.3	7.6	139	200	-0.65	-1.83	-2.84	84.7
B1	9/30	13.2	7.6	137	197	-0.66	-1.84	-2.84	79.3
B1	9/30	13.2	7.7	133	193	-0.56	-1.69	-2.94	77.0
B1	9/30	13.2	7.6	128	192	-0.73	-2.00	-2.88	72.2
B1	10/1	13.1	7.7	123	203	-0.62	-1.78	-2.96	18.4
T9	10/1	13.1	7.7	125	203	-0.63	-1.84	-2.98	18.4
T9	10/1	13.2	7.7	134	203	-0.58	-1.84	-2.94	18.4

REFERENCES

Adams, C., and Swinnerton, A. (1937). The solubility of limestone. Trans. Am. Geophys. Union 18: 504-508.

Aley, T., and Fletcher, M. W. (1976). The water tracer's cookbook. Missouri Speleology 16 (6): 32p.

Barr, T. C., Jr. (1961). Caves of Tennessee (Tennessee Division of Geology Bulletin 64).

Bloxsom, D., Jr. (1955). Sinking Cove Cave System. Troglodyte 1 (9).

Bögli, A. (1980). Karst Hydrology and Physical Speleology (Berlin: Springer-Verlag).

Bretz, J. H. (1942). Vadose and phreatic features of limestone caverns. J. Geol. 50: 675-811.

Brook, G. A., Folkoff, M. E., and Box, E. O. A global model of soil carbon dioxide. Earth Surface Processes and Landforms (in press).

Brook, G. A., and Ford, D. C. (1978). The origin of labyrinth and tower karst and the climatic conditions necessary for their development. Nature 275: 493-496.

Brown, M. C., Wigley, T. L., and Ford, D. C. (1969). Water budget studies in karst aquifers. J. Hydrol. 9: 113-116.

Brucker, R. W. (1966). Truncated cave passages and terminal breakdown in the Central Kentucky Karst. Bull. Natl. Speleol. Soc. 28: 171-178.

Coleman, J. C. (1945). An indicator of waterflow in caves. Geol. Mag. 82: 138-139.

Corbel, J. (1959). Erosion en terrain calcaire. Ann. Geogr. 68: 97-120.

Crawford, N. C. (1978). Subterranean stream invasion, conduit cavern development, and slope retreat: a surface-subsurface erosion model for areas of carbonate rock terrain overlain by less soluble and less permeable caprock. Unpublished PhD Dissertation, Clark University.

Davis, W. M. (1930). Origin of limestone caverns. Geol. Soc. Am. Bull. 41: 473-628.

Deike, G. H., and White, W. B. (1969). Sinuosity in limestone solution conduits. Am. J. Sci. 267: 230-241.

Douglas, I. (1964). Intensity and periodicity in denudation processes with special reference to the removal of material in solution by rivers. Z. Geomorph. 8: 453-473.

(1968). Some hydrologic factors in the denudation of limestone terrains. Z. Geomorph. 12: 241-255.

Drake, J. J. (1980). The effect of soil activity on the chemistry of carbonate groundwaters. Water Resources Research 16(2): 381-386.

Drake, J. J., and Wigley, T. M. L. (1975). The effect of climate on the chemistry of carbonate groundwater. Water Resources Research 11: 958-962.

Ferguson, C. C., and Stearns, R. G. (1968). Geologic Map of the Pitcher Ridge Quadrangle, Tennessee. (State of Tennessee, Department of Conservation, Division of Geology).

Folk, R. L. (1959). Practical petrographic classification of limestones. Bull. Am. Assoc. Pet. Geol. 43: 1-38.

Ford, D. C., and Ewers, R. O. (1978). The development of limestone cave systems in the dimensions of length and depth. Can. J. Earth Sci. 15: 1783-1798.

Hack, J. T. (1966). Interpretation of Cumberland Escarpment and Highland Rim, south-central Tennessee and northern Alabama. Geol. Surv. Prof. Pap. (U.S.) 524-C.

Harmon, R. S., White, W. B., Drake, J. J., and Hess, J. W. (1975). Regional hydrochemistry of North American carbonate terrains. Water Resources Research 11: 963-967.

Hayes, C. W., and Campbell, M. R. (1894). Geomorphology of the southern Appalachians. Natl. Geogr. Mag. 6: 63-126.

Hunter, D. R. (1978). Petrographic and geochemical study of carbonate rocks in the Bangor-Lowermost Pennington interval, Monteagle Mountain, Tennessee. Unpublished MS Thesis, Dept. of Geology, University of Georgia, Athens.

Jennings, J. N. (1971). Karst (Cambridge, Mass.: MIT Press).

Johnson, L. (1978). Happenings at Sinking Cove. Speleonews 22(4): p.52.

Malott, C. A. (1937). Invasion theory of cavern development. Proc. Vol. Geol. Soc. Am. 1937: p.323.

Marker, M. (1980). A systems model for karst development with relevance for southern Africa. S. Af. Geogr. J. 62: 151-163.

Martel, E. (1921). Nouveau traite des eaus souterraines (Peris: Delagrave).

Pohl, E. R. (1955). Vertical shafts in limestone caves. Occ. Paper - Natl. Speleol. Soc. 2.

Quinlan, J. F., and Rowe, D. R. (1977). Hydrology and water quality in the Central Kentucky Karst: Phase I. Management Report 12, National Park Service, Uplands Field Research Laboratory, Mammoth Cave, Kentucky.

Rhoades, R., and Sinacori, M. N. (1941). The pattern of groundwater flow and solution. J. Geol. 49: 785-794.

Sawatzky, D.L. (1977). LINANL - LINeament ANaLysis procedure. U.S. Geological Survey (unpublished manuscript).

Shuster, E. T., and White, W. B. (1971). Seasonal fluctuations in the chemistry of limestone springs: a possible means of characterizing carbonate aquifers. J. Hydrol. 14: 93-128.

Smith, D. I. (1965). Some aspects of limestone solution in the Bristol region. Geogr. J. 131: 44-49.

Smith, D. I., and Atkinson, T. C. (1976). Processes, landforms and climate in limestone regions. In Derbyshire, E. (Ed.), Geomorphology and Climate (Chichester: Wiley), pp. 367-409.

Smith, M. O. (1978). The Boulder (5th) entrance to Sinking Cove Cave, Franklin County, Tennessee. Birmingham Grotto Newsletter, May.

Sun, C. H., Dept. of Geography, University of Georgia, Athens.

Sweeting, M, M, (1973). Karst Landforms (New York: Columbia University Press).

Swinnerton, A. C. (1932). Origin of limestone caverns. Geol. Soc. Am. Bull. 43: 663-694.

Tennessee Cave Survey, Shelbyville, Tennessee.

Tennessee Valley Authority, Data Management Section (R. Beebe, supervisor).

Thornthwaite, C. W. and Mather, J. R. (1955). Instructions and tables for computing potential evapotranspiration and the water balance. Publications in Climatology 10: 181-311.

Thrailkill, J. V. (1968). Chemical and hydrologic factors in the excavation of limestone caves. Geol. Soc. Am. Bull. 79: 19-45.

Trudgill, S. T. (1975). Measurement of erosional weightloss of rock tablets. pp. 13-19 in Shorter Technical Methods, British Geomorphological Research Group Technical Bulletin 17.

Zötl, J. G. (1965). Tasks and results of karst hudrology. In Stelcl, O. (Ed.), Problems of the Speleological Research (Prague), pp. 141-145.